Spring 2016

Anti-Predator Responses of Squid Throughout Ontogeny

Carly Anne York
Old Dominion University

Recommended Citation

ANTI-PREDATOR RESPONSES OF SQUID THROUGHOUT ONTOGENY

by

Carly Anne York
B.S. December 2007, Elon University
M.S. August 2011, Western Kentucky University

A Dissertation Submitted to the Faculty of
Old Dominion University in Partial Fulfillment of the
Requirements for the Degree of

DOCTOR OF PHILOSOPHY

ECOLOGICAL SCIENCES

OLD DOMINION UNIVERSITY
May 2016

Approved by:

Ian Bartol (Director)

Lisa Horth (Member)

Kent Carpenter (Member)

Sara Maxwell (Member)

Paul Krueger (Member)

Joseph Thompson (Member)

ABSTRACT

ANTI-PREDATOR BEHAVIOR OF SQUID THROUGHOUT ONTOGENY

Carly Anne York
Old Dominion University, 2016
Director: Dr. Ian K. Bartol

Multiple sensory modalities and a complex array of escape behaviors have evolved as components of anti-predator responses in squids. The goals of this study include: (1) examine the role of the lateral line analogue and vision in successful predator evasion; (2) measure kinematics of escape jetting; (3) document how chromatic patterning, posturing and inking in squid change in response to predators; and (4) investigate escape jet hydrodynamics of squid. Given that squids undergo considerable morphological, ecological, and behavioral changes throughout ontogeny, the goals above were all investigated across different life history stages. To test the respective roles of vision and the lateral line analogue, squid of different life stages were recorded in the presence of natural predators under light and dark conditions with their lateral line analogue intact and ablated via a pharmacological technique. Anti-predator behaviors of squid throughout ontogeny were studied in a series of predator-prey trials using high-speed videography. Additionally, the hydrodynamics and kinematics of high velocity escape jets in squid were examined using a combination of 2D/3D velocimetry. The lateral line analogue played a role in initiation of an escape response at the earliest life stages, and continued to contribute to successful evasion by aiding visual cues in juvenile/adult squid. Paralarvae relied heavily on stereotyped swimming behaviors and translucent coloration to avoid capture, while juvenile and adults used multiple cues associated with the predator's approach to determine whether posturing or inking and escape jetting is the most suitable anti-predator behavior.

Throughout ontogeny, squid produced two escape jet patterns: (1) *escape jet I* characterized by short rapid pulses resulting in vortex ring formation and (2) and *escape jet II* characterized by long high volume jets, often with a leading edge vortex ring. Paralarvae exhibited significantly higher propulsive efficiency (94.55%) than adult squid (87.71%) during jet ejection. These results indicate that all life stages of squid are well adapted for predator avoidance; they employ multiple sensory modalities for predator detection, use a variety of anti-predator behavioral responses, and utilize a highly efficient and flexible escape jet to maximize escape from predation.

"Jetting animals are just hearts set free…"
O'Dor and Webber, 1991

ACKNOWLEDGMENTS

TABLE OF CONTENTS

LIST OF TABLES

LIST OF FIGURES

CHAPTER 1

INTRODUCTION

Predation is a major factor in the biology of organisms and influences a species' life history and behavior (Polis, 1981). An animal whose form and behavior aids in predator avoidance or escape will increase its probability of survival to reproductive age. As a result, there is a possibility for greater reproductive success relative to animals that are unable to avoid predators (Alcock, 1993). As almost all animals are subject to predation, a wide variety of adaptations have evolved to reduce detection by predators and, if detected, escape successfully. Primary defenses function to decrease exposure to a predator, and often involve crypsis and cryptic behavior. Secondary defenses are brought into play once the animal has been detected and often include a threat or escape behavior (Hanlon and Messenger, 1996).

The unique anti-predator defenses of cephalopods include having high sensory acuity, using adaptive coloration, generating ink, and employing a powerful escape jet. The wide variety of techniques for predator avoidance makes cephalopods a particularly interesting organism for the study of anti-predator behavior and biomechanics. While cephalopods are themselves predators, they also serve as food to many higher predators of the ocean, including fish, marine mammals, sea birds, and even other cephalopods, and are therefore an integral component of marine food webs (Clarke, 1996; Piatkowski et al., 2001). Despite being a highly sought after food source, cephalopods have survived since the Cambrian era, as evidenced by the fossil record (Kröger et al., 2011).

Cephalopod Sensory Systems

The eyes are the most prominent sensory feature of cephalopods (Budelmann, 1996) with

the optic lobes being the most dominant region of the brain (Young, 1962). Resembling the vertebrate eye, the squid eye incorporates a large posterior chamber, lens, iris, retina, choroid, sclera and argenta (Budelmann, 1994). However, there are several key differences between the cephalopod and vertebrate eye anatomy. Cephalopods have a rhabdomeric structure of the retina in which there are no rods or cones, as found in other mollusks and arthropods (Mäthger et al., 2009). The visual image also falls directly on the photoreceptor cells without interneurons, as found in the retina of vertebrates (Budelmann, 1994). The photoreceptors contain only one visual pigment peaking in spectral sensitivity around 480-500 nm (Budelmann, 1996), rendering cephalopods colorblind, which has been confirmed in behavioral studies (Mäthger and Hanlon, 2006). Unlike the eyes of most teleost fish, cephalopods have motile pupils that respond to changes in illumination. The time required for pupil closure is far less than in most other animals. The common cuttlefish (*Sepia officinalis*) and brief squid (*Lolliguncula brevis*) require only 0.32 s and 0.49 s, respectively, to attain half maximal pupil constriction, while the fastest teleost fish response is 0.75 s (Douglas et al., 2005). Cephalopods have laterally placed eyes and consequently see their environment monocularly. As the eyes are utilized individually, the pupils of coleoid cephalopods respond independently to light (Douglas et al., 2005) and exhibit asymmetrical constriction under increasing irradiance levels (McCormick and Cohen, 2012). The highly evolved visual system of cephalopods likely plays a large role in predator detection and initiation of an escape response.

In addition to their complex visual system, cephalopods can detect disturbances from small water movements using mechanoreceptors on their head and arms, which resemble hair cells in the fish lateral line system (Bleckmann et al., 1991; Budelmann and Bleckmann, 1988). The fish lateral line consists of the superficial and canal neuromasts. The superficial neuromasts

have the highest response rates to direct-current and low frequency flows, while the canal neuromasts respond best to high frequency flows (Coombs et al., 2001; Montgomery et al., 2001). With both types of neuromasts, hair cell cilia housed under a gelatinous cupula are stimulated by water motion. The cupula has a distinct infrastructure organization that enhances the mechanical coupling of the ciliary bundles under the hair cells (Shadwick and Lauder, 2006). The cephalopod lateral line analogue is not as well described as the fish lateral line. It consists of polarized epidermal hair cells that have several kinocilia and an axon extending from their base (Budelmann and Bleckmann, 1988). Polarization occurs in a precise pattern (anteriorly, posteriorly, left and right), allowing the animals to respond to water movements as low as 18.8 µm/s, which is equivalent to the sensitivity of fish lateral lines (Bleckmann et al., 1991). The epidermal lines respond to bursts of sinusoidal water movements with a receptor potential in a phasic-tonic manner (Bleckmann et al., 1991). In the squid *Loligo vulgaris*, five epidermal lines are present on each side of the head running in an anterior-posterior direction (Budelmann and Bleckmann, 1988).

The lateral line of fishes plays a large role in detecting a predator (Feitl et al., 2010). Larval zebrafish (*Danio rerio*) react swiftly (within 30 ms) to the flow field produced by an attacking predator via a C-start escape response that quickly moves the fish out of the predator's path (Hale, 1999; McHenry et al., 2009). The C-start is initiated when neuromasts comprising the lateral line are stimulated by pressure gradients generated by an oncoming predator (McHenry et al., 2009; Wainwright et al., 2007). There are two pressure gradients that can stimulate C-starts, one produced by the push of water in front of the predator and another by suction generated by the predator during mouth opening. Interestingly, Stewart et al. (2013) demonstrated that larval zebrafish have most success at evading predators when they react to the push of water in front of

the predator, as opposed to the suctional flows, and when they are positioned at an optimal intermediate distance away from the predator. Fishes generally lack canal neuromasts during early ontogenetic stages, which also has an impact on escape success. In herring larvae (*Clupea harengus*), responsiveness to predator attacks is very low in newly formed larvae, but increases with size as the lateral line canal system develops (Blaxter and Fuiman, 1990). The role of the lateral line in these escape responses has been confirmed by lateral line ablation, whereby the escape response rapidly diminishes with ablation but returns with hair cell regeneration (Feitl et al., 2010; McHenry et al., 2009). To date, no research has been performed on the lateral line analogue of cephalopods to assess whether it plays a similar role in predator detection at any life history stage.

Cephalopod Anti-predator Behavior

An array of complex behaviors is associated with escape responses in cephalopods (Hanlon and Messenger, 1996; Staudinger et al., 2011; Wood et al., 2010). Along with a jet-driven escape, a widely used strategy for predator evasion in cephalopods is camouflage (Hanlon et al., 1994; Hanlon et al., 1999; Mäthger and Hanlon, 2007; Messenger, 2001). Cephalopods can adapt their color and body patterning quickly according to various features in their environment via chromatophores and iridophores (Sutherland et al., 2008). Chromatophores are complex organs containing a large compartment of pigment granules (Florey, 1966), including those that are yellow, orange, red, brown and black (Fingerman, 1970; Messenger, 2001). No blue or green pigments are found in cephalopods (Messenger, 2001). Each chromatophore organ contains an elastic sacculus with pigment granules and is surrounded by a series of 15-25 radial muscles. These muscles are under nervous control and therefore expansion and contraction can occur

rapidly and selectively to create patterns (Florey, 1966). Squid generally have two layers in their skin, a superficially located layer of chromatophores and an underlying layer of structural reflector cells called iridophores (Mäthger et al., 2009). Chromatophore and iridophore arrangement varies among taxa (Boyle and Rodhouse, 2008). Expanding and retracting chromatophores over the iridophores influences the light that is reflected (Mäthger and Hanlon, 2007; Sutherland et al., 2008). Chromatophores are also used to produce a countershading effect, which eliminates any silhouette or shadow created by downward light (Boyle and Rodhouse, 2008). During countershading, the dorsal chromatophores are expanded and the ventral chromatophores are retracted, while the side of the mantle and the arms are graded between the two extremes (Hanlon and Messenger, 1996).

Cephalopods use crypsis in the form of body patterning and chromatophore change during secondary defense behaviors to maximize the effectiveness of escape jets (Hanlon et al., 1994). A typical response to a threat is the "blanch-ink-jet" maneuver (Hanlon and Messenger, 1996; Hanlon et al., 1994). During this sequence, the cephalopod blanches white and ejects ink as it jets away. This visually confuses the predator and allows for an escape. Many intraspecific body patterns are highly stereotyped; however, it is unclear whether the chromatophore change in the "blanch-ink-jet" maneuver is a fixed-action pattern (Hanlon et al., 1994). The secretion of ink can occur in several forms. One method is producing a pseudomorph, which is a blob of ink that is held together by mucus. The pseudomorph typically is the size of the cephalopod, which serves to distract a predator while the animal escapes. Another method is to create a cloud of ink behind which the cephalopod can disappear (Hanlon and Messenger, 1996). There are several other shapes of ink such as "ropes" and "puffs" that have been observed in nature (Bush and Robison, 2007). Squid ink also contains chemicals that elicit escape responses in nearby

conspecifics (Gilly and Lucero, 1992). L-dopa and dopamine are largely responsible for the chemical signals (Lucero et al., 1994). There is also anecdotal evidence that chemicals in ink may block olfactory or taste receptors in predators (Caldwell, 2005; Hanlon and Messenger, 1996). Little research is currently available on how this anti-predator behavior sequence changes throughout life history stages.

Escape Jet Biomechanics and Hydrodynamics

The escape response of cephalopods is largely driven by jet propulsion, which is produced by the rapid expulsion of water from the mantle cavity through a funnel aperture (O'Dor, 1988; Packard, 1969; Young, 1938). Water is drawn into the mantle cavity around the sides of the head through intakes via mantle expansion produced by radial muscle contraction and elastic recoil of connective tissue fibers. Circular muscles in the mantle then contract to pressurize the water in the mantle cavity, resulting in the closure of the intakes (Young, 1938). A high velocity jet is produced when water is forcibly expelled through the funnel, which has relatively small cross-sectional area. The funnel is flexible and capable of directing the jet anywhere within a hemisphere below the body, allowing the animal to move in various directions (Bartol et al., 2001a). Estimates of peak jet velocity range between 2.9 and 6.9 m/s for octopus and cuttlefish and between 6.7 and 11 m/s for squid (Shadwick, 1995). The high velocity created by the jet allows for quick evasion from the path of a predator. The motor systems of the mantle and funnel presumably allow for control of the trajectory, volume, and flow speed of escape jets (Otis and Gilly, 1990), though variation in escape jetting has not been documented to date.

The mantle hydrostatic system that allows for jet propulsion consists of a three-

dimensional arrangement of circular and radial fibers and connective tissue (Thompson and Kier, 2001a). The mantle cavity is enclosed by a wall of flexible muscle with an array of connective tissue within the mantle musculature. There are two distinct muscle types of circular muscle fibers in the mantle: superficial mitochondria rich (SMR) fibers and central mitochondria poor (CMP) fibers. SMR fibers have a large core of mitochondria, have high succinic dehydrogenase activity, and have a high ratio of oxidative to glycolytic enzymes. These fibers are present in thin (i.e., 50 to 200 μm) layers at the inner and outer zones of the circular muscle fibers (Bone et al., 1981; Mommsen et al., 1981). CMP fibers make up the circular muscle fibers of the central zone and have a small core of mitochondria, low succinic dehydrogenase activity, and a low ratio of oxidative to glycolytic enzymes (Bone et al., 1981; Mommsen et al., 1981). The SMR circular muscle fibers are similar to the red muscles of vertebrates and provide power for ventilation of the mantle cavity and slow prolonged swimming (Bartol et al., 2001a; Bartol et al., 2008; Gosline et al., 1983; Thompson et al., 2008). In contrast, the CMP circular muscle fibers are similar to the white muscles of vertebrates and provide power for short, high powered jets (Bartol et al., 2001a; Gosline et al., 1983; Thompson et al., 2008). Bartol (2001a) correlated mantle kinematics with electromyography records and found that SMR activity occurs at low speeds, increased CMP activity occurs at intermediate speeds and full activation of CMP fibers occurs at high speeds in the squid *L. brevis*.

Although current hydrodynamic research on squid does not focus on escape jets, a large body of knowledge has been acquired on jet propulsion in steady swimming. Many studies have examined swimming energetics of squid (Bartol et al. 2001a; Finke et al., 1996; O'Dor, 1982; O'Dor et al., 1991; O'Dor et al., 1995; Webber and O'Dor, 1986), but fewer studies have addressed the hydrodynamics of squid locomotion. An examination of the forces acting on adult

squid (*Loligo opalescens* and *Illex illecebrosus*) was provided by O'Dor (1988), and Anderson and DeMont (2000) examined propulsive efficiency and unsteady hydrodynamics of *D. pealeii*. Bartol et al. (2001b) found that small squid, such as *L. brevis,* use a suite of behavioral fin and jet strategies with speed and provided qualitative descriptions of vortex ring formation. These flow features are especially intriguing because they may provide thrust benefits through acceleration of fluid via entrainment and added mass effects (Krueger and Gharib, 2003). Subsequent studies involving more quantitative digital particle image velocimetry (DPIV) measurements (Bartol et al., 2008; 2009a; 2009b) and volumetric velocimetry (Bartol et al. 2016) have shown that vortex ring formation is a common feature of the wakes of squid. Bartol and his colleagues have shown that several different types of jet flow patterns are produced by squid of different life history stages. In juvenile and adult brief squid, two principal jet modes occur: (1) *jet mode I*, where ejected fluid rolls into an isolated vortex ring and (2) *jet mode II*, where ejected fluid forms into a leading vortex ring that pinches off from a long trailing jet (Bartol et al., 2008; Bartol et al., 2009b). *Jet mode I* is associated with greater propulsive efficiency, lower slip and higher frequency of fin activity, while *jet mode II* is associated with greater time-averaged thrust and lift forces and is used more heavily than the first jet mode. *D. pealeii* paralarvae produce jets consisting of elongated vortical ring structures but with no clear pinch-off as present in *jet mode II* of larger size classes (Bartol et al., 2009a; Bartol et al., 2009b). Bartol et al. (2009a) suggested that the absence of pinch-off may be a product of either (1) viscous diffusion blurring the separation between the ring and jet or (2) vortex ring formation being preempted by viscous diffusion such that a vortical tail remains behind the ring. Bartol et al. (2008, 2009a, 2009b) found that not only do flow features differ between paralarval and juvenile/adult squid, but that paralarval squid also have higher propulsive efficiency during jet ejection than older squid.

In addition to jet propulsion, lateral fins in sepioids and squids play an important role in stability, steering, and thrust/lift production. Undulatory motions of the fins alone are used during hovering or small movements (Anderson and Grosenbaugh, 2005; Bartol et al., 2001a; Hoar et al., 1994a; O'Dor, 1988). Cephalopods lack the rigid skeletal support elements that extend through the fins of teleost fishes. Instead, the fins consist of a three-dimensional array of musculature that serves as both the effector of movement and the support for the movement (Kier, 1988). The fins of the brief squid function as stabilizers during tail-first swimming at low speeds, but shift to propulsors as speed increases. During arms-first swimming, the fins primarily provide lift with a reduced role in thrust production (Stewart et al., 2010). Recent volumetric velocimetry studies has provided further support for the role of fins as stabilizers and producers of lift and thrust, with 3D visualizations revealing that complex fin and fin/jet flows are common during steady swimming (Bartol et al., 2016). Although the jet is largely responsible for the majority of thrust associated with an escape response, the fins potentially play an important role for stability and steering, though this has not been addressed in the literature to date.

The basic framework for producing an escape jet is thought to be stereotyped regardless of the life history stage and size of the animal (Thompson and Kier, 2001), though variations in wake topology are certainly possible with slight modifications to this underlying framework. The series begins with the mantle hyper-inflating, which allows the mantle cavity to fill with water. The collar flaps then close and the anterior edge of the mantle begins to contract. Next, the fins fold against the side of the mantle and the remainder of the mantle contracts, rapidly expelling water through the funnel (Thompson and Kier, 2001). Although the basic approach to escape jetting is conserved across ontogeny, it is likely that other components of the escape-response, such as mantle/funnel kinematics and fin use, vary through life history stage as several of the

major elements of jet propulsion change throughout ontogeny. Squid undergo major morphological changes throughout ontogeny that affect both jet propulsion and fin use (Hoar et al., 1994a; Okutani, 1987; Packard, 1969). Paralarvae have small rounded bodies with rudimentary fins. This forces hatchlings to rely primarily on jet propulsion for locomotion (Bartol et al., 2008). Juveniles and adults have less rounded bodies and larger, more developed fins (Hoar et al., 1994a). In the oval squid (*Sepioteuthis lessoniana*), the weight-specific peak thrust of jet propulsion and the mechanics of the circumferential muscles of the mantle change significantly from hatchling to juvenile/adult stages (Thompson and Kier, 2002). Juvenile and adult squid also have smaller relative funnel apertures than paralarvae (Thompson and Kier, 2001). Additionally, ontogenetic changes occur in the relative amplitude of mantle contraction, relative maximum amplitude of mantle hyperinflation and relative maximal mantle contraction during escape jetting (Thompson and Kier, 2001). Given these morphological and behavioral changes, locomotive escape responses are likely variable throughout ontogeny. In particular, escape jet propulsive efficiency, bulk jet wake properties and locomotive escape strategies are expected to change with life stage.

As squids grow from hatchlings to adults they also experience a variety of flow regimes (Bartol et al., 2008; Thompson and Kier, 2002). The Reynolds number (Re) describes the relationship between the size of the animal, the speed of the animal, and the kinematic viscosity of the fluid media with the following equation:

$$\text{Re} = lU/v \quad \text{(Lighthill, 1975)},$$

where l is a characteristic length of the organism, U is the velocity of the organism in the fluid and v is the kinematic viscosity of the fluid. Re characterizes the relationship between inertial forces and viscous forces felt by the swimming animal (Vogel, 2013). At high Re ($>10^3$) inertial

forces dominate, while at low Re (<1), viscosity is dominant. At intermediate Reynolds numbers ($1<\text{Re}<10^3$), both inertial and viscous forces play important roles (Vogel, 2013). Paralarval squids often operate at Re of $1\text{-}10^2$, while juveniles and adults operate at Re of $10^3\text{-}10^6$ (Bartol et al., 2008). Given the wide Re regimes experienced by squid throughout ontogeny, it is likely that escape response dynamics will vary significantly with life history stage.

Objectives

The purpose of this study is to evaluate anti-predator defenses of squid throughout ontogeny. Three general areas of research are explored: (1) sensory biomechanics, whereby I explore the role of vision and mechanoreceptors in predator avoidance throughout ontogeny; (2) anti-predator behavior, whereby I document body patterning, posturing and inking throughout ontogeny; and (3) hydrodynamics and kinematics of the escape jet, whereby I focus on the swimming mechanics of escape responses to assess vortex-wake flow structure, propulsive efficiency, escape speeds and accelerations throughout ontogeny. Although the physiology and morphology of the visual system of cephalopods has been studied extensively, the role of the visual system for predator avoidance has not been quantified. Moreover, mechanoreception and its importance for predator detection relative to the visual system has been largely ignored. Given that similar mechanoreception systems in fishes are important for predator detection, it is likely that the lateral line analogue in squids is integral to their ability to detect and escape predators. Although it is well known that inking often occurs in predation events, documentation of inking patterns in squids during predator confrontations has not been performed to date. Additionally, considerable research has been conducted on how the chromatophore organs create patterns that can reduce detection. However, a further investigation of chromatophore changes

throughout the escape response is needed to fully understand how chromatophore patterns can increase survivability. Currently, little research has focused specifically on the hydrodynamics and kinematics of escape responses in cephalopods. While jets associated with steady swimming have been studied in some squid species, nothing is known about the hydrodynamics of escape jets, including data on peak jet velocities, vorticity structure, and propulsive efficiency. Most importantly, none of the areas above have been explored throughout an ontogenic range of squids.

This dissertation includes 4 data chapters that focus on escape responses of squid throughout ontogeny. In Chapter 2, I describe a pharmaceutical mechanoreceptor ablation technique and demonstrate for the first time that this approach can be performed successfully on cephalopods. I also provide the first data documenting that the lateral line analogue, together with the visual system, is important for predator detection and survival in juvenile/adult squid. In Chapter 3, I document escape responses in ablated and non-ablated squid in light and dark conditions to examine the relative roles of vision and the lateral line analogue in survival throughout ontogeny. For Chapter 4, I document how chromatic patterning, posturing and inking in squid change in response to predators throughout ontogeny and measure kinematic variables associated with squid-predator interactions to better understand the behavioral cues that trigger anti-predator responses. Finally, in Chapter 5, I study the hydrodynamics of escape jetting in squid throughout ontogeny using 2D and 3D velocimetry, with an emphasis on documentation of vortex wake structures and propulsive efficiency. Collectively, the four chapters above represent the most comprehensive assessment of escape responses in squid throughout ontogeny to date.

CHAPTER 2

LATERAL LINE ANALOGUE AIDS VISION IN SUCCESSFUL PREDATOR

EVASION FOR BRIEF SQUID *LOLLIGUNCULA BREVIS*

INTRODUCTION

Cephalopods rely on multiple sensory systems for detection of predators (Budelmann, 1996). The eyes are the most prominent sensory feature of cephalopods with the optic lobes being the dominant region of the brain (Young, 1962). The highly evolved visual system of cephalopods likely plays a large role in predator detection and initiation of an escape response. However, to date, the role of vision relative to other sensory modalities in predator evasion has not been examined in any cephalopod.

In addition to their complex visual system, cephalopods have a sensory system that resembles the lateral line system of fishes (Bleckmann et al., 1991; Budelmann, 1996; Budelmann and Bleckmann, 1988). The cephalopod lateral line analogue consists of polarized epidermal hair cells that have several kinocilia and an axon extending from their base (Budelmann and Bleckmann, 1988). Polarization occurs in a precise pattern (e.g., anteriorly, posteriorly, left and right), allowing the animals to respond to water movements as low as 18.8 µm/s, which is equivalent to the sensitivity of fish lateral lines (Bleckmann et al., 1991). Behavioural responses have also been elicited in cuttlefish (*Sepia officinalis*) by stimulating their lateral line analogue using a wide range of frequencies (10-600 Hz) (Komak et al., 2005). While fish can react swiftly to the flow field produced by an attacking predator using their lateral line system (McHenry et al., 2009; Stewart et al., 2013), it is unknown if the lateral line analogue of cephalopods plays a similar role in predator detection. The goal of this study was to develop a

technique to successfully ablate cephalopod sensory hair cells, and test the hypothesis that the lateral line analogue of squid (*Lolliguncula brevis*) aids vision in successful predator evasion.

MATERIALS AND METHODS

Animal collection and maintenance

Lolliguncula brevis (2.5 cm-6.0 cm dorsal mantle length (DML)) used in this project were captured by otter trawl in Wachapreague, VA, USA. Squid were kept in 1.2 m diameter circular tanks using protocols described in Hanlon (Hanlon, 1990). Animals were allowed to acclimate for at least 2 h before experiments. Only animals that appeared healthy and exhibited normal behaviour were utilized. For the lateral line analogue ablation validation (see below), *Doryteuthis pealeii* paralarvae were purchased from the Marine Biological Laboratory, Woods Hole, MA, and maintained in a recirculating seawater system at a salinity of 30-32‰ and at temperatures of 19-24°C until hatching.

Lateral line analogue ablation validation

Antibiotic solutions have successfully been used for lateral line ablation in fish studies (Harris et al., 2003; McHenry et al., 2009; Stewart et al., 2013); however, the technique had never been performed on cephalopods and therefore validation of this approach was required. To determine the appropriate concentration of the neomycin sulphate solution for lateral line analogue ablation, a series of antibiotic trials were conducted. *Doryteuthis pealeii* paralarvae were used in the antibiotic trials because of the large number available and small body size, which is conducive for scanning electron microscopy (SEM) prep. Paralarvae were divided into four treatment groups (N=15 per group): 0 μM, 150 μM, 250 μM and 500 μM neomycin

sulphate. Paralarvae were placed into the antibiotic solution for one hour, and then were anesthetized using water at 5°C before fixation. SEM was employed to survey the success of ablation within each of the experimental groups. For SEM, the squid were placed overnight in a fixative (concentrations: 3% glutaraldehyde, 6% sucrose, 0.5% tannic acid, 0.065M Sörensen's buffer), rinsed and stored in a buffer (concentration: 1% glutaraldehyde, 6% sucrose, 0.065M Sörensen's buffer) and then dehydrated in a graded ethanol series. Specimens were dried using the chemical drying agent hexamethyldisilazane and mounted on aluminium stubs with double-stick tape. Specimens were sputter-coated with 15-30 nm gold and examined with a Hitachi S-3400N JEOL 6300-F field emission scanning electron microscope at an accelerating voltage of 15kV. SEM images revealed consistently successful lateral line ablation after being treated with 500 μM neomycin sulphate solution (Fig.1). Similar protocols were used with *L. brevis* juveniles to confirm lateral line ablation at this treatment concentration. Based on successful ablation in *D. pealeii* hatchlings and *L. brevis* juveniles, a 500 μM concentration was selected for predator-prey experiments. Although this treatment was effective at decreasing the number and integrity of lateral line hair cells, the lateral line regeneration capabilities of squid were not tested and are not currently known. Observation of both *D. pealeii* and *L. brevis* after treatment showed that squid maintained normal behaviours and did not lose any orientation abilities that would indicate damage to the statocycsts.
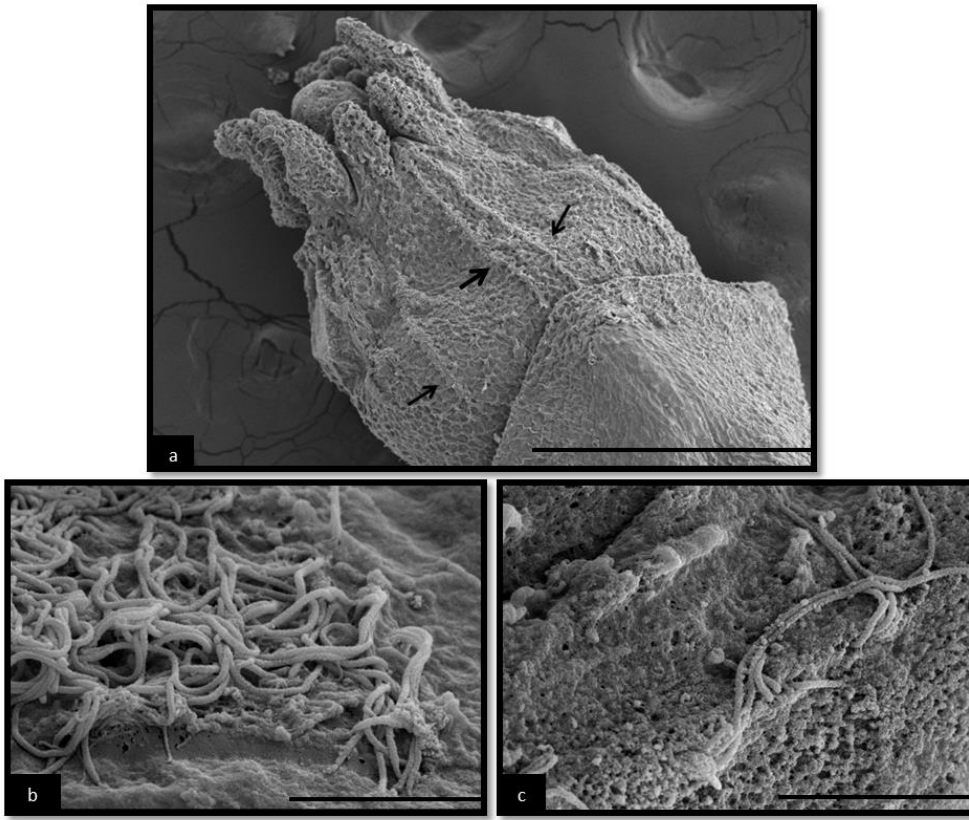
Figure 1. SEM images of the lateral line analogue shown on a *Doryteuthis pealeii* paralarvae. Lines of hair cells on the head highlighted with arrows (a); close-up views of sensory hair cells of the lateral line analogue (b); sensory hair cells after treatment with a 500 μM solution of neomycin sulphate (c). The majority of hair cells were destroyed completely after treatment with the remaining hair cells being porous and heavily damaged. Scale bar for a = 400 μm; b, c =5 μm.

Predator-prey experiments

Predator-prey interaction experiments were used to evaluate the use of vision and mechanoreception in predator evasion. Trials took place in a 1.2 m diameter x 0.76 m deep round tank lined with gravel substrate. The arena was lined with curtains to avoid disturbing acclimating animals. Black plastic sheeting was used to block light during the dark trials. For each experiment, a single squid was placed in an arena with two flounder (13.2 cm and 15.5 cm total length). Flounder have shown successful captures for the relative prey size presented in this study (Staudinger and Juanes, 2010), and were chosen as predators due to their exceptional vision in both bright and dark conditions (Horodysky et al., 2010). Multiple predators were used to increase the odds of a predation event. The flounder were fed live squid prior to the trials so that they could become proficient in squid capture before data collection. Food was withheld 24 h prior to the start of all trials to standardize predator hunger.

One hour prior to trials, squid were placed in a container, which either held the neomycin sulphate solution for ablation groups or untreated water for the non-ablation groups. Prior to the start of each trial, a cylinder made of 5 mm plastic mesh was lowered into the experimental tank and a single squid was placed inside for a 30 min acclimation period. The trials commenced when the partition was raised above the tank and the flounder and squid were allowed to interact. Each trial ran for 10 min before surviving squid were removed. Four different conditions were tested: 1) light non-ablated, 2) light ablated, 3) dark non-ablated, and 4) dark ablated. Separate squid (N=10) were tested in each treatment condition. All interactions were recorded *ad libitum* by a single observer. Interactions used for subsequent statistical analysis were defined as: (1) successful predator strikes, (2) unsuccessful predator strikes, and (3) approaches where a strike

was not initiated because of an escape response by the squid.

Statistical analysis

Statistical analysis was performed in SPSS (v. 18 SPSS Inc., Chicago, IL, USA). The proportion of interactions survived for each squid was calculated to show success relative to the number of capture attempts. Since this measure does not reveal the total number of interactions survived, the sum of interactions survived for each squid in each treatment group was also calculated. All data were tested for normality using Shapiro-Wilk tests. Data from several groups varied from normality (all $p \leq 0.02$), and therefore all data were transformed prior to parametric analysis. A regression was performed on the total number of interactions survived and the mantle length of the squid in each condition to determine the relationship between size and survivability. No significance was found (all $p \geq 0.10$), and thus all sizes were pooled for further analysis. Analysis of variance (ANOVA) was performed on the total number of interactions survived and the proportion of interactions survived in each treatment group. Means and standard deviations are presented unless otherwise noted.

RESULTS

Successful predator evasion differed among the four treatment conditions (Table 1). The proportion of interactions survived significantly differed across treatment groups ($F_{3,36}=6.16$, $p=0.002$; Fig.2). Tukey post-hoc comparisons showed the light non-ablated group (mean=1±0.00) had higher proportion of interactions survived than the dark ablated group (mean=0.33±0.44), $p=0.001$). Additionally, the light ablated group (mean=0.78±0.34) showed higher survivability than the dark ablated group (mean=0.33±0.44, $p=0.046$).

Table 1: Descriptive information for each treatment group.

Treatment Condition		N	DML±S.E. (cm)	Total # Squid Survived	Total # Interactions Survived (pooled)	Range # Interactions Survived (per squid)
Light	Non-ablated	10	4.2 ± 0.3	10	60	4-11
	Ablated	10	3.9 ± 0.3	6	34	0-5
Dark	Non-ablated	10	3.9 ± 0.4	5	22	0-4
	Ablated	10	3.9 ± 0.3	2	15	0-4
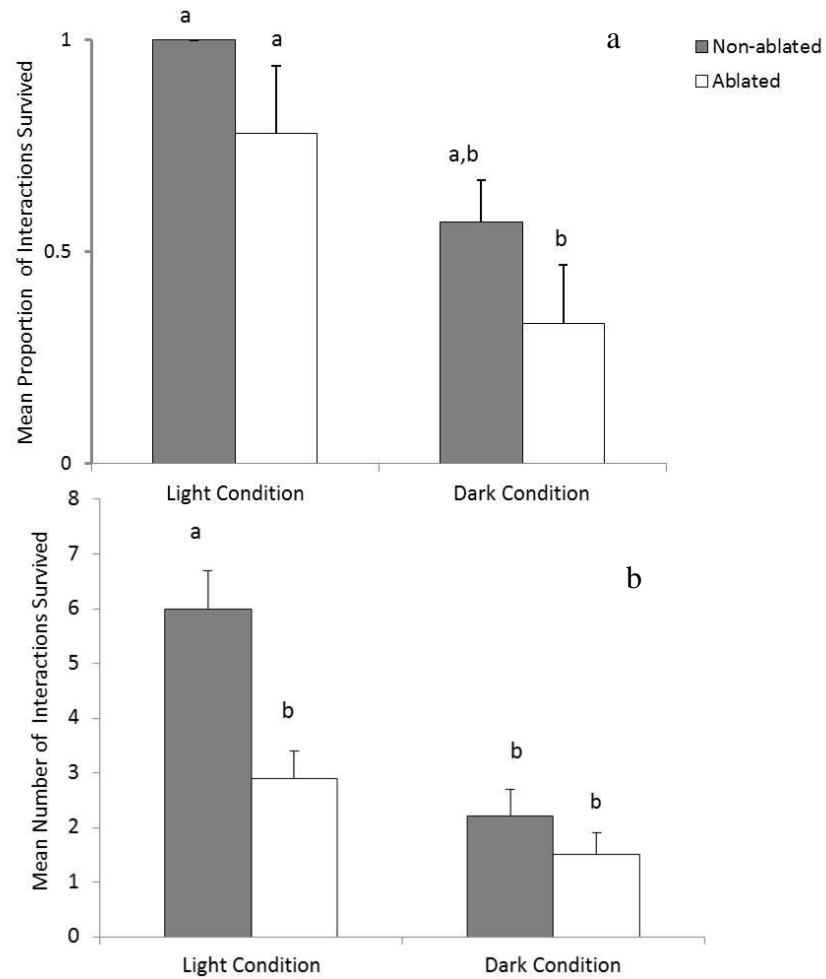
Figure 2. Survivorship for non-ablated and ablated squid during light and dark conditions. Mean proportion of interactions survived in each treatment group (a) and mean number of interactions survived (b) in each treatment group. Bars with different letters are significantly different. Mean ± s.e.m. are presented.

While not significant at α=0.05, the light non-ablated group, exhibited a trend in higher proportion of interactions survived, relative to the dark non-ablated group (mean=0.5±0.50, p=0.056). The mean number of interactions survived differed significantly across treatment groups ($F_{3,36}$=8.69, p<0.001). Tukey post-hoc comparisons of the four groups indicate that the light non-ablated group (mean=6.00±2.20) had significantly higher mean number of interactions survived than the light ablated group (mean=2.90±1.52, p=0.031), the dark non-ablated group (mean=2.20±1.62, p=0.002) and the dark ablated group (mean=1.50±1.27 , p<0.001) (Fig. 2).

DISCUSSION

The results of this study indicate that both vision and the lateral line analogue provide sensory information for successful predator evasion. The light non-ablated group survived a higher number of interactions than the light ablated and dark treatment groups, indicating the importance of both sensory systems. The observed higher proportion of interactions survived for the light non-ablated group relative to the dark ablated group, and the trend in higher proportion of interactions survived for the light non-ablated versus the dark non-ablated group demonstrate that vision is the most important modality (of the two tested here) for predator avoidance. The higher mean proportion of interactions survived in the light ablated than dark ablated group provides further support for this conclusion. Increased number of interactions survived, in the light non-ablated than the light ablated group, however, suggests that the lateral line analogue also plays a role in predator evasion even when vision can be utilized. Although the dark non-ablated and dark-ablated groups were not significantly different, there was a 30% decline in the total number of animals that survived when the lateral line analogue was ablated indicating that

having the sensory hair cells intact aided survival in dark conditions as well.

This study provides, to our knowledge, the first examination of the role of the lateral line analogue in cephalopods for predator avoidance. The lateral line analogue appears to play a similar role to the fish lateral line, serving as a sensory component to predator evasion (McHenry et al., 2009; Stewart et al., 2013). Although vision and the lateral line analogue clearly contribute to survival, there are other sensory modalities that could potentially add to successful predator evasion. Olfactory cues were likely present and could have alerted the squid to the predator's presence. Additionally, mechanoreceptors within the muscle or on the fins could have detected a pressure wave created by an approaching predator. It is possible that several sensory components not tested here contribute to successful predator avoidance; therefore further research is needed to examine other potential sensory modalities involved in predator detection and evasion in cephalopods. This study, however, demonstrates for the first time that mechanoreceptor ablation techniques can be performed successfully on cephalopods and the lateral line analogue, together with the visual system, is important for predator detection and survival.

CHAPTER 3

MULTIPLE SENSORY MODALITIES USED BY SQUID IN SUCCESSFUL

PREDATOR EVASION THROUGHOUT ONTOGENY

INTRODUCTION

Hydrodynamic stimuli provides important information for aquatic animals, and consequently most taxa have developed a sensory system for the detection of water movements and pressure fluctuations (Bleckmann, 1994; Coombs et al., 1989b). Over the past two decades, many studies have brought to light the functional significance of the fish lateral line, a system of hair cells that detects animal flows/pressure fields (Bleckmann, 1994; Bleckmann and Zelick, 2009; Coombs et al., 1989a; Coombs et al., 1989b; Engelmann et al., 2000; Montgomery et al., 1995). The role of the lateral line in fish predator-prey interactions has been investigated using lateral line ablation techniques, whereby the escape response rapidly diminishes with ablation, but returns with hair cell regeneration (Feitl et al., 2010; McHenry et al., 2009; Stewart et al., 2013). In fish, the C-start escape response is initiated when neuromasts comprising the lateral line are stimulated by pressure gradients generated by an oncoming predator (McHenry et al., 2009; Wainwright et al., 2007). Larval zebrafish (*Danio rerio*) react swiftly (within 30 ms) to the flow field produced by an attacking predator via a C-start escape response that quickly moves the fish out of the predator's path (Hale, 1999; McHenry et al., 2009).

While the vertebrate lateral line systems have been well studied, hydrodynamic receptor systems are also commonly used among invertebrates for predator evasion. In fact, the ability to detect fluid motion is found throughout many aquatic invertebrate groups from protozoans to lower chordates (Coombs et al., 1989b). For example, copepods are capable of sensing flow

using setae along the first antenna, which can alert them to an oncoming predator (Fields and

Yen, 2002; Heuch et al., 2007; Viitasalo et al., 1998; Visser, 2001; Yen et al., 1992). The setae

extend into the surrounding fluid environment, allowing copepods to detect predator flows

within a three-dimensional volume surrounding the copepod body (Browman et al., 2011; Doall

et al., 2002). Another invertebrate example are tunicates, which also have specialized sensory

receptor cells along their tentacles that sense hydrodynamic cues from predators (Burighel et al.,

2003).

Like fishes and the invertebrates described above, cephalopods also have flow sensing

structures. Squid and cuttlefish have epidermal hairs along their head and arms that resemble the

lateral line system of fishes (Bleckmann et al., 1991; Budelmann, 1994; Budelmann, 1996;

Budelmann and Bleckmann, 1988; Sundermann, 1983). This lateral line analogue is not as well

described as the fish lateral line system. It consists of polarized epidermal hair cells that have

several kinocilia and an axon extending from their base (Budelmann and Bleckmann, 1988).

Polarization occurs in a precise pattern (e.g., anteriorly, posteriorly, left and right), allowing the

animals to detect water movements as low as 18.8 µm/s, which is equivalent to the sensitivity of

fish lateral lines (Bleckmann et al., 1991). Behavioural responses have been elicited in cuttlefish

(*Sepia officinalis*) by stimulating their lateral line analogue using a wide range of frequencies

(10-600 Hz) (Komak et al., 2005). In addition, York and Bartol (2014)(see Chapter 2)

demonstrated that ablation of the lateral line analogue leads to reduced survivability of juvenile

and adult squid (*Lolliguncula brevis*) when interacting with a predator.

One important advantage of squid in predator evasion is their reliance on multiple

sensory systems for detection of predators (Budelmann, 1996). In addition to the lateral line

analogue system, cephalopods have a highly evolved visual system, with prominent eyes and

dominant optic lobes useful for predator detection and initiation of escape responses (Budelmann, 1994; Budelmann, 1996; Young, 1962). Resembling the vertebrate eye, the cephalopod eye incorporates a large posterior chamber, lens, iris, retina, choroid, sclera and argenta (Budelmann, 1994). Additionally, a squid's visual acuity is approximately 5-10 minutes of arc (Muntz and Johnson, 1978), and recordings from the optic lobe have revealed that the fusion frequency, i.e. the number of flashes of light perceived per second, is between 20 and 60 Hz and intensity dependent (Bullock and Budelmann, 1991). Both of these values are comparable to measurements of the vertebrate eye (Budelmann, 1994). Used together, visual processing and flow sensing represent a powerful integrated mechanism for predator detection in cephalopods.

Many organisms live in distinct environments during different life stages of their development, requiring their sensory systems to change throughout ontogeny. While cephalopods do not experience a distinct metamorphosis, and therefore do not have true larva (squid hatchlings are called paralarvae) (Shea and Vecchione. 2010), hatchlings are nonetheless ecologically different from older life history stages (Robin et al., 2014; Shea and Vecchione, 2010; Young and Harman, 1988). Unlike juveniles and adults, which are capable of powerful long distance locomotion (Robin et al., 2014), paralarvae are planktonic and cover only short distances by active swimming, often moving through the water column in diel vertical migrations (Boyle and Boletzky, 1996; Robin et al., 2014). Moreover, although squid do not experience a distinct metamorphosis, paralarvae do indeed differ morphologically from older life stages, having a more rounded mantle, relatively smaller arms, a proportionally larger funnel, and rudimentary fins (Boletzky, 1974; Okutani, 1987; Packard, 1969). Important physiological changes also occurs throughout ontogeny, with paralarvae having greater proportions of surface

mitochondria rich (SMR) mantle fibers (Preuss et al. 1997), shorter thick myofilament lengths (Thompson and Kier, 2006; Thompson et al. 2010), and less coordination of giant and non-giant motor systems (Preuss and Gilly, 2000) relative to adults. Additionally, the brain volume of squids increases exponentially with age and different regions of the brain develop at distinct points through ontogeny (Kobayashi et al., 2013).

Squids undergo morphological, physiological and ecological changes throughout ontogeny (Boyle and Boletzky, 1996), and therefore may perceive predators differently at various life stages, as is the case with certain fishes and invertebrates. Because herring larvae (*Clupea harengus*) lack canal neuromasts during early ontogenetic stages, they have reduced responsiveness to predator attacks, but increase their wake sensing capabilities with size as the lateral line canal system develops (Blaxter and Fuiman, 1990). Squids do not appear to have a canal neuromast system, but they still may exhibit important differences in hair cell sensitivity with ontogeny given differences in ecology, morphology, and physiology with life stage. Additionally, the visual capabilities of alewife (*Alosa pseudoharengus*), yellow perch (*Perca flavescens*) and bloaters (*Coregonus hoyi*) improve throughout ontogeny, and these changes may lead to improvements in predator avoidance due to the increased ability to detect potential predators (Miller et al., 1993). Crustaceans also undergo considerable reorganization of their visual systems throughout ontogeny, where larvae have eyes that are structurally suited for orientation and vertical migration, whereas adults are capable of more elaborate visual tasks such as navigation, prey recognition and capture, mate selection and communication (Cronin and Jinks, 2001). Given the variation of sensory capabilities seen in other taxa, it is likely that differences in ecology, morphology, and physiology of squid throughout ontogeny translate to differences in their abilities to perceive an oncoming predator. No information is currently

available on the role of vision and the lateral line analogue in predator evasion throughout multiple life history stages of squid.

While it has been shown that the lateral line analogue plays a role in successful predator detection in juvenile and adult squid (see Chapter 2), the kinematics of predator-prey interactions have not been examined for squid under different light conditions and levels of lateral line analogue ablation. Additionally, the relative roles of the lateral line analogue and vision throughout ontogeny have not been explored in any cephalopod. Therefore, this study addresses two primary questions: 1) are epidermal hairs and vision both important for successful predator evasion in squid throughout ontogeny, and 2) do orientation angles, swimming velocities, accelerations, and response times change throughout ontogeny when visual cues and the lateral line analogue are modified.

MATERIALS AND METHODS

Animal collection and maintenance

This project was conducted in accordance with Old Dominion University's Institutional Animal Care and Use Committee (Protocol #12-016). Paralarval *Doryteuthis pealeii* (dorsal mantle length (DML) = 0.18 cm) and juvenile and adult *Lolliguncula brevis* (DML=3.0-7.0 cm) were used for this research. Despite their abundance in the Chesapeake Bay, coastal Atlantic, and Gulf of Mexico as juveniles and adults, *L. brevis* egg mops are extremely difficult to locate and obtain. Therefore, *D. pealeii* was selected to study early ontogenetic stages. *D. pealeii* is a reasonable substitute for *L. brevis* because both species have similar body size, fin size and shape, and ecological niches as paralarvae (Bartol et al., 2008).

D. pealeii paralarvae were purchased from the Marine Biological Laboratory, Woods Hole, MA, and maintained in buckets with drilled 5 cm diameter holes covered by mesh (for water circulation). The buckets were suspended in a larger 450-gallon recirculating seawater system at a salinity of 30-32‰ and at temperatures of 19-24°C until hatching. Upon hatching, paralarvae were separated to track their age. Squid *L. brevis* used in this project were captured by otter trawl in Wachapreague, VA, USA. Trawls were conducted in August, September and October as the catch probabilities are highest in these months (Bartol et al., 2002). After capture, squid were transferred to a 114 L, circular holding tank (Angler Livewells, Aquatic Eco-Systems, Inc., Apopka, FL, USA) fitted with a portable battery powered aerator (Model B-3, Marine Metal Products Co., Inc., Clearwater, FL, USA) for transport to the lab. Squid were then placed in 450-gallon seawater systems configured with several forms of filtration (e.g., BioBalls, protein skimmers, ozone filtration, etc.), where they were maintained until the experiments were performed. Seawater was maintained at temperatures and salinities equivalent to those of the capture sites (19-22 °C; 30-35 ‰). A moderate current flow was maintained to promote active swimming and squid were fed a diet of live *Palaemonetes pugio* and *Fundulus heteroclitos* as suggested by Hanlon et al. (Hanlon, 1990; Hanlon et al., 1983). Squid were allowed to acclimate for at least 2 h prior to experimental trials. Only those animals that appeared healthy and exhibited normal behaviours were used. In total, 80 paralarval squid and 40 juvenile and adult squid were selected for this study.

Two summer flounder (*Paralichthys denatus*) (13.2 cm and 15.5 cm body length (BL)) and mummichogs (*Fundulus heteroclitus*) (1.3 cm and 1.5 cm BL) were purchased from the Marine Biological Laboratory, Woods Hole, MA, and maintained in a recirculating seawater system at salinities of 30-32‰. The flounder and mummichogs were fed live squid (*L.brevis* and

D. pealeii, respectively) for one week prior to experimental trials so that they could become proficient in squid capture before data collection. Although we are using different fish species for the paralarvae and juvenile/adult trials, the species chosen reflect predators that the squid often encounter in each ontogenetic phase in the waters of the mid-Atlantic region, with the goal of documenting behaviors that reflect natural conditions.

Predator-prey experiments

Predator-prey interaction experiments were used to evaluate the importance of vision and the lateral line analogue in predator evasion. Lateral line ablation was accomplished with a 500 µm neomycin solution, which is commonly used in ablation studies in fish (Harris et al., 2003) and which has been validated as an effective technique in squid (see Chapter 2). One hour prior to trial acclimation, squid were placed in a container that either held the neomycin sulphate solution for ablation groups or untreated seawater for the non-ablation groups. Four different conditions were tested: 1) light non-ablated, where the trials were held in bright light conditions with squid having intact hair cells; 2) light ablated, where the trials were held in bright light conditions with squid having ablated hair cells; 3) dark non-ablated, where the trials were held in dark conditions with squid having intact hair cells; and 4) dark ablated, where the trials were held in dark conditions with squid having ablated hair cells.

Paralarvae trials were conducted in a 10x10 x10 cm clear acrylic tank. Two DALSA Falcon video cameras (DALSA Corp., Waterloo, ON, Canada; 1400 x 1024 pixel resolution, 100 frames per second) outfitted with a 25 mm lens (FOV=2.7x3.7 cm) were positioned above the arena for a dorsal view, and another DALSA Falcon outfitted with a 25 mm lens was positioned beside the tank for a lateral view. A 500-watt halogen light provided illumination for the light

experimental trials. An IR56 infrared light (C&M Vision Technologies Inc., Houston, TX, USA) was used to illuminate the working section during the dark trials. Video frames from the cameras were stored in real time on hard disk using a CLSAS capture card (IO Industries, London, ON, Canada) and Streams 5 software (IO Industries, London, ON, Canada). For each experiment, 5-10 paralarvae were placed in the arena with two small mummichogs (*Fundulus heteroclitus*). Food was withheld from the mummichogs 24 h prior to the start of all trials. Multiple predators were used to increase the frequency of predation events. At the beginning of each trial, the squid were placed in the arena for a 30 min acclimation period. After the acclimation period, the fish were added and the experiments commenced. Each trial lasted 10 minutes, after which the fish were removed and surviving paralarvae were returned to their holding tank.

The experimental set-up for the adult and juvenile trials is described in York and Bartol (2014) (see Chapter 2) and briefly repeated here for convenience. Trials took place in a 1.2 m diameter x 0.76 m deep round tank with a crushed coral substrate. The arena was lined with curtains to avoid disturbing acclimating animals. A UNIQ UP-685 CL high-speed color camera (Uniq Vision; 659 x 494 pixel resolution, 110 frames per second) outfitted with a 5 mm lens (FOV = 130 cm x 170 cm) was suspended from scaffolding over the tank. Video frames from the cameras were stored in real time on hard disk using a CL160 capture cards (IO Industries, London, ON, Canada) and Video Savant 4.0 software (IO Industries, London, ON, Canada). Four 500-watt halogen lights provided illumination for the light experimental trials. Infrared lighting was used for dark treatments; however, the lighting did not provide sufficient lighting for detailed kinematic measurements (see below).

For each juvenile and adult experiment, a 40 cm diameter cylinder made of 5 mm plastic mesh was lowered into the experimental tank containing two summer flounder *Paralichthys*

denatus, and a single squid was placed inside the mesh cylinder for a 30 min acclimation period. The trials commenced when the cylinder partition was raised above the tank, and the flounder and squid were allowed to interact. Each trial ran for 10 min; after this time any surviving squid were removed. Multiple predators again were used to increase the odds of a predation event, and as was the case for paralarval trials, food was withheld from the predators 24 h prior to the start of all trials. Ten separate squid were tested in each of the four treatment conditions. Each group contained squid of similar sizes (mean ± s.d: light non-ablated = 4.2±0.3 cm DML; light ablated= 3.9±0.3 cm DML; dark non-ablated= 3.9 ±0.4 cm DML; dark ablated= 3.9±0.3 cm DML).

Frame-by-frame position tracking of the squid body features was accomplished using image tracking software (Hedrick, 2008). Infrared lighting used during the dark trials for juveniles and adults did not provide sufficient lighting to capture detailed kinematic measurements and were therefore excluded from analysis. In juveniles and adults, eight points were tracked: (1) mouth of fish, (2) middle of the fish body, (3) tail of squid, (4) eye of squid, (5) tip of the squid mantle, (6) tip of squid arms, (7) leading edge of ink, and (8) trailing edge of ink. In paralarvae, four points were tracked in both dorsal and lateral views: (1) mouth of fish, (2) middle of the fish body, (3) tip of the squid mantle, and (4) eye of squid. The tracked points were used to determine (1) distance between the predator and prey at the initiation of escape response, (2) the minimum distance between predator and prey, (3) the velocity of the squid at the beginning of the interaction, (4) the maximum and mean velocity of the predator and prey during the encounter, (5) the time the prey reached maximum velocity after initial predator recognition, (6) the maximum acceleration of the predator and prey, (7) time when maximum acceleration was reached and (8) distance between predator and prey at point of maximum

acceleration. These parameters were calculated using Matlab routines developed in-house. The routine performed a low pass filter of the data using a cutoff frequency between 10-20 Hz and a 2nd order Butterworth filter. The double filter operation increases the effective order of filtering to the 4th order.

The angular orientation of squid relative to the approaching predator (θ) and the angular orientation of the squid escape trajectory (ϕ) were measured at the initiation of the predator's attack and over several frames of the escape response, respectively (Fig. 3A). θ was the angle between the squid's longitudinal axis and the line connecting the tip of the predator rostrum to the squid's center of mass, whereas ϕ was the angle between the line connecting the tip of the predator rostrum to the prey's center of mass and the path of the escape over multiple frames. Predator-squid distance (d) was measured from the predator's rostrum to the closest component of the squid. Interactions were divided into four groups of angular orientations for both θ and ϕ: (1) < 45°, (2) 46°-90°, (3) 91°-135°, (4) 136°-180°. These groupings were useful in determining whether the predator approached the squid from an anterior, lateral or posterior direction, as well as for determining the direction of the squid escape trajectory (Fig. 3B).

Statistical analysis

Statistical analysis including t-tests, ANOVAs and MANOVAs were performed in SPSS (v. 18 SPSS Inc., Chicago, IL, USA). The proportion of escape responses and interactions survived for each squid was calculated to show success relative to the number of capture attempts. All data were tested for normality using Shapiro-Wilk tests. Data from several groups varied from normality (all $p \leq 0.02$), and therefore all data were transformed via arcsine transformation prior to parametric analysis. A regression was performed on the total
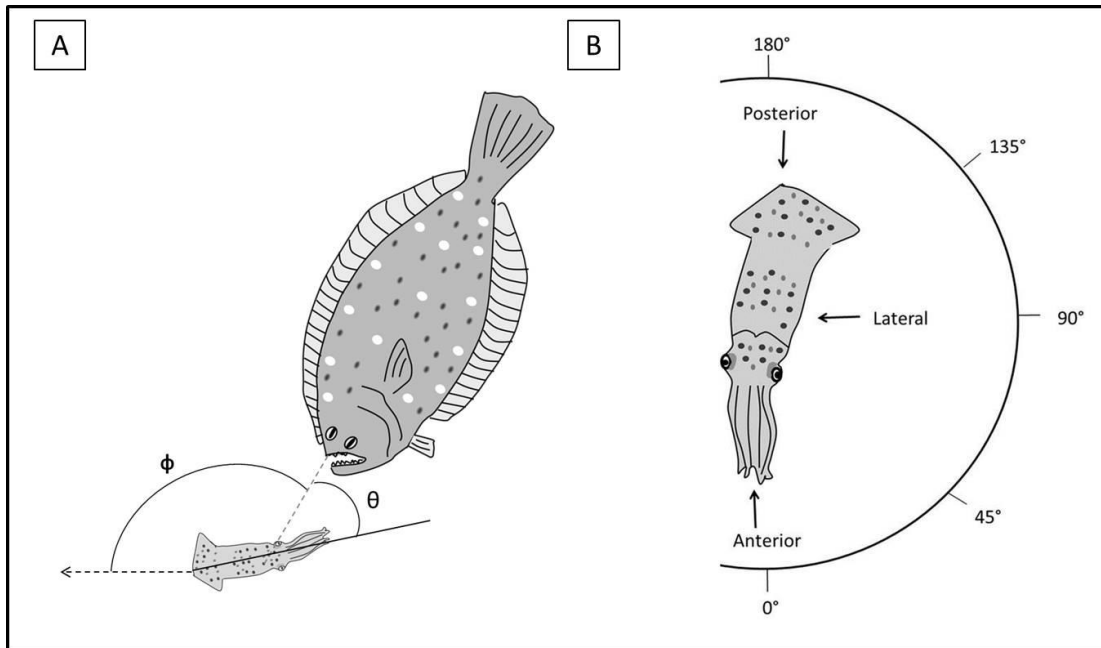
Figure 3. Angular orientation of squid during interactions with predator. A) The angular orientation of squid to approaching predator (θ) was the angle between the squid's longitudinal axis (solid black line extending from squid) and the line connecting the tip of the predator's upper rostrum to the squid's center of mass (dashed grey line). The angular orientation of the squid escape jet (φ) was the angle between the line connecting the tip of the predator's upper rostrum to the prey's center of mass and the path of the escape over multiple frames (dashed arrow extending from squid). B) Diagram of squid orientations. Interactions were divided into four groups of angular orientations for both φ and θ: 1) < 45°, (2) 46°-90°, (3) 91°-135°, (4) 136°-180°.

number of interactions survived and the mantle length of the juvenile and adult squid in each

condition to determine the relationship between size and survivability, and no significance was

found (all p≥0.10). Additionally, kinematic measurements were compared between juveniles and

adults with no significant differences found (all p≥0.05), and thus all juvenile and adult squid

were pooled into one ontogenetic group for further analysis. Paralarvae, which had consistent

dorsal mantle lengths of 0.18 cm, were considered a second ontogenetic group.

As there were often multiple predator-prey encounters per trial, kinematic parameters

were compared between multiple encounters to access differences as the trial progressed;

however, no significant differences were found in any of the kinematic parameters tested

(ANOVA: all p>0.05). Therefore, measurements from multiple encounters were averaged per

individual for further comparison between treatment groups. Analysis of variance was used to

compare survival and escape between treatment groups through ontogeny. Multivariate analysis

of variance (MANOVA) was used to compare kinematic variables in squid among treatment and

ontogenetic groups.

RESULTS

Paralarval and Juvenile/Adult Escape and Survival

Overall success in predator-prey interactions differed significantly among treatment

groups within paralarvae ($F_{6,152}$ = 3.205, p=0.005,Wilk's $_\Delta$ = 0.788, η^2=0.112). Significant

differences were found among the mean proportion of paralarvae that initiated an escape

response within each treatment group ($F_{3,77}$=5.08, p=0.003; Fig.4A). Tukey post-hoc tests

revealed that both the light, non-ablated paralarval group (mean proportion for escape=

0.68±0.47) and the dark non-ablated paralarval group (mean proportion escape= 0.76±0.44) had

a higher proportion of escape responses than the dark ablated paralarval group (mean proportion escape= 0.29±0.46). Additionally, the light, ablated paralarval group (mean proportion escape= 0.33±0.48) had a significantly lower proportion of escape responses than the dark, non-ablated condition (mean proportion escape= 0.76±0.44). Although not statistically significant at α=0.05, light ablated paralarvae exhibited a trend in lower proportion of escape responses (0.33±0.48) than the light non-ablated paralarvae (p=0.08). The number of paralarvae that survived interactions with the predator also significantly differed according to treatment groups ($F_{3,77}$=2.78, p=0.04: Fig. 4B), with greater survival being detected for both light treatment groups and the dark, non-ablated group relative to the dark ablated group (mean proportion survival= 0.06±0.25).

When paralarval data are compared with juvenile and adult data reported in Chapter 2 significant differences were found between the two groups in the proportion of escape responses and the proportion of squid that survived in each treatment group. Juveniles and adults were more likely to initiate an escape response than paralarvae in all four treatment groups (all p<0.05; Fig 4A). Juveniles and adults also had significantly greater survival than paralarvae in all treatments (all p<0.05; Fig. 4B).

Paralarvae Kinematics

The mean velocity, maximum velocity and maximum acceleration of the predator did not significantly vary among the four treatment groups (MANOVA: $F_{9,151}$ = 1.28, p=0.251, Wilk's $_\Delta$ = 0.836, η^2=0.058), indicating that the fish behaved similarly throughout the paralarvae trials irrespective of treatment level. No differences in the escape kinematics of paralarvae were found among the four treatment conditions (MANOVA: $F_{15,166}$ = 0.973, p=0.485, Wilk's $_\Delta$ = 0.792,
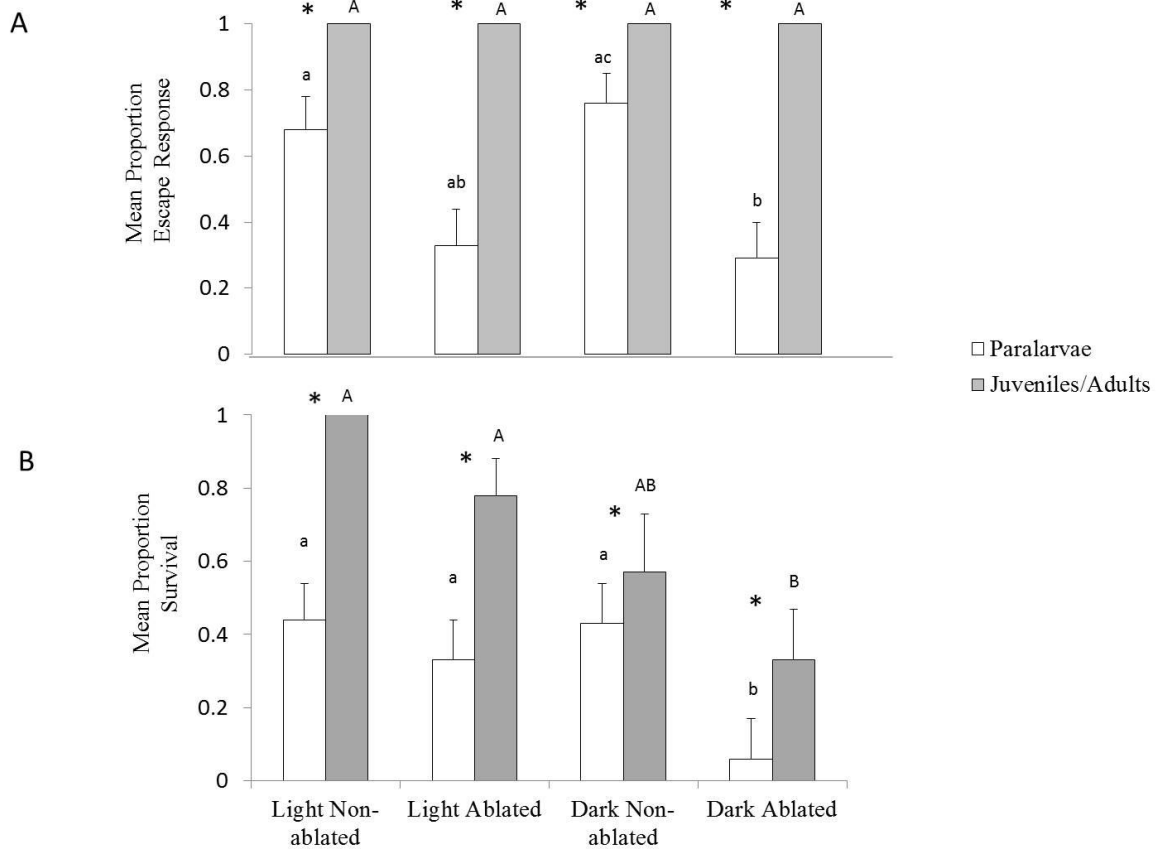
Figure 4. Mean proportion of escape responses (A) and surviving individuals (B) for paralarval and juvenile/adult squid. Non-ablated and ablated squid in light and dark conditions are shown. Lower case letters indicate significant differences among paralarvae treatment conditions and upper case letters indicate differences among juvenile/adult treatment groups. Bars with the same letters are not significantly different (Tukey *post hoc* comparison tests). Significant differences between paralarvae and juvenile/adults in each treatment group are indicated with asterisks. Non-transformed means and s.e.m. are presented. Juvenile/adult data derive from Chapter 2.

$\eta^2=0.075$). Indeed, neither the mean nor maximum velocity of the paralarval squid differed among treatment groups (mean velocity: $F_{3,64}= 0.89$, p=0.45; maximum velocity: $F_{3,64}=0.60$, p=0.62)(Fig. 5A, 5B). Additionally, no differences were found in the time to reach maximum velocity ($F_{3,64}=0.89$, p=0.45)(Fig. 5D) or maximum acceleration of the paralarval squid ($F_{3,64}=2.49$, p=0.07)(Fig. 5C). Furthermore, the distance between the predator and prey at the initiation of the escape response, minimum distance between predator and prey, and the velocity of the squid at the beginning of the interaction were not found to be significantly different among treatment groups (all p>0.05). No significant correlation was detected between the mean velocity of the approaching predator and the escape response of the squid within all treatment groups (all p>0.05).

Throughout all of the treatment groups, the angular orientation of the squid to the approaching predator (θ) was 0°-90°. Within this narrow angular range, there were some significant differences in θ among the treatment groups ($F_{3,62}=3.34$, p=0.025; Fig.6A,C). In particular, squid in the light, ablated group oriented themselves at lower angles (mean= 26.08±17.14°) than the dark, non-ablated group (mean=55.55±24.41°; p=0.01). The mean angle of the squid's escape trajectory (ϕ) did not differ by treatment group ($F_{3,62}=0.12$, p=0.94; Fig. 6B,D), with all mean angles falling between 90 and 180°. Inking behavior was not observed among the paralarval squid.

Juvenile and Adult Kinematics

As mentioned earlier, interactions in the dark conditions involving juveniles and adults were not recorded with high resolution due to insufficient lighting and were therefore excluded from kinematic analysis. The mean velocity, maximum velocity and maximum acceleration of
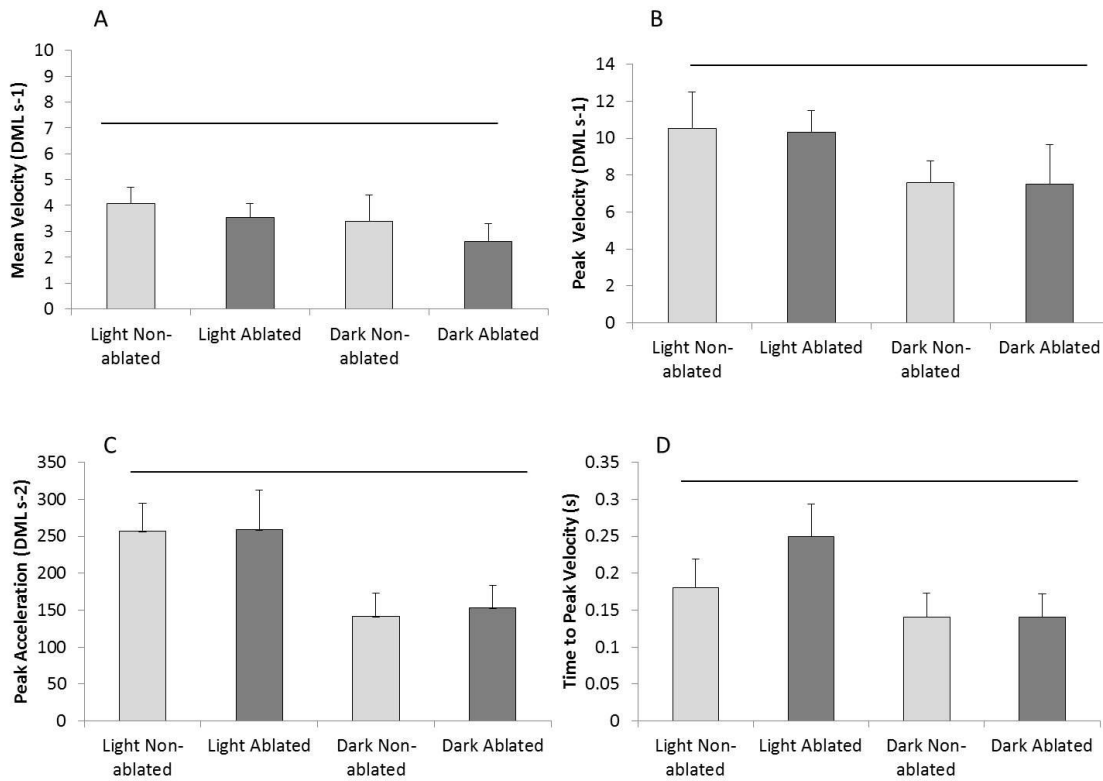
Figure 5. Kinematics of the paralarval escape responses. A) The mean velocity of the paralarval escape response in each treatment group. B) The peak velocity of the escape response. C) The peak acceleration of the escape response. D) The time to peak velocity in each treatment group. Non-transformed means and s.e.m. are presented. No differences were found among the treatment groups as indicated by horizontal bars.

Figure 6. Angular orientation of the squid to the predator (θ) (A, C) and paralarval escape trajectories (ϕ) during predator encounters (B, D). A and B represent light conditions, whereas C and D represent dark conditions. The grey color represents the non-ablated treatment group and the black represents the ablated treatment group. Each sectional increment in the diagrams represents two squid.

the predator did not significantly differ between light ablated and light non-ablated treatments ($F_{3,16}$ = 1.06, p=0.393, Wilk's $_\Delta$ = 0.83, η^2=0.166), indicating that the fish behaved similarly throughout the trials. Conversely, significant differences in squid kinematics were found throughout the treatment groups ($F_{8,11}$ = 4.13, p=0.005, Wilk's $_\Delta$ = 0.25, η^2=0.75). The mean velocity of the squid's escape response was significantly higher in non-ablated than ablated light conditions ($F_{1,19}$ =8.98, p=0.008, non-ablated= 29.20±17.2 DML s^{-1}, ablated= 10.4±9.73 DML s^{-1}) (Fig. 7A). Additionally, significant differences were found between the maximum velocity of the squid in the light non-ablated and ablated groups ($F_{1,19}$ =5.84, p=0.002) with the non-ablated group having significantly higher peak velocities (65.29±28.78 DML s^{-1}) than the ablated group (27.08±18.78 DML s^{-1})(Fig. 7B). The time for squid to reach maximum velocity also differed between treatment groups ($F_{1,19}$ =10.35, p=0.005), with the ablated group taking significantly longer to respond than the non-ablated group (non-ablated= 0.49±0.35 s, ablated= 0.93±0.26 s; Fig.7D). The maximum acceleration reached by the squid also differed according to treatment group ($F_{1,19}$ =5.84, p=0.026), with the ablated group only reaching half of the acceleration of the non-ablated group (non-ablated= 437.16±249.31 DML s^{-2} ablated= 210.04±161.7 DML s^{-2})(Fig. 7C).

The squid in both treatment groups actively oriented between 0° and 90° during all predator interactions; however the ablated group had a significantly higher mean angle towards the predator (θ) than the non-ablated group ($F_{1,19}$=2.92, p=0.01; non-ablated= 38.5±11.86°; ablated= 69.00±30.94°; Fig.8). The mean angle of escape trajectories (ϕ) did not differ between non-ablated and ablated groups $F_{1,19}$=0.93, p=0.37; non-ablated= 148±5.47°, ablated= 144±11.94°; Fig. 8). Interestingly, the ablated group demonstrated a lower proportion of inking
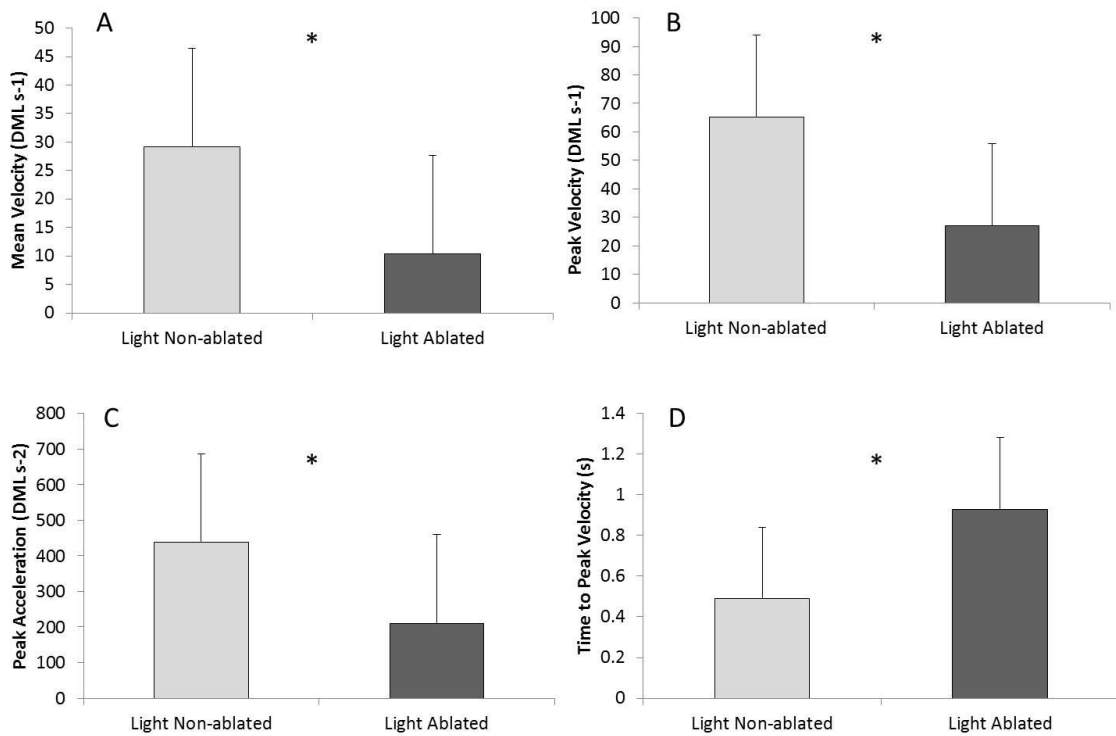
Figure 7. Kinematics of the juvenile and adult escape responses. A) The mean velocity (DML s^{-1}) of the escape response in each treatment group. B) The peak velocity (DML s^{-1}) of the escape response. C) The peak acceleration (DML s^{-2}) of the escape response. D) The time to peak velocity (s) in each treatment group. Non-transformed means and s.e.m. are presented. Asterisks denote significant differences.
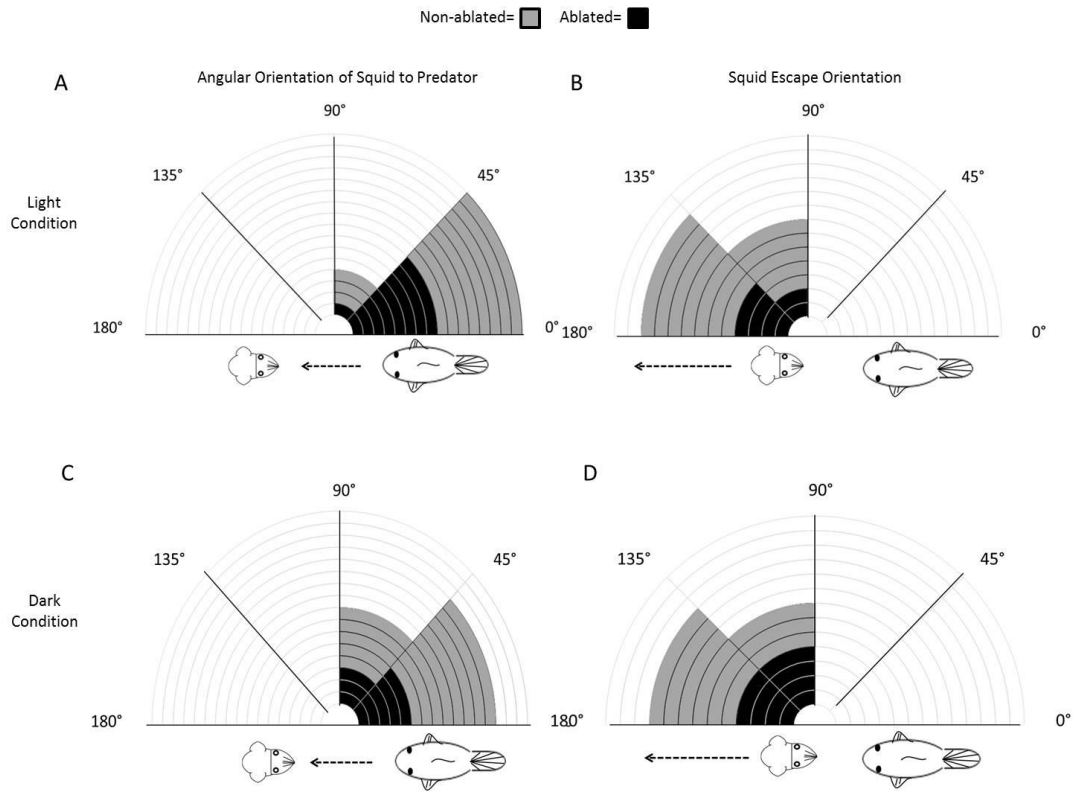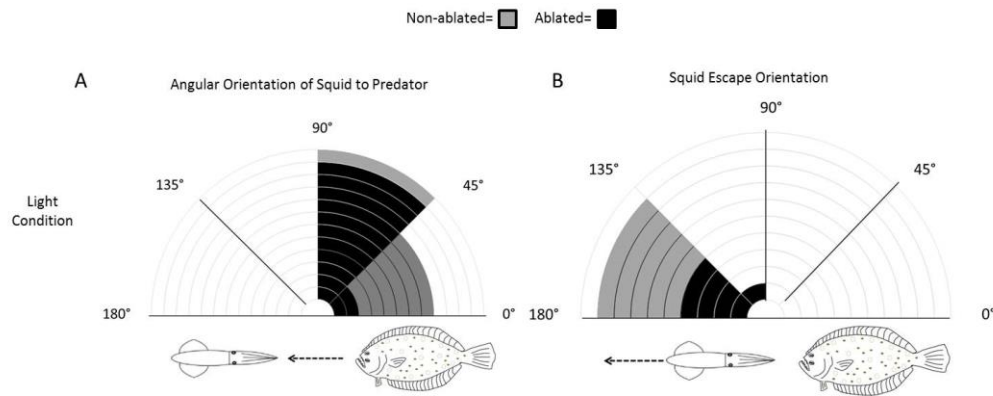
Figure 8. Angular orientation of the squid to the predator (θ)(A) and juvenile and adult squid escape trajectories (φ) during predator encounters (B) under lighted conditions. The grey color represents the non-ablated treatment group and the black represents the ablated treatment group. Each sectional increment in the diagrams represents two squid.

events than the non-ablated group ($F_{1,19}$ =2.18, p=0.038, non-ablated= 0.52±0.35 proportion ink events, ablated= 0.22±0.22 proportion ink events).

When inking was performed, both ablated and non-ablated groups inked at similar distances from the predator (t_7=0.19, p=0.90; non-ablated= 2.65±1.11 DML, ablated= 2.41±2.96 DML). Other kinematic parameters (distance between the predator and prey at the initiation of escape response, minimum distance between predator and prey, the velocity of the squid at the beginning of the interaction) were not significantly different between treatment groups (all p>0.05). Additionally, no significant correlation was detected between the mean velocity of the approaching predator and the escape response of the squid within either treatment group (all p>0.05).

DISCUSSION

The findings of this study demonstrate for the first time that both vision and the lateral line analogue provide sensory information for initiation of an escape response and successful predator evasion in squid throughout ontogeny. Cephalopod vision has been viewed as the dominant sensory modality used in predator detection due to the well-developed complex nature of cephalopod eyes (Budelmann, 1994; Budelmann, 1996). Cephalopods have a wide visual field that can extend over 360° in the horizontal plane, allowing them to detect predators within an extensive sensory sphere (Cronin, 2005; Messenger, 1968). Despite the highly advanced visual system, there are many situations where visual cues are reduced and/or unreliable, such as in turbid waters, at night, in complex environments where visual indicators are overwhelming, or in cases where predators are well camouflaged (Budelmann, 1994; Budelmann, 1996). Under these conditions, cephalopods can benefit from other sensory systems, such as the lateral line

analogue, which is sufficiently sensitive to detect a swimming 1-meter fish at a distance of about 30 meters away, even when vision is disabled (Budelmann, 1994).

The use of the lateral line analogue was evident in paralarval squid where significantly different escape responses were observed among the four treatment groups. In both the light and dark conditions, the non-ablated groups showed a higher proportion of escape responses than the dark ablated group. A clear trend in higher proportion of escape responses for light non-ablated paralarvae versus light ablated paralarvae was also noted. Together these results indicate that the lateral line analogue plays a role in initiation of an escape response in paralarvae. Interestingly, there was no difference in the initiation of an escape response of the paralarvae in the light non-ablated and dark non-ablated conditions, as would be expected given the importance of the visual system in cephalopods. This unexpected finding may derive from reduced visual capabilities at early ontogenetic stages, though this topic has not been examined to date. If paralarvae do indeed have reduced visual capabilities during early ontogeny, the sensory function of the lateral line analogue may be relatively more important for paralarvae than older life stages, when the visual system is fully developed.

The lack of survival differences across the light ablated, light non-ablated and dark non-ablated treatments in paralarvae is likely due to swimming speed differences between the prey (squid) and predator (fish). The mean velocity of the predator (2.31 cm s^{-1}) was much higher than that of the paralarvae (0.75 cm s^{-1}), making successful escape difficult even when the lateral line analogue and visual systems were accessible. Interestingly, when both visual and lateral line sensing were removed (i.e., the dark ablated treatment), survival was lowest, indicating use of these two sensory modalities in concert is important for successful predator evasion for paralarvae. These results are consistent with previous studies on zebrafish, where zebrafish

larvae with intact lateral line systems are able to avoid many more attacks than larvae with ablated lateral line systems (Stewart 2013). As described in Chapter 2, light non-ablated adult/juvenile squid have a higher proportion of interactions survived (1.00±0.00) than dark ablated squid (0.33±0.44) and exhibit a trend in higher proportion of interactions survived than dark non-ablated squid (0.57±0.50). These results demonstrate that vision is an important modality for predator avoidance in addition to the lateral line analogue. The higher mean proportion of interactions survived in light ablated adults (0.78±0.34) than dark ablated adults (0.33±0.44) provides further support for this conclusion.

Significant differences were found in the proportion of escape responses and survival between the paralarvae and older squid throughout the treatment conditions. Overall, juveniles and adults performed more escape responses than paralarvae, which led to a significantly higher rate of survival for juveniles and adults in all treatment conditions. This result may reflect different anti-predator strategies of squid throughout ontogeny, whereby paralarvae use different approaches to compensate for an underdeveloped nervous system and life in a more viscous flow regime (Re paralarvae = $1\text{-}10^2$; Re juvenile and adults = $10^3\text{-}10^6$) (Chen et al., 1996; Bartol et al., 2009). In 32% of the predator-prey interactions, paralarvae did not change their behavior as a predator was approaching, other than orienting arms-first to the predator. The juveniles and adults, however, always responded to an approaching predator with an escape response, regardless of ablation treatment. Unlike juveniles and adults, paralarvae often rely on a repertoire of stereotyped behaviors, such as circling and spiraling in combination with a clear body pattern, to avoid predation over employing a directed escape response (see Chapter 4). This reliance on random, constant motion may be the paralarvae's best defense given presumed sensory limitations during early ontogeny and residence in a highly viscous flow field. Nonetheless,

reduction in the frequency of escape jetting likely produced the observed differences in escape responses and survival.

In juveniles and adults, the kinematics of the escape responses under lighted conditions (detailed kinematic analysis was not performed in dark conditions because of camera resolution issues) differed based on ablation conditions. The mean velocity of the juvenile and adult's escape response was significantly higher for non-ablated versus ablated squid, with the ablated group having mean velocities of 10.4 ± 9.73 DML s^{-1}, while the non-ablated group had mean velocities of 29.20 ± 17.2 DML s^{-1}. The peak velocity of the ablated group (27.08 ± 18.78 DML s^{-1}) was also significantly lower than the peak velocity of the non-ablated group (65.29 ± 28.78 DML s^{-1}). Additionally, the time for the squid to reach maximum velocity was almost half a second longer in the ablated versus non-ablated group, and the ablated group only reached approximately half of the peak acceleration of the non-ablated group. Collectively, these results strongly suggest that juveniles and adults use their lateral line analogue to sense the hydrodynamic signatures of oncoming prey, similar to zebrafish (*Danio rerio*), which detect the bow wave generated by an approaching predator using their lateral line system (Stewart et al., 2014). When flow sensing hairs are disabled through ablation, the squid reacts more slowly and with a lower velocity escape response than those with intact sensory hairs, thereby leading to reduced survivability. These results make sense given the sensitivity of the lateral line analogue to flow perturbations (Bleckmann et al. 1991) and its importance as an early warning system for predators.

Another potential reason for reduced survivability of ablated juvenile and adult squid is their lower frequency of inking events than non-ablated squid. Juvenile and adult squid in the non-ablated group inked in 52% of predator-prey interactions, whereas ablated squid inked in

only 22% of interactions. Previous studies have indicated that an inking event is one of the most important anti-predator behaviors for successful predator evasion with a > 50% increase in survival occurring in squid *Doryteuthis pealeii* when inking is used during attacks by fish versus when it is not (Staudinger et al., 2011). In addition to ink causing visual confusion during predator encounters, chemicals in the ink are also thought to block olfactory or taste receptors in predators, causing them to abandon their approach (Caldwell, 2005; Hanlon and Messenger, 1996). Thus, reduced inking in ablated squid likely played some role in reduced survivorship. Interestingly, unlike the juveniles and adults, the paralarval squid did not demonstrate any inking behavior and this may have contributed to lower survivorship in paralarvae. The reason for this is unclear as paralarval squid can produce ink. However, perhaps the lack of inking in paralarvae is a reflection of more restrictive use of this defense given the high energetic requirements of producing ink (Wood et al., 2008) coupled with the need to allocate high levels of energy toward development (Russo et al., 2003).

While the paralarvae did show differences in the proportion of escape jets employed across treatment groups, there were no differences in mean or peak swimming velocity, time to reach peak swimming velocity or acceleration across the treatment groups. The lack of observed kinematic differences may derive from an underdeveloped motor system at this ontogenetic stage. The squid mantle undergoes muscular changes throughout ontogeny, where the superficial, mitochondria rich (SMR) fibers are used for jetting as paralarvae, but central, mitochondria-poor (CMP) fibers increase in number and produce the power for an escape jet as juveniles and adults (Preuss et al., 1997a). To produce an escape jet, the squid nervous system is comprised of giant axons that generates a powerful all-or-none contraction of the circular muscle fibers of the mantle (Young, 1938), as well as parallel non-giant motor axons that can generate equally strong

contractions, but require repetitive firing (Gilly et al., 1996; Prosser and Young, 1937). During escape responses, juvenile and adult squid show two recruitment patterns for the giant axons where either (1) a stereotyped escape response is driven by a single giant axon spike, or (2) a more complex escape jet is produced by a synchronized recruitment of non-giant and giant motor neurons (Otis and Gilly, 1990). Paralarvae squid hatch with functional giant and non-giant motor systems (Marthy, 1987; Martin, 1965; Preuss et al., 1997a), but concerted recruitment of the two systems does not become fully established until several weeks post-hatching (Preuss and Gilly, 2000). The paralarvae examined in this study were 24-48 h post hatching. Therefore it is likely the paralarval escape responses were driven by the single giant motor neuron, whereas more complex and variable escape responses were demonstrated in the juveniles and adults through recruitment of non-giant axon activity. This is supported by observations that paralarvae responded with a similar kinematic jet response, regardless of predator approach, whereas juveniles and adults showed greater variation in the escape response (e.g., variation in velocity, time to peak velocity and acceleration), particularly in the ablated groups. Additionally, the basal lobe system of the brain, which is associated with the control of movements in cephalopods, increases in size exponentially throughout ontogeny (Kobayashi et al., 2013), which may also relate to control over the escape response in predator-prey interactions.

Throughout all of the predator-prey interactions, the squid actively oriented themselves at angles of 0° - 90° relative to the oncoming predator. While it is conceivable that this positioning is driven by a preference for the fish to attack the anterior portion of the prey, the squid in this study consistently kept their arms towards the predator once the threat was detected (typically at the beginning of the experimental trial). Thus the observed orientation angles most likely reflect a behavioral preference by the squid. This position is advantageous for hydrodynamic sensing

given the anterior position of the lateral line analogue along the arms and head of the animal. By positioning themselves anteriorly, the squid are able to detect hydrodynamic cues produced by the oncoming predator with the greatest population of hair cells. This is important as other studies on fish lateral line systems have revealed greatest escape success when fish prey are orientated with maximum hair cell exposure to the oncoming predator (Stewart et al., 2014). For example, zebrafish larvae escape oncoming predators most effectively when they are positioned laterally to the predator because this orientation exposes the maximum area of the fish lateral line (Coombs et al., 1989b; Stewart et al., 2014). Furthermore, previous studies have indicated fish that move much faster than an approaching predator should execute a fast start (i.e., C-start) at a right angle from the predator's heading to maximally increase their distance from the predator (Weihs and Webb, 1984), which was supported by Stewart et al. 2014. Squid do not produce body-derived C-starts for escape; they use an escape jet. When oriented anteriorly to a predator, squid can more readily perform a tail-first escape jet (the predominant orientation for escape responses) to maximally increase their distance from the predator. In the juveniles and adults, the ablated group positioned themselves at a higher angle to the predator than the non-ablated group, which indicates that without lateral line analogue sensory input, they are less capable of sensing the predator, particularly its bow wave, and unable to position themselves optimally for their escape response. The paralarvae in the light, ablated group, however, had lower angles than the dark, non-ablated group. This result suggests that vision may be important for optimal positioning for escape jetting. Nonetheless, optimal positioning does not necessarily guarantee an escape response, as significantly less escape responses were recorded in the light ablated group relative to the dark non-ablated group, indicating that the lateral line analogue input is crucial for successful escape at the paralarval stage

The escape response of squid is driven primarily by a rapid powerful jet, which propels the animal away from the predator. The flexible funnel can direct the jet at any angle within a hemisphere below the body (Ward and Wainwright, 1972) and the funnel can even alter the jet trajectory during an escape jet (Otis and Gilly, 1990). Based on geometric models, escaping with a trajectory of 180° corresponds to maximizing the distance from a predator approaching at a speed lower than that of the prey (Domenici, 2002; Domenici et al., 2011). Non-ablated juvenile and adult squid in this experiment performed escape jets at speeds as high as 256.70 cm s^{-1} (63.15 DML s^{-1}), whereas the predator only approached peak velocities of 86.51 cm s^{-1} (6.55 BL s^{-1}). Given this speed discrepancy, juvenile and adult escape trajectories close to 180° provide good spatial separation from the approaching predator. While squid *L. brevis* are highly maneuverable (Jastrebskey et al., *in press*), they maintained largely straight escape paths when responding to a predator. In juveniles and adults, 90% of all the squid examined performed an escape trajectory between 136-180°. Paralarvae, however, had more variable escape trajectories with 42% of escapes falling between 90-135° and only 58% between 136-180°. Unlike the juveniles and adults, the paralarvae did not achieve higher peak velocities than the predator, with the squid reaching only mean velocities of 0.75 cm s^{-1} (4.16 DML s^{-1}) while the fish reached 2.31 cm s^{-1} (1.53 BL s^{-1}). Given the inability of paralarvae to outswim the predator along a similar rectilinear path, it certainly seems reasonable that paralarvae would select other escape angles than 180° and even employ random, more unpredictable escape paths. Indeed, employing multiple swimming paths decreases the probability that predators will lock onto repeated escape behaviors and improves survivability (Domenici et al., 2011). Interestingly, survival of paralarvae with escape trajectories of 90-135° did not differ from those with trajectories of 136-180° across those treatment groups with survivorship exceeding 0%. These results support the

conclusion that unpredictable escape trajectories are advantageous during the paralarval life history stage.

Throughout ontogeny, squid are prey targets for many marine predators, including fish, marine mammals, sea birds, and even other cephalopods, making predator detection an extremely important aspect of survival to reproductive age (Clarke, 1996; Piatkowski et al., 2001). Additionally, squid undergo substantial morphological, ecological and physiological transitions as they develop from planktonic paralarvae to larger, more neurologically advanced adults. This is the first study to examine the use of multiple sensory modalities in predator detection throughout ontogeny of squid. Our findings indicate that the lateral line analogue plays a role in predator detection and initiation of escape responses at the earliest life stages, and continues to contribute to successful evasion by aiding visual cues in juvenile and adult squid. These results provide novel insight into the sensory modalities used by squid to evade predators from the earliest life stages to maturity.

CHAPTER 4

ANTI-PREDATOR BEHAVIOR OF SQUID THROUGHOUT ONTOGENY

INTRODUCTION

Throughout their lives, squids are prey targets for many marine predators, including fish, marine mammals, sea birds, and even other cephalopods, making them an integral component of marine food webs (Clarke, 1996; Mather, 2010; Piatkowski et al., 2001; Wood et al., 2008). An array of complex behaviors have evolved as components of anti-predator responses in squids (Hanlon and Messenger, 1996). Along with a jet-driven escape, a widely used strategy for predator evasion in cephalopods is camouflage (Barbosa et al., 2008; Hanlon and Messenger, 1996; Messenger, 2001). Postural displays are also commonly used to deter a predator from attacking (Bush et al., 2009; Hanlon et al., 1999; Huffard, 2006), and inking is often employed to confuse oncoming predators and allow time for escape (Bush and Robison, 2007; Hanlon and Messenger, 1996; Wood et al., 2010). Collectively, these responses provide a wide behavioral repertoire for predator avoidance.

The ability of squid to change body patterning and color quickly is central to their camouflage and postural display strategies (Hanlon and Messenger, 1996). Chromatophores, the organs largely responsible for color change and body patterning, contain a large compartment of pigment granules (Florey, 1966), including those that are yellow, orange, red, brown and black, with the pigment color combination varying with species (Fingerman, 1970; Messenger, 2001). Each organ contains an elastic sacculus with pigment granules and is surrounded by a series of 15-25 radial muscles to contract and expand the chromatophore (Messenger, 2001). These muscles are under nervous control and therefore expansion and contraction can occur rapidly and

selectively to create a wide variety of patterns (Hanlon and Messenger, 1996; Messenger, 2001). The complexity of patterns that squid can produce are correlated to their habitat complexity, with species living in coral reefs, rock reefs or kelp showing the highest number of chromatic components and pattern combinations (Hanlon and Messenger, 1996). Different body patterns have also been described during mating, antagonistic displays and predator avoidance (Barbato et al., 2007; Hanlon and Messenger, 1996; Hanlon et al., 1994; Hanlon et al., 1999). Furthermore, squid perform a wide repertoire of deimatic behaviors that involve chromatic, postural and locomotor components, which are intended to signal a warning to a predator (Cornwell et al., 2009; Hanlon and Messenger, 1996; Hanlon et al., 1994; Hanlon et al., 1999; Jantzen and Havenhand, 2003; Staudinger et al., 2011).

In addition to crypic behavior, inking events are often employed to maximize the effectiveness of an escape response by confusing predators (Hanlon and Messenger, 1996; Staudinger et al., 2011; Wood et al., 2010). A typical response to a predation threat is the "ink-blanche-jet" maneuver, during which the cephalopod ejects ink as it jets away and blanches white (Hanlon and Messenger, 1996; Hanlon et al., 1994). Inking can occur in several forms, such as a 'pseudomorph', which is a blob of ink that is held together by mucus and approximates the volume of the cephalopod, serving to distract a predator while the animal swims off. Another method is to create a cloud of ink behind which the cephalopod can disappear (Bush and Robison, 2007; Hanlon and Messenger, 1996). Several other shapes of ink release have been observed, including 'ropes' and 'puffs' (Bush and Robison, 2007). Squid ink also contains chemicals such as L-dopa and dopamine that elicit escape responses in nearby conspecifics (Gilly and Lucero, 1992; Lucero et al., 1994; Wood et al., 2008; Wood et al., 2010). Not only do the chemicals in this ink potentially warn conspecifics, they may block olfactory or taste

receptors in predators, causing them to abandon their approach (Caldwell, 2005; Hanlon and Messenger, 1996).

Although the various anti-predator behaviors have been well studied in some species of adult squid, little is known about how squid respond to threats throughout ontogeny. Cephalopods undergo major morphological and morphometric changes throughout their life and alter their ecological niches (Boyle and Boletzky, 1996). While cephalopods do not experience a distinct metamorphosis, and therefore do not have true larva, hatchlings are ecologically distinct from older life history stages (Robin et al., 2014; Shea and Vecchione, 2010; Young and Harman, 1988). The term "paralarva" is used instead of 'larva', and is defined as a newly hatched cephalopod that has a unique mode of life from the adults, often with an endpoint identified by changes in morphological characteristics (Shea and Vecchione, 2010). Moreover, relative to the adult, paralarvae have a more rounded mantle, relatively smaller arms, a proportionally larger funnel, and rudimentary fins (Boletzky, 1974; Okutani, 1987; Packard, 1969). Ecologically, paralarvae differ from older squid in that they cover shorter overall distances by active swimming driven primarily by the jet (Bartol et al., 2009a), move through the water column in diel vertical migrations (Boyle and Boletzky, 1996; Robin et al., 2014), and reside in an intermediate Reynolds number (Re) regime (Re~$1-10^2$) (Bartol et al., 2008; Bartol et al., 2009a; Thompson and Kier, 2002; Webber and O'Dor, 1986). Conversely, many juvenile and adult squids are capable of powerful and long distance locomotion covering significant horizontal distances, generally employ less vertical migratory behavior, though there are certainly some species that undergo significant vertical migrations (Boyle and Rodhouse, 2008), and operate in a higher Re regime (Re~$10^3 – 10^6$) (Bartol et al., 2009b; O'Dor, 1988). Paralarvae squid also have largely transparent bodies with relatively fewer chromatophores than juvenile

and adult stages (Messenger, 2001; Okutani, 1987), suggesting they likely use camouflage differently than juveniles and adults.

Although it is clear there are large physical, behavioral, and ecological differences in the life history stages of squid, few studies have examined how anti-predator behavior changes from paralarvae to adults. The goal of this study is to (1) document how chromatic patterning, posturing and inking in squid change in response to predators throughout ontogeny and (2) measure kinematic variables associated with squid-predator interactions to better understand the behavioral cues that trigger anti-predator responses.

MATERIALS AND METHODS

Animal collection and maintenance

This project was conducted in accordance with Old Dominion University's Institutional Animal Care and Use Committee (Protocol #12-016). Paralarval *Doryteuthis pealeii* (dorsal mantle length (DML) = 0.18 cm) and juvenile/adult *Lolliguncula brevis* (DML = 3.0-7.0 cm) were used for this research. Little information is currently available on the breeding habits of *L. brevis*, and they are extremely difficult to obtain as hatchlings. Therefore, *D. pealeii* was selected to study early ontogenetic stages. *D. pealeii* is a reasonable substitute for *L. brevis* because both species have similar body size, fin size and shape, and ecological niches as paralarvae (Bartol et al., 2008). Additionally, juvenile and adult *L. brevis* demonstrate similar body patterning to juvenile and adult *D. pealeii* (Hanlon et al., 1999).

D. pealeii paralarvae were purchased from the Marine Biological Laboratory, Woods Hole, MA, and maintained in a recirculating seawater system at a salinity of 30-32‰ and at temperatures of 19-24°C until hatching. Once the paralarvae hatched they were kept in separate

containers to keep track of age. *L. brevis* used in this project were captured by otter trawl in Wachapreague, VA, USA. Trawls were conducted in August, September and October as the catch probabilities are highest in these months (Bartol et al., 2002). After capture, squid were transferred to a 114 L, circular holding tank (Angler Livewells, Aquatic Eco-Systems, Inc., Apopka, FL, USA) fitted with a portable battery powered aerator (Model B-3, Marine Metal Products Co., Inc., Clearwater, FL, USA) for transport to the lab. Squid were maintained in 450-gallon seawater systems in the lab with several forms of filtration (e.g., BioBalls, protein skimmers, ozone filtration, etc.). Seawater was maintained at temperatures and salinities equivalent to those of the capture sites (19-22 °C; 30-35 ‰). A moderate current flow was maintained to promote active swimming and squid were fed a diet of live *Palaemonetes pugio* and *Fundulus heteroclitos* as suggested by Hanlon et al. (Hanlon, 1990; Hanlon et al., 1983). Squid were allowed to acclimate for at least 2 h prior to experimental trials. Only those animals that appeared healthy and exhibited normal behaviors were used. In total, 60 paralarval squid and 20 juvenile/adult squid were selected for this study.

Two summer flounder (*Paralichthys denatus*) (13.2 cm and 15.5 cm total length) and two mummichogs (*Fundulus heteroclitus*) (1.3 cm and 1.5 cm total length), were purchased from the Marine Biological Laboratory, Woods Hole, MA, and maintained in a recirculating seawater system at a salinity of 30-32‰. The flounder and mummichogs were fed live squid (*L.brevis and D. pealeii*, respectively) for one week prior to experimental trials so that they could become proficient in squid capture before data collection. Although we used different fish species for the paralarvae and juvenile/adult trials, the species chosen reflect predators that the squid are most likely to encounter in each ontogenetic phase in the waters of the mid-Atlantic region, with the goal of documenting behaviors that reflect natural conditions.

Predator-prey experiments

Paralarvae trials were conducted in a 10x10x10 cm clear acrylic tank. A DALSA Falcon video camera (DALSA Corp., Waterloo, ON, Canada; 1400 x 1024 pixel resolution, 100 frames per second) outfitted with a 25 mm lens (FOV = 2.7x3.7 cm) was positioned above the arena. A 500 watt halogen light provided illumination for the experimental trials. Video frames from the cameras were stored in real time on hard disk using a CLSAS capture card (IO Industries, London, ON, Canada) and Streams 5 software (IO Industries, London, ON, Canada). For each experiment, 5-10 paralarvae were placed in the arena with the two mummichogs (*Fundulus heteroclitus*), which are a natural predator for paralarvae squid. Multiple predators were used to increase the frequency of predation events. At the beginning of each trial, the squid were placed in the arena for a 10 minute acclimation period. After the acclimation period, the fish were added and the experiments commenced. Each trial lasted 10 minutes, after which the fish were removed and surviving squid were returned to their holding tank.

Adult and juvenile trials took place in a 1.2 m diameter x 0.76 m deep round tank with a crushed coral substrate. The arena was lined with curtains to avoid disturbing acclimating animals. A UNIQ UP-685 CL high-speed color camera (Uniq Vision; 659 x 494 pixel resolution, 110 frames per second) outfitted with a 5 mm lens (FOV = 130x170 cm) was suspended from scaffolding over the tank. Four 500-watt halogen lights provided illumination for the experimental trials. For each experiment, a single squid was placed in the arena with two summer flounder (*Paralichthys denatus*). Multiple predators again were used to increase the probability of a predation event. Prior to the start of each trial, a 12 cm diameter cylinder composed of 5 mm plastic mesh was lowered into the experimental tank and a single squid was placed inside the cylinder for a 30 minute acclimation period. The trials commenced when the

partition was raised above the tank and the flounder and squid were allowed to interact. Each trial lasted 10 min, after which the squid was removed from the arena and returned to its holding tank. Video frames from the cameras were stored in real time on hard disk using CL160 capture cards (IO Industries, London, ON, Canada) and Video Savant 4.0 software (IO Industries, London, ON, Canada).

Behavioral Responses and Kinematics

Kinematic variables were measured using National Institute of Health's public domain software ImageJ (http://rsb.info.nih.gov/ij/). Predator-squid distance (*d*), angular orientation of squid to approaching predator (θ), angular orientation of the squid escape trajectory (ϕ), and orientation (i.e., tail-first or arms-first body position) were measured at the initiation of each squid's defensive response to the predator (i.e., at the beginning of inking, posturing, and/or body patterning). Predator-squid distance (d) was measured from the predator's rostrum to the closest component of the squid. θ was the angle between the squid's longitudinal axis and the line connecting the tip of the predator rostrum to the squid's center of mass., whereas ϕ was the angle between the line connecting the tip of the predator rostrum to the prey's center of mass and the path of the escape over multiple frames (Fig. 9). Interactions were divided into four groups of angular orientations for both θ and ϕ: (1) < 45°, (2) 46°-90°, (3) 91°-135°, (4) 136°-180. These groupings were useful in determining whether the squid oriented themselves in an anterior, lateral or posterior direction towards the approaching predator, as well as for determining the direction of the squid escape trajectory).

Body postures were grouped into two categories: (1) "splayed arms" where the arms were spread apart with minimal contact between the arms, and (2) "raised arms" where unilateral or

bilateral raising of the arms was observed, often with 4-arm groupings occurring on one or both sides of the body (Hanlon et al., 1994) (Fig. 10). These postures were the only two observed and therefore other postures observed in cephalopods were not included in this study. Several types of body patterns were examined in juveniles and adults including: (1) clear body, where chromatophores are retracted, rendering the animal mostly translucent; (2) dark body, where most chromatophores are expanded producing a dark body coloration; (3) banded pattern, where chromatophores are expanded in striped sections across the mantle, fins, head and/or arms; and (5) dark arms and clear body, where chromatophores are retracted on the body but expanded along the head and arms. Unlike juveniles and adults,the range of body patterns displayed by paralarval *D. pealeii* has not been previously reported. Based on our observation of paralarvae in the presence of a predator, three body patterns were identified: (1) clear body, where the chromatophores are not contracted, rendering the animal mostly translucent; (2) intermediate body, where the chromatophores are partially contracted; and (3) dark body, where the chromatophores are contracted fully, producing a dark body coloration. The mean areas of three chromatophores on the dorsal portion of mantle were measured on each individual (N=60) to determine the body pattern category during the predator encounter.

Inking patterns were grouped according to the following categories: (1) "ropes", (2) "pseudomorph", (3) "puffs", and (4) "clouds". Ink "ropes" consist of long continuous streams of ink (Bush and Robison, 2007), while a "pseudomorph" is described as a dense blob of ink that is approximately the same size and shape as the cephalopod (Hanlon & Messenger 1996). "Puffs" are defined as short releases of ink that quickly dissipate (Bush and Robison, 2007).
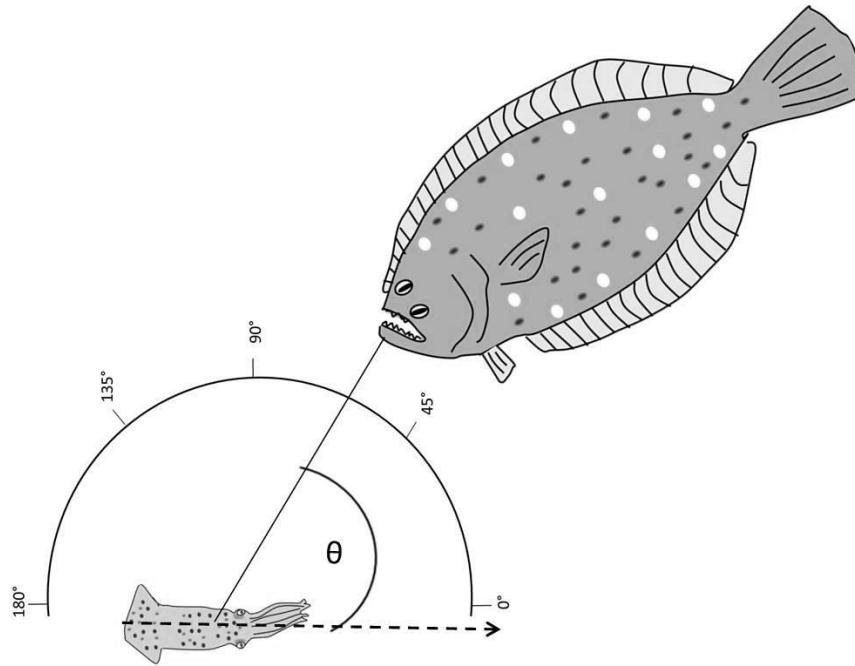
Figure 9. Angular orientation of squid during interactions with predator. A) The angular orientation of squid to approaching predator (θ) was the angle between the squid's longitudinal axis (dashed black line) and the line connecting the tip of the predator's upper rostrum to the squid's center of mass (solid black line). Interactions were divided into four groups of angular orientations for θ: 1) < 45°, (2) 46°-90°, (3) 91°-135°, (4) 136°-180°.
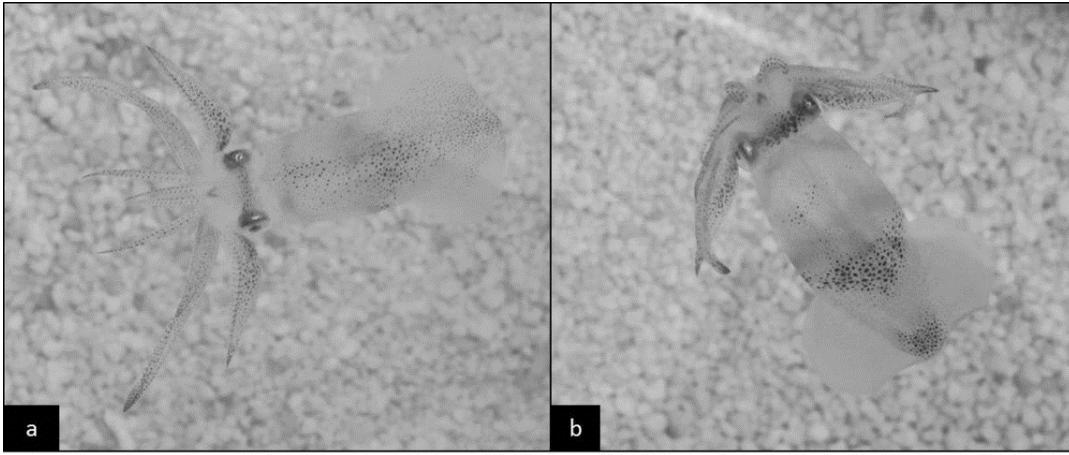
Figure 10. Squid body postures examined in this study: (a) "splayed arms" where all eight arms are spread outward, (b) "raised arms" where there is unilateral or bilateral raising of groups of arms.

Cephalopods can also create diffuse "clouds" during escape responses that generally involve large volumes of ejected ink with irregular borders (Hanlon and Messenger, 1996) (Fig.11).

The swimming velocity of squid during escape jets, which occur in conjunction with inking, was also measured. Several kinematic components of the predator's approach were considered, including the velocity of the predator during the interaction, overall distance travelled by the predator and the distance travelled before a response was initiated for paralarval, juvenile and adult squid. The velocity of the fish was determined by measuring displacement from the beginning of the approach to the end of the attack (usually denoted by the fish catching the squid or changing trajectory) divided by the duration of the attack. The velocity of the squid was determined by measuring the net displacement from the beginning of the escape response to the end (denoted either by capture or ceasing to jet) divided by the duration of the escape response.

Statistical Analysis

Statistical analysis was performed in SPSS (v. 18 SPSS Inc., Chicago, IL, USA). Paralarve squid (N=60) were treated as a single ontogenetic group as they consistently had a dorsal mantle length of 0.18 cm. Juvenile squid were those animals 3.0–5.0 cm DML (N=9), while adults were animals 5.1–7.0 cm DML (N=11). When individuals had multiple predator-prey interactions, mean proportions were calculated for body pattern type, posture type, and ink shape. Different predator-prey interactions were considered for postural encounters and inking encounters. Before analysis, all data were tested for normality using Shapiro-Wilk tests. The proportion data deviated from normality (all $p<0.05$) and thus were arcsine transformed prior to
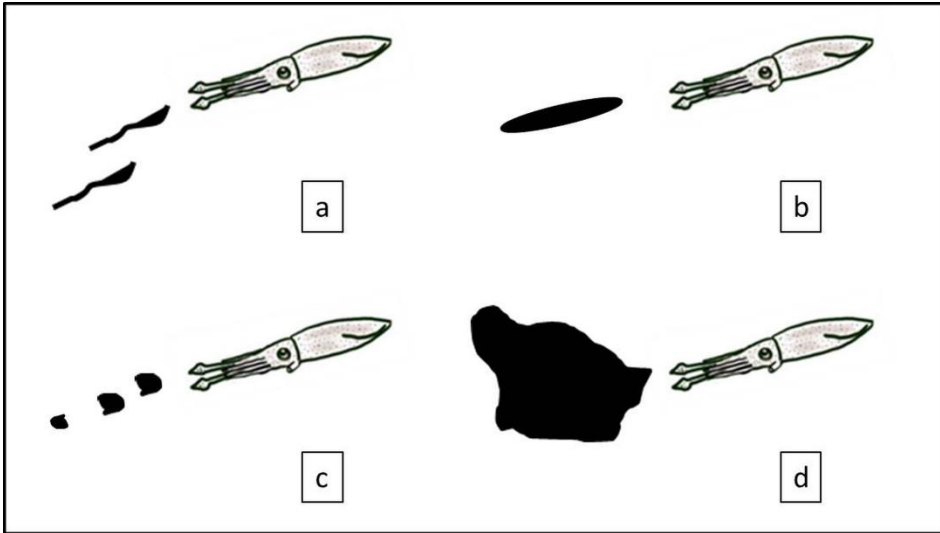
Figure 11. Schematics of inking patterns examined in predator-prey experiments (modified from Bush and Robison, 2007). Inking patterns include: (a) ink "ropes", which consist of long continuous streams of ink; (b) a "pseudomorph", which is described as a dense blob of ink that is approximately the same size and shape as the cephalopod; (c) "puffs", which are short releases of ink that quickly dissipate; and (4) "clouds" that generally involve large volumes of ejected ink with irregular borders.

parametric analysis. No differences were found between juveniles and adults (t-tests: all p>0.05) for any of these variables, and therefore data were combined for further analysis of this group (N=20). Kinematic variables (predator-squid distance (d), angular orientation of squid to approaching predator (θ), angular orientation of the squid escape trajectory (ϕ), and body orientation) associated with inking events and posturing events were compared via independent two-tailed t-tests. For analysis of squid behaviors and predator distance, comparisons were made between behavioral events that occurred in the beginning of the interaction ($\leq$50% total distance) and the end of the interaction (>50% total distance).

Independent two-tailed t-tests were used to compare orientation, posture, inking events and body patterns between the two size class groups. Analysis of variance (ANOVA) was performed to compare groups of angular positions and behavioral responses (body patterning, posture events, inking events). The average proportion of interactions with inking events and with body patterning (i.e., posturing and/or chromatic changes) were calculated for each individual squid and ANOVAs were performed on these data to determine preference when confronted with a predator. Significance was tested at $p<0.05$ and all means are presented $\pm$ standard deviation unless otherwise noted.

RESULTS

Paralarvae kinematics

Throughout the predator-prey interactions, paralarval squid did not demonstrate posturing and only one inking event was recorded. Significantly more predator-prey interactions occurred while paralarval squid were oriented with arms towards the predator versus tail-first relative to the approaching predator (t-test: $t_{118}=16.4$, $p<0.001$), with only five total interactions (0.08%)

occurring while the paralarvae were oriented tail-first. Paralarvae responded to an approaching predator with an escape jet in only 35% of total interactions. When paralarvae did respond, the mean average swimming velocity during escape jetting was 32.42±15.66 squid dorsal mantle lengths (DML) s^{-1}. Distance and velocity of the predator did not determine whether an escape jet was performed (distance t-test: t_{58} =-0.36, p=0.71; velocity t-test: t_{58} =-1.4, p=0.17). The distance that the predator travelled, however, played a role in whether an escape jet was performed by the squid (t-test: t_{58}=-2.55, p=0.01), with escape responses occurring at larger predator travel distances (mean travel distance=0.67±0.31 predator body lengths (PBL)) than non-escape responses (mean travel distance=0.45±0.39 PBLs). No difference in θ or ϕ was found between escape and non-escape responses (angular orientation of the squid relative to the approaching predator: t-test: t_{58}= 1.3, p=0.20; squid escape trajectory t-test: t_{58}=-0.12, p=0.91).

For the 65% of predator-prey interactions that did not result in an escape jet, the paralarvae performed stereotyped swimming behaviors that potentially could aid in predator avoidance. These behaviors included swimming repetitively in a circle in both the xy and xz plane, varying in diameter from 1-3 DML (Fig.12a). In some cases the paralarvae exhibited no net displacement during these circular motions (i.e., starting and ending points of the loop were the same), whereas in other cases, net displacement was present, resulting in movement in a spiral pattern (Fig. 12b). Additionally, several different forms of jetting were performed. These included short, pulsed, sequential jets in which the squid moved rectilinearly through the water column in either an arms-first or tail-first orientation over relatively short distances, distinguishing these jets from larger displacement escape jets (Fig. 12c). Erratic zig-zag jetting, in which the paralarvae employed short vectored jets with multiple changes in direction, was found in both arms-first and tail-first orientations (Fig. 12d). The paralarvae also exhibited
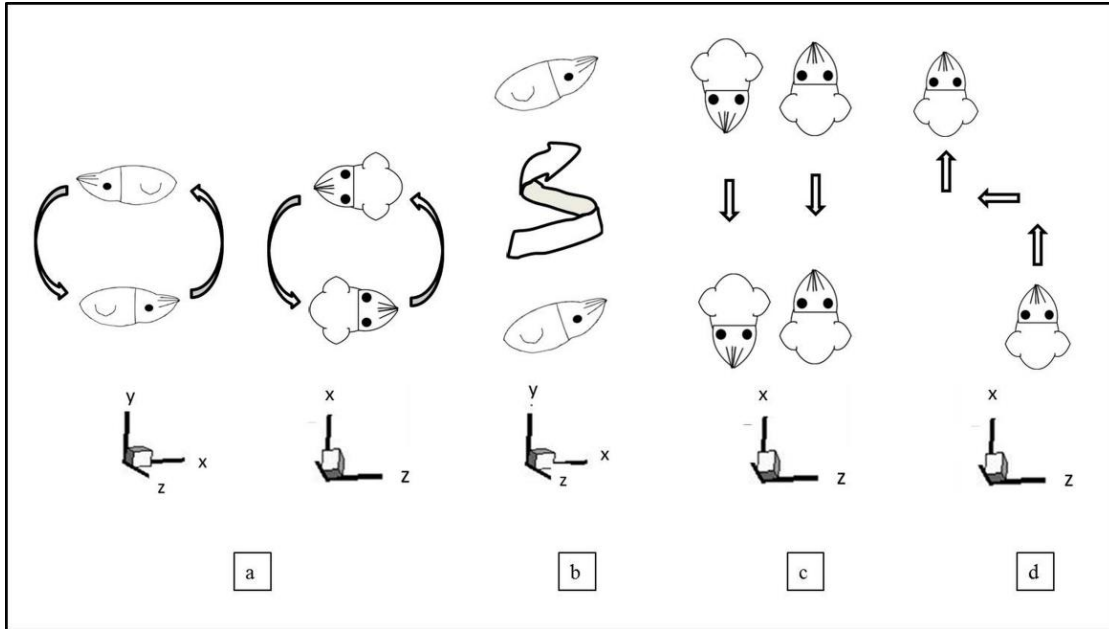
Figure 12. Stereotyped swimming behaviours of paralarvae squid: (a) swimming repetitively in a circular pattern in both the xy and xz plane; (b) swimming in a spiral pattern; (c) pulsed sequential jets in which the squid moved rectilinearly through the water column in either an arms-first or tail-first orientation; (d) erratic zig-zag jetting, in which the paralarvae employed short vectored jets with multiple changes in direction (squid perform this pattern in both tail-first and arms-first orientations; arms-first orientation is depicted here).

rolling (rotation about the x-axis or y-axis) and pitching (rotation about the z-axis), but these behaviors were unlikely to have anti-predator benefits as there was no translational motion.

Juveniles/adults kinematics

Response initiation distance was significantly greater for those juvenile/adult squid exhibiting only postural responses versus those demonstrating ink/escape responses (t-test: t_{17}= -7.1, p<0.001; Fig. 13a). Squid showing only postural displays (i.e., raised or splayed arms) also were associated with lower predator approach velocities than those exhibiting an ink/escape response (t-test: t_{19}=-3.03, p=0.006) (Fig. 13b). Interestingly, squid using ink/escape responses were also associated with greater overall predator travel distances than those showing only postural responses (t-test: t_{18}= -5.25, p< 0.001; mean predator travel distance=2.52±0.34 PBL (ink/escape response), 0.68±0.35 PBL (postural response)). No significant differences in response initiation distance were found between 'splayed arm' postural responses, which were only displayed during tail-first orientations, and 'raised arm' postural responses, which were only observed during arms-first orientations (t-test: t_{19}=0.25, p=0.80), nor was there a significant difference in the velocity of the approaching predator between the two behaviors (t-test: t_{10}= 1.34, p= 0.21). The squid was more likely to actively position itself anteriorly facing the predator when the predator was within 2.5 predator body lengths of the squid (t-test: t_{16}=-2.20, p=0.046). However, predator-prey distance did not affect the specific body pattern or inking pattern selected (all p> 0.05).

Inking and escape jet differences through ontogeny
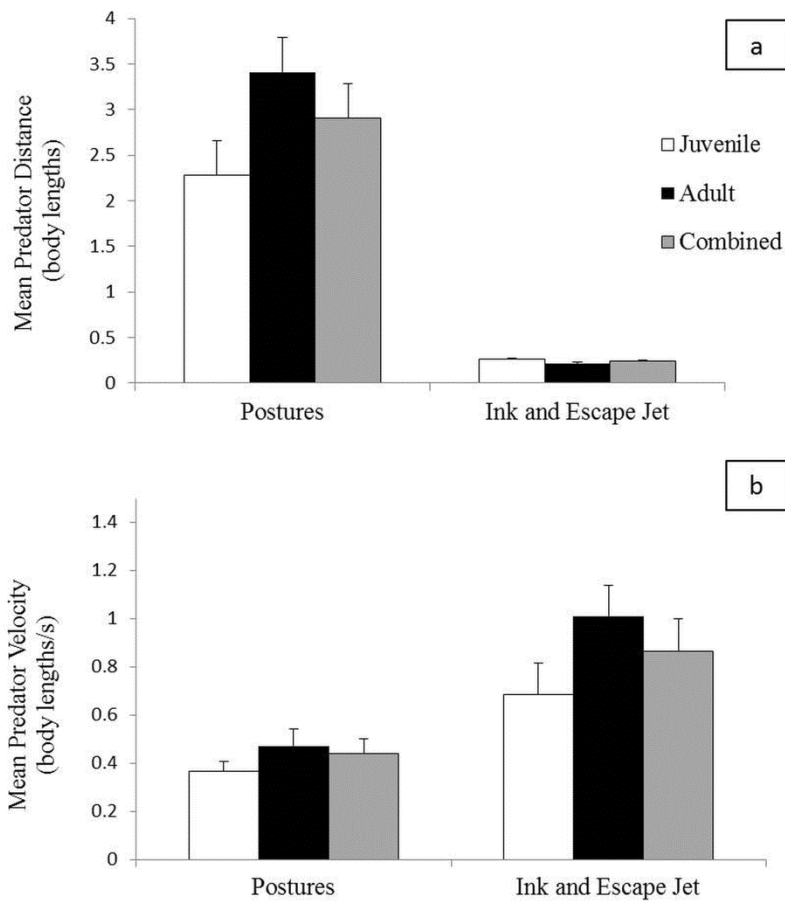
Figure 13. The mean (a) distance of predator from the squid when the squid initiated a behavioral response, expressed in predator body lengths (PBL) and (b) velocity of the predator approach when squid initiated a behavioral response, expressed in PBL s^{-1}. Significant differences between juvenile and adult squid were not evident, and thus juvenile and adult data were pooled for analysis (grey bars). Paralarval squid did not demonstrate postures or frequent inking behaviour and were therefore excluded from this figure. Mean ± s.e.m is presented.

The juvenile and adult squid in this study responded to an oncoming predator with an inking event in approximately 60% of all interactions. Inking events were always exhibited in sequence with an escape jet, where inking occurred either at the initiation of the escape jet (61%) or at another point throughout the escape jet (39%). Inking in paralarvae only occurred in 0.02% of all interactions. Significant differences were found in relative swimming velocities during escape responses between paralarval squid and juvenile/adult squid (ANOVA: $F_{3,121}=89.36$, $p<0.001$). Tukey post-hoc analysis revealed paralarvae have significantly slower escape responses (mean=32.42 ± 15.66 DML s^{-1}) than juveniles/adults (mean= 47.9 ± 1.41 DML s^{-1}, $p=0.001$) (Fig.14). However, no significant differences in predator approach velocities were found between paralarvae (mean=1.75 ± 3.17 PBL s^{-1}) and juveniles/adults (mean=1.14 ± 0.43 PBL s^{-1}). In paralarvae, escape was only initiated in 35% of interactions, leading to an overall survival rate of only 40%, whereas juveniles and adults survived all interactions in these trials.

The proportion of inking events during encounters varied significantly with the angular orientation of the squid relative to the approaching predator for juveniles/adults (ANOVA: $F_{2,16}=$ 14.1, $p< 0.001$); inking events were more prevalent when θ were 46-90º (mean proportion of inking events=0.90 ± 0.25) compared with $\theta<45º$ (mean proportion of inking events=0.45 ± 0.33, $p>0.001$). The squid escaped at speeds significantly greater than the predator approach for both age groups (paralarvae: $p<0.001$; juveniles/adults: $p<0.001$; Fig.14). Juvenile/adult squid demonstrated a significantly higher proportion of inking events when displaying a clear body pattern than when displaying other body patterns (ANOVA: $F_{2,16}=5.47$, $p<0.015$). No significant differences were found between squid postures, i.e., splayed arms vs. raised arms, based on θ (all $p>0.05$). The average angular orientation of the squid escape trajectory (ϕ) was $152.34\pm35.23º$. ϕ did not influence the selection of postures (ANOVA: $F_{1,14}=0.09$, $p=0.77$),
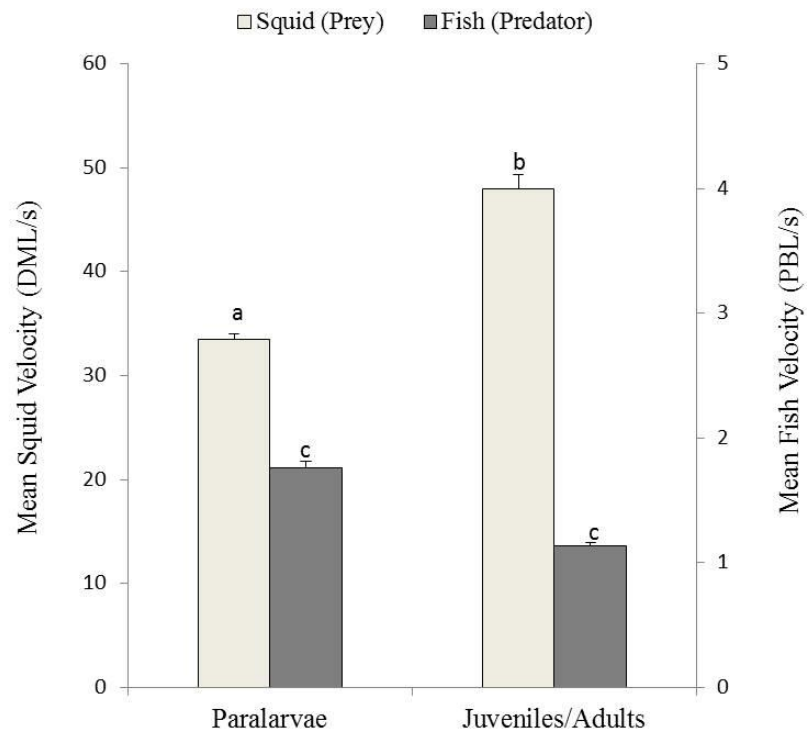
Figure 14. The mean velocity of the fish and the squid when an escape jet was performed during predator-prey interactions for paralarval and juvenile/adult trials. 100% of the juvenile squid survived the encounters; 40% of paralarvae survived the encounters. Bars with different letters are significantly different. Mean ± s.e.m. are presented.

orientation (ANOVA: $F_{1,16} > 0.16$, all $p > 0.69$) or proportion of ink and escape events (ANOVA: $F_{2,16} = 0.49$, $p = 0.62$).

Body pattern differences through ontogeny

Different body patterns were observed for paralarvae and juveniles/adults. Paralarvae demonstrated clear body patterning (N=33, mean area of chromatophores= $2.74 \times 10^{-5} \pm 1.13 \times 10^{-5}$ cm²), intermediate body patterning (N=18, mean area of chromatophores= $1.45 \times 10^{-4} \pm 9.86 \times 10^{-6}$ cm²), and dark body patterning (N=9, mean area of chromatophores= $2.50 \times 10^{-4} \pm 5.50 \times 10^{-5}$ cm²). The mean area of the chromatophores in the three body classifications were significantly different, indicating that they are indeed three distinct body patterns (ANOVA: $F_{2,57} = 379.7$, $p < 0.001$; Fig. 15). The proportion of clear, intermediate and dark body patterning displayed during predator-prey responses were significantly different for paralarvae (ANOVA: $F_{2,177} = 12.4$, $p < 0.001$). Tukey post-hoc tests revealed that clear body patterns (mean proportion=0.55 ± 0.50) were used significantly more often than intermediate body patterns (mean proportion= 0.31 ± 0.43, $p < 0.001$) and dark body patterns (mean proportion=0.15 ± 0.36, $p=0.007$, Fig. 16a). The velocity of the approaching predator did not affect the body pattern selection of the paralarvae (all $p > 0.05$), nor did the angle of the predator approach (θ), distance of the predator or distance travelled by the predator at the time of the interaction (all $p > 0.05$). When responding to an approaching predator, juvenile and adult squid were significantly more likely to demonstrate the banded pattern than the dark body, dark arms with clear body, or clear body pattern (ANOVA: $F_{3,76} = 26.1$, $p < 0.001$; Fig. 16b). When the juvenile/adult squid responded with an inking event (something that is very rare for paralarvae), it was significantly more
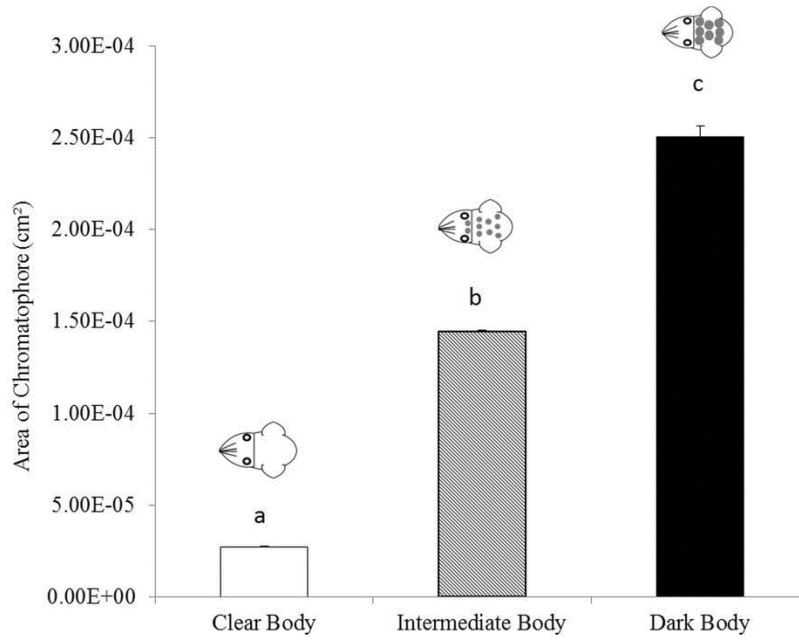
Figure 15. Distinct body patterns of paralarvae during predator-prey interactions and the associated mean area of chromatophores in the clear body, intermediate body and dark body patterns. Bars with different letters are significantly different. Mean ± s.e.m. presented.
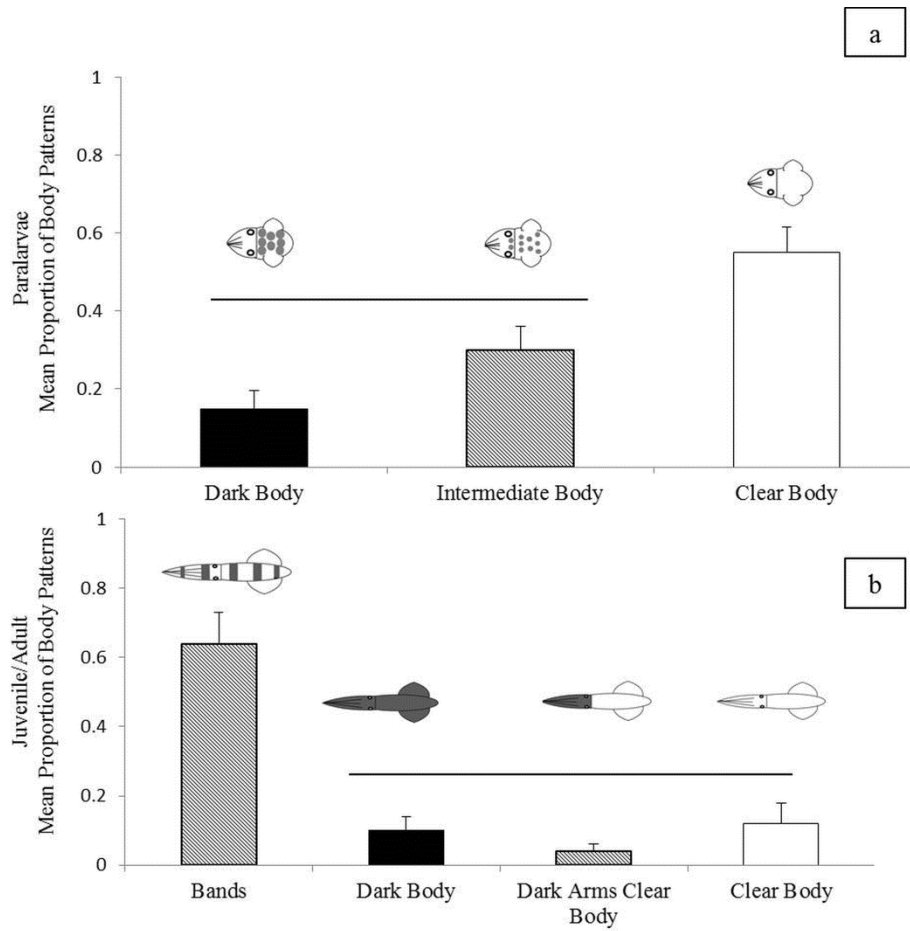
Figure 16. Mean proportion of body patterns demonstrated in (a) paralarvae, and (b) juvenile/adult squid during predator approaches. Mean ± s.e.m. is presented. Lines above bars indicate no significant difference.

likely to be in the form of a 'pseudomorph' than a 'cloud' or 'puff' (ANOVA: $F_{2,57} = 91.2$, $p<0.001$). The rope shape was not observed in these experiments.

DISCUSSION

The results of this study reveal the unique differences in anti-predator strategies of squid as they undergo morphological and ecological transformations throughout ontogeny. Paralarval squid did not react to an oncoming predator with posturing or consistent inking responses, as only one inking event occurred throughout all of the trials. Instead, they either produced an escape jet (35% of encounters) or demonstrated routine stereotypical behaviors (65% of encounters) in the presence of a predator. In contrast, juvenile and adult squid exhibited frequent inking/escape jetting and postural responses to an oncoming predator, with the selection of anti-predator behavior being impacted by characteristics of the predator's approach. During the slower predator approaches, the juvenile/adult squid were more likely to posture, while faster approaches triggered inking and escape jet responses. In juveniles/adults, postural responses were favored when the predator was positioned at large distances from the squid while inking responses were selected when the predator was close to the squid. Additionally, postural displays were selected when the predator travelled only a short distance toward the squid, while ink responses were used when the predator travelled a significantly greater distance toward the squid. Postural displays are likely an attempt to dissuade the predator at the beginning of the attack while minimizing energy expenditure associated with an inking response (Wood et al. 2008). Inking is then utilized only when crypsis or posturing has failed and the predator continues with its approach, as was seen in this study.

In many cephalopods, inking provides a distraction to oncoming predators, allowing them to escape from reach (Hanlon and Messenger, 1996). Additionally, the chemical properties of ink can act as a predatory deterrent as it disrupts the sensory systems of the predator (Derby, 2007; Gilly and Lucero, 1992; Wood et al., 2010). The juvenile and adult squid in this study responded to an oncoming predator with an inking event in approximately 60% of all interactions, whereas only one inking event was recorded in the paralarvae (0.02% of all interactions). It is possible that paralarvae are more selective in their use of inking events given the high energetic requirements of producing ink (Wood et al., 2008) coupled with the need to allocate high levels of energy toward development (Russo et al., 2003). In addition, juveniles and adults showed proportionally more inking events with clear body patterns relative to other body patterns and inking and escape jetting were always coupled, a sequence of behaviors that is consistent with the "ink-blanche-jet" maneuver described earlier. In juveniles/adults, the 'pseudomorph' shape was produced more often than 'rope', 'puff' or 'cloud' shapes. This is consistent with previous observations, where shallow-dwelling cephalopods commonly use 'pseudomorphs' (Hanlon and Messenger, 1996), while a wider variety of shapes are evident in deep sea species (Bush and Robison, 2007). In several instances, the flounder were distracted by the 'pseudomorph' and directed their approach towards the ink instead of the squid. Ink has also been shown to act as a conspecific alarm cue that could be used when swimming in schools (Wood et al., 2008; Wood et al., 2010). *L. brevis* do school in their natural habitat (I. Bartol, pers. obs.), and it is possible that the 'pseudomorph' not only acts as a decoy but also a social warning cue. Although 'pseudomorphs' were found to be the most common ink response observed in the present study, it is conceivable that the 'rope' and 'puff' shapes, which involve smaller sequential ink release

patterns, are used as conspecific alarms. Since the experimental trials only considered one squid per trial, this social alarm possibility was not tested directly.

Both paralarvae and juveniles/adults showed impressive average escape velocities of 32.42 ± 15.66 and 47.9 ± 1.47 DML s^{-1}, respectively. In fish, average escape velocities range only from approximately 14-23 BL s^{-1} in larvae (Williams et al., 1996) and roughly 20-28 BL s^{-1} in adults, depending on the species (Gibb et al., 2006). The velocities found here were markedly higher than those reported in Chapter 3 as only sequences where an escape jet was performed were used for analysis. The juvenile/adult squid reached significantly higher relative swimming velocities than the paralarvae in these experiments, which is likely reflective of the unique hydrodynamic and morphological conditions that squid encounter throughout ontogeny. Paralarvae operate at low to intermediate Reynolds numbers and must overcome high viscous forces, while juveniles and adults operate at higher Reynolds numbers where inertial forces are greater and gliding through the water column is more prevalent (Bartol et al., 2008). Additionally, relative to paralarvae, juvenile and adult squid have more streamlined bodies and larger, more developed fins to provide additional propulsive forces to complement the jet, at least at the start of the escape jet (Bartol et al., 2009a; Bartol et al., 2009b; Hoar et al., 1994a; Stewart et al., 2010). Both paralarvae and juveniles/adults escaped at speeds greater than the approaching fish, leading to a 100% survival rate for juvenile and adults, but only a 40% survival rate for paralarvae. In Chapter 3, the predator had a higher mean velocity than the squid, however sequences in which the squid was performing stereotyped behaviors, or did not respond to the oncoming predator at all, were included in velocity measurements. The low survival rate of paralarvae is a reflection of the absence of an escape response in many encounters, not their inability to escape a predator, as their swimming velocity during escape jetting was significantly

higher than the velocity of the predator approach when they did initiate an escape response. Paralarvae only responded with an escape jet in 35% of all interactions, whereas the juveniles and adults always responded with an escape jet when a posture failed to deter the approaching predator. The absence of any escape response in such a high percentage of paralarvae is intriguing and may relate to a reduction in the effectiveness of epidermal hair cells in early ontogeny, which have been shown to play an important role in predator wake sensing (see Chapters 2, 3).

One of the most striking ontogenetic differences found in this study was the unique use of stereotyped behaviors by paralarvae, but not other life history stages. These behaviors included swimming movements such as repetitive circling, spinning and erratic jetting that were not seen in juveniles or adults. Since the paralarvae often did not change their behavior as a predator was approaching, it is possible that they rely heavily on their repertoire of stereotyped behaviors and clear body patterning to elude potential predators in the water column until they develop better neural and motor control, which can produce more complex body patterning and enhance hydrodynamic sensing capabilities. Indeed, the ability of paralarval squid to coordinate sensory inputs and motor outputs improves within the first month of hatching (Chen et al., 1996; Preuss and Gilly, 2000), suggesting that chromatophore control and hair cell functionality also increase throughout this period. Therefore, coupling stereotyped swimming strategies with transparency in the earliest days of hatching, when posturing is less achievable and sensing capabilities are limited, is a reasonable predator avoidance strategy for paralarvae. Although brief squid vary in size from juvenile to adult, they maintain similar ecological niches and thrive in the same environment during these ontogenetic stages (Bartol et al., 2002). Therefore it is likely that similar behaviors are effective at deterring predators over these ontogenetic stages, which is

consistent with the findings reported here. The number of chromatophores increases on the mantle and fins of squid as their size increases (Dubas et al., 1986); however, the proportion of the body that is shaded to produce patterns stays approximately the same in juveniles and adults (banded pattern in juvenile= 34% shaded; banded pattern in adult= 41% shaded).

In this study, paralarval squid demonstrated the clear body pattern significantly more often than intermediate or dark patterns. It is likely that maintaining a clear body pattern is advantageous given the planktonic nature of paralarvae. By sustaining a transparent state, the paralarvae allow for maximum transmission of background light, making them difficult to detect in the water column (Okutani, 1987; Zylinski and Johnsen, 2011). However, for adults and juveniles, the banded body pattern was demonstrated far more than the dark body, clear body or dark arms with a clear body patterns. This banded body patterning was used during both 'splayed arm' and 'raised arm' postures. Banded patterns were also seen throughout the predator's attack and did not vary based on the predator approach distance. The banded body pattern potentially acts as disruptive coloration, making it more difficult for a predator to identify the squid as prey (Hanlon and Messenger, 1996). It is likely that the coloration, in addition to body postures, allows the squid to look larger and more threatening to predators (Hanlon and Messenger, 1996; Staudinger et al., 2011), an option that planktonic paralarvae do not have given their inherently small size and more limited coloration palette. This banded body pattern is also used by adult *D. pealeii* in combination with descending in the water column and laying on the substrate to hide from cruising predators (Staudinger et al., 2011). The *L. brevis* examined in this study did not demonstrate the behavior of dropping to the substrate. Instead they remained high in the water column throughout their behavioral response to the predator. Conceivably, this was because flounder typically have an ambush style of attack, where they remain camouflaged until striking,

as suggested by Staudinger et al. (2011). However, the majority of attacks made by the flounder in this study were not ambush style. The flounder were usually active and visible prior to striking, and they began their attack from as far as 1.1 m away from the squid. It is likely, nonetheless, that if a different type of predator was used, the brief squid would have shown this behavior as well (i.e., dropping to substrate), as *L. brevis* and *D. pealeii* share similar ecological niches and therefore have likely adapted similar anti-predator tactics.

Although the direction of the predator's approach did play a role in the behavior of the juvenile and adult squid, it did not affect the behavioral response of paralarvae. These differences are likely the result of an underdeveloped sensory system in paralarvae (Chen et al., 1996), particularly the polarized lateral line analogue, which plays an integral role in successful predator detection (Chapters 2 and 3; York and Bartol, 2014). The lateral line analogue runs in an anterior-posterior direction along the head and each of the arms of the squid (Budelmann and Bleckmann, 1988). The wake of predators approaching the squid from different angles clearly will trigger different hair cells along the head and arms, potentially eliciting graded behavioral responses depending on the number and location of hair cells stimulated. Given that the paralarvae considered in the present study were only one day old and their sensory systems were not fully developed (Chen et al., 1996), it is conceivable that the lateral line analogue was not yet sufficiently integrated with neural processing centers to affect a wide range of behaviors based on the direction of the predator's approach. However, as shown in Chapter 3, the lateral line is nonetheless important for predator detection and survival at early ontogenetic stages, even if their behavioral repertoire is limited. Clearly, further research is needed to fully understand how hydrodynamic cues stimulate the lateral line analogue and how this input contributes to behavioral escape responses throughout ontogeny.

Throughout all of the predator-prey interactions, 80% of the juvenile/adult squid were oriented arms-first in an angular position (θ) between 0° and 90° relative to the oncoming predator, with an average θ of 57º. Paralarvae were also likely to orient themselves in an arms-first position with an average θ of 42°. By facing the predator anteriorly, the squid can perform a fast escape jet in a tail-first heading, an orientation that contributes to higher swimming speeds with greater aperture throughput for jet ejection relative to the arms-first mode (Bartol et al., 2001b; Bartol et al., 2009a; Bartol et al., 2009b). Additionally, this position is advantageous for sensory perception, especially for optimal orientation of epidermal hair cells. Fish that move much faster or slower than a predator orient laterally to the predator and execute a fast start at a right angle form the predator's heading to maximally increase their distance from the predator (Weihs and Webb, 1984), which was supported by Stewart et al. 2014 (Stewart et al., 2014). The squid in this study, however, squid mostly oriented themselves anteriorly to the oncoming predator, not laterally. This strategy makes sense in light of the morphological differences between the fish and squid mechanoreceptors. Unlike fish that have mechanoreceptors along the length of their bodies, squid have lateral line analogue hairs only along the head and arms but not the mantle. Thus, if squid were to position themselves laterally to the predator, a more limited portion of the lateral line analogue would be receiving direct hydrodynamic cues from the predator's approach. By positioning themselves anteriorly to the predator, they are exposing the maximum area of epidermal hair cell lines in the direction of the oncoming predator. Furthermore, the proportion of total inking events varied based on the angular orientation of the squid relative to the approaching predator, with anterior and lateral approaches (46-90º) triggering more inking and escape events than approaches from other angles, potentially

indicating that hydrodynamic cues received by the lateral line analogue play a role in inking behavior.

The anti-predator behavioral responses recorded for juveniles and adults in this study are consistent with previous research (Hanlon et al., 1994; Hanlon et al., 1999; Mather, 2010; Staudinger et al., 2011). Staudinger et al. (2011) found that the likelihood of survival when adult *D. pealeii* exhibit deimatic postures and inking events increases when confronted by a predator. In *D. pealeii* deimatic posturing involves having the arms and tentacles extended, which is similar to the 'splayed arm' posture observed in the present study for *L. brevis*, making the squid appear larger and more threatening. When this posture is exhibited in *D. pealeii*, 88% of the attacks are abandoned by the predator (Staudinger et al., 2011), indicating it is a successful anti-predator strategy to employ in the earliest stages of the predator's approach. We also found a high level of predator abandonment (51%) when a splaying arm or raised arm posture was exhibited. Posturing was employed when the predator was far away, while inking was used at shorter distances. When the predator was close and approaching at high velocities, the squid exhibited an inking response and escape jet, behaviors that have been shown to provide a high probability of escape (Staudinger et al., 2011). All of the juvenile and adult squid used in this study avoided capture, indicating that their suite of anti-predator behaviors is extremely effective.

Cephalopods undergo enormous morphological and ecological transitions as they develop from planktonic paralarvae to larger, more neurologically advanced adults. Each life stage has unique challenges that demand effective strategies for survival. This study is the first to examine anti-predator behavior of squid throughout ontogeny. Our findings indicate that anti-predator behavior of squids changes throughout development, with divergent strategies used in the

paralarval and juvenile/adult stages. Paralarvae had fewer behavioral responses directly linked to an oncoming predator compared with juvenile/adult stages, and tended to maintain a clear body pattern while either escape jetting or demonstrating stereotyped swimming behaviors, making them elusive to predators. Juveniles and adults, on the other hand, were adept at varying their response according to the predator approach and balancing the energetic requirements of escape with the urgency of the situation. The observed variances in anti-predator strategy indicate that squid utilize suitable adaptations for their changing morphology and ecological niche to maximize survival throughout ontogeny.

CHAPTER 5

HYDRODYNAMICS AND KINEMATICS OF ESCAPE JETS THROUGHOUT

ONTOGENY

INTRODUCTION

Escape responses are used by many animals as their primary survival tactic against

predation (Bullock, 1984). Typically, escape responses are characterized by extremely fast

reaction times and high accelerations (Domenici et al., 2011). A number of species, including

scallops (Cheng and DeMont, 1996; Cheng et al., 1996; Dadswell and Weihs, 1990), jellyfish

(Daniel, 1983; Daniel, 1985; Demont and Gosline, 1988; Katija et al., 2015), salps (Bone and

Trueman, 2009; Madin, 1990) and frogfish (Fish, 1987) accomplish an escape response through

jet propulsion. Cephalopods, including the chambered *Nautilus*, octopuses, cuttlefishes and

squids, are well known for their rapid escape jet responses. Unlike many octopuses and

demersal cuttlefishes that can burrow and hide from predators, squids reside exclusively in the

water column throughout ontogeny with predators approaching them from all directions. Thus,

they require highly effective escape responses for survival.

The jet propulsive escape response of squids is produced by the rapid expulsion of water

from the mantle cavity through a funnel aperture (O'Dor, 1988; Packard, 1969; Young, 1938).

Water is drawn into the mantle cavity around the sides of the head through intakes via mantle

expansion produced by radial muscle contraction and elastic recoil of connective tissue fibers.

Circular muscles in the mantle then contract to pressurize the water in the mantle cavity,

resulting in the closure of the intakes (Young, 1938). A high velocity jet is produced when water

is forcibly expelled through the funnel, which has relatively small cross-sectional area. The

funnel is flexible and capable of vectoring the jet within a hemisphere below the body, which can

propel the animal in various directions (Bartol et al., 2001a). Estimates of peak jet velocity

range from 2.9 - 6.9 m/s for octopus and cuttlefish and 6.7 - 11 m/s for squid (Shadwick, 1995).

These high velocity jets accelerate the animal, allowing for quick evasions from oncoming

predators. The axonal system of cephalopods together with their muscular hydrostatic systems

(i.e., mantle and funnel) presumably allow for control of the animal's trajectory, ejected water

volume, and flow speed of escape jets (Otis and Gilly, 1990), though variation in escape jetting

has not been documented to date.

Although the hydrodynamics of squid escape jets have not been examined extensively, a

number of studies have focused on steady routine jet propulsion in squid, with studies of both

swimming energetics (Bartol et al., 2001a; Finke et al., 1996; O'Dor, 1982; O'Dor, 2002; O'Dor

and Webber, 1991; O'Dor and Webber, 2011; Thompson and Kier, 2001; Webber and O'Dor,

1986; Wells and O'Dor, 1991) and hydrodynamics (O'Dor, 1988; Anderson and DeMont, 2000;

Bartol et al., 2001b; Anderson and Grosenbaugh, 2005; Bartol et al., 2008; Bartol et al., 2009a;

Bartol et al., 2009b; Stewart et al., 2010; Staff et al. 2014; Bartol et al., 2016). Many of the

recent hydrodynamic studies have quantified velocity vector fields around steadily swimming

squid and explored propulsive efficiency based on velocimetry measurements (Anderson and

Grosenbaugh, 2005; Bartol et al., 2008; Bartol et al., 2009a; Bartol et al., 2009b; Bartol et al.,

2015), some of which have shown that flows from the fins and jet can involve complex vortical

flows (Bartol et al., 2009a; Bartol et al., 2009b; Stewart et al., 2010; Bartol et al., 2016).

However, to date, no study has explicity considered the hydrodynamics of the escape jet and how

escape jetting may change throughout ontogeny.

During ontogeny, squid undergo major morphological and physiological changes that

affect their locomotive abilities (Boyle and Boletzky, 1996). While squid do not experience a

distinct metamorphosis, and therefore do not have true larva (they are known as paralarvae (Shea and Vecchione, 2010)), hatchlings are ecologically distinct from older life history stages (Robin et al., 2014; Shea and Vecchione, 2010; Young and Harman, 1988). Moreover, relative to the adult, paralarvae have a more rounded mantle, relatively smaller arms, a proportionally larger funnel, and rudimentary fins (Boletzky, 1974; Okutani, 1987; Packard, 1969). Paralarvae also hold a proportionally greater volume of water in their cavities and have shorter thick filaments in the mantle muscles to provide jetting power (Gilly et al., 1991; Preuss et al., 1997b; Thompson and Kier, 2001; Thompson and Kier, 2006). Ecologically, paralarvae differ from older squid in that they cover shorter overall distances by active swimming driven primarily by the jet (Bartol et al., 2009a), move through the water column in diel vertical migrations (Boyle and Boletzky, 1996; Robin et al., 2014), and reside in an intermediate Reynolds number (Re) regime (Re~1-10^2) (Bartol et al., 2008; Bartol et al., 2009a; Thompson and Kier, 2002; Webber and O'Dor, 1986). Conversely, many juvenile and adult squids are capable of powerful and long distance locomotion covering significant horizontal distances, generally employ less vertical migratory behavior (Boyle and Rodhouse, 2008), and operate in a higher Re regime (Re~$10^3 - 10^6$) (Bartol et al., 2009b; O'Dor, 1988).

Bartol et al. (2008, 2009a, 2009b) have shown that several different types of jet flow patterns are produced by squid of different life history stages during steady rectilinear swimming. In juvenile and adult brief squid *L. brevis*, two principal jet modes occur: (1) *jet mode I*, where ejected fluid rolls into an isolated vortex ring and (2) *jet mode II*, where ejected fluid forms into a leading vortex ring that pinches off from a long trailing jet (Bartol et al., 2008; Bartol et al., 2009b). *Jet mode I* is associated with greater propulsive efficiency, lower slip and higher frequency of fin activity, while *jet mode II* is associated with greater time-averaged thrust

and lift forces and is used more heavily than the first jet mode. *D. pealeii* paralarvae produce steady jets consisting of elongated vortical ring structures but with no clear leading ring pinch-off, as is the case in *jet mode II* of larger size classes (Bartol et al., 2009a; Bartol et al., 2009b). Bartol et al. (2009a) suggested that the absence of pinch-off may be a product of either (1) viscous diffusion blurring the separation between the ring and jet or (2) vortex ring formation being preempted by viscous diffusion such that a vortical tail remains behind the ring (Bartol et al. 2009b). Bartol et al. (2008, 2009a, 2009b) found that not only do flow features differ between paralarval and juvenile/adult squid, but that paralarval squid also have higher propulsive efficiency during jet ejection than older squid during steady swimming when considering the whole range of modes.

In this study we expand upon our knowledge of squid hydrodynamics by focusing on high velocity escape responses throughout ontogeny. We use 2D and 3D velocimetry and high-speed videography to study flow features and kinematics of escape jets. The primary objectives of this study were to: 1) document kinematics of escape jetting, 2) examine escape jet velocity and vorticity and 3) compute propulsive efficiency of escape responses using direct measurements of bulk properties of the jet wake. These objectives were examined along a continuum of life history stages from paralarvae to adults.

MATERIALS AND METHODS

Paralarval *Doryteuthis pealeii* (dorsal mantle length (DML) = 0.18 cm) and juvenile (DML= 3.0-5.0 cm) and adult *Lolliguncula brevis* (DML = 5.1-7.0 cm) were used for this research. Little information is currently available on the breeding habits of *L. brevis*, and they are extremely difficult to obtain as hatchlings. Therefore, *D. pealeii* was selected to study early

ontogenetic stages. *D. pealeii* is a reasonable substitute for *L. brevis* because both species have similar body size, fin size and shape, and ecological niches as paralarvae (Bartol et al., 2008).

D. pealeii eggs were purchased from the Marine Biological Laboratory, Woods Hole, MA, and maintained in floating buckets with mesh openings within a recirculating seawater system at a salinity of 30-32‰ and at temperatures of 19-24°C until hatching. Once the eggs hatched, the paralarvae were separated so that their age could be tracked. *L. brevis* used in this project were captured by otter trawl in Wachapreague, VA, USA. Trawls were conducted in August, September and October as the catch probabilities are highest in these months (Bartol et al., 2002). After capture, squid were transferred to a 114 L, circular holding tank (Angler Livewells, Aquatic Eco-Systems, Inc., Apopka, FL, USA) fitted with a portable battery powered aerator (Model B-3, Marine Metal Products Co., Inc., Clearwater, FL, USA) for transport to the lab. Squid were maintained in 450-gallon seawater systems with several forms of filtration (e.g., BioBalls, protein skimmers, ozone filtration, etc.). Seawater was maintained at temperatures and salinities equivalent to those of the capture sites (19-22 °C; 30-35 ‰). A moderate current flow was maintained to promote active swimming and squid were fed a diet of live *Palaemonetes pugio* and *Fundulus heteroclitos* as suggested by Hanlon et al. (Hanlon, 1990; Hanlon et al., 1983). Squid were allowed to acclimate for at least 24 h prior to experimental trials. Only animals that appeared healthy and that exhibited normal behaviors were used.

Paralarvae DPIV Experiments

Digital particle image velocimetry (DPIV) has been successfully used to collect hydrodynamic data in paralarval squid (Bartol et al., 2009b; Bartol et al., 2008). We followed similar protocols to these studies, but provide a generalized overview of our approaches here for

convenience (see above papers for greater detail). For experimental trials, 3-8 paralarvae were added to a Plexiglas holding chamber (4.0x6.0x2.5 cm). Multiple squid were added to the chamber to increase the probability of imaging an escape jet within a limited field of view. A total of 52 trials were performed and a total of 170 animals were considered. The chamber was filled with seawater (30-32‰, 16-19°C) seeded with neutrally buoyant, silver-coated hollow glass spheres (mean diameter=14 µm, Potters Industries, Valley Forge, PA, USA). The spheres were illuminated within a 0.5-2.0 mm parasagittal plane using two (A and B) pulsed Nd:YAG lasers and a laser optical arm (wavelength-532 nm, power rating= 350mJ pulse^{-1}; LABest Optronics, Beijing, China). Each laser was operated at 14 Hz (7 ns pulse duration) with a 1-4 ms separation between laser A and B pulses. A UNIQ UP-1830CL video camera (1024 x 1024 pixel resolution; paired images collected at 15Hz; Uniq Vision, Inc., Santa Clara, CA, USA) outfitted with a VZM 450i zoom lens (Edmund Optics, Barrington, NJ, USA) and interfaced with a CL-160 capture card (IO industries, Inc., London, Ontario, Canada), which was used for image acquisition.

In addition to the UNIQ UP-1830CL video camera, two high-speed DALSA Falcon video cameras (Teledyne Dalsa, Inc., 1400 x 1200 pixels, 100 fps), each outfitted with Fujinon CF25HA-1 25 mm lenses, were used. To prevent over exposure of frames from the laser, each high-speed camera was fitted with a filter to block 532 nm wavelengths. One camera was positioned above the working section to record images from a dorsal perspective and the other was positioned directly beside the UNIQ camera for an expanded lateral field of view. A series of 40W lights equipped with a filter to transmit wavelengths >600 nm provided illumination for the high-speed DALSA cameras. A Kodak Wratten 58 green filter that transmits wavelengths of

410-600 nm was mounted to the UNIQ UP-1830CL video camera to prevent over exposure from the 40W halogen lights.

For analysis of the DPIV data, each image was subdivided into a matrix of 32x32 pixel interrogation windows. Using a 16 pixel offset, cross-correlation was used to determine the particle displacement within interrogation windows comprising the paired images. These cross correlations were performed in *Pixelflow*^{TM} software (FG Group LLC, San Marino, CA, USA)(Willert and Gharib 1991). Particle shifts that were three pixels greater than their neighbors were removed as outliers and the data were smoothed to remove high frequency fluctuations. Using *Pixelflow*^{TM} software, velocity vector and vorticity contour fields were determined. Window shifting was performed to improve the accuracy of the results (Westerweel et al., 1997).

Juvenile and Adult Experiments

Animals considered in these experiments included juvenile (N=22) and adult (N=26) *L. brevis*. For experimental trials, a water tunnel with a 15x15x44 cm working section (Model 502(s) Engineering Laboratory Design, Lake City, MN, USA) was filled with seawater seeded with 50 μm plastic polyamide light reflective particles (Dantec Dynamics, Skovlunde, Denmark) and matching conditions in the squid's holding tanks (salinity=30 ppt, temperature= 24°C, pH= 8-8.2, and ammonia levels <0.2 ppm). Each animal was added to the tunnel and allowed to acclimate for 5 minutes under low flow (3 cm s^{-1}) conditions before beginning trials. After the animal had acclimated to the water tunnel, the flow velocity was increased to prompt swimming. A range of tunnel speeds from 2-7 cm s^{-1} were presented to the squid in the tunnel. Escape jets were generally elicited by startling the squid using laser pulses, although some escape jet sequences were also recorded without laser provocation. All of the escape jets analyzed in this

study involved squid swimming against the flow with minimal change in vertical position over the jet cycle period.

Defocusing digital particle tracking velocimetry (DDPTV) data were collected together with kinematic data (see description below) for juvenile/adult size classes. The DDPTV technique and hardware were developed by Dr. Morteza Gharib's lab (California Institute of Technology, Pasadena, CA, USA) at Caltech with further commercial development by TSI, Inc. and is currently marketed as the V3V^{TM} system. For DDPTV data collection, a 14x14x10 cm region of the working section was illuminated using two pulsed Nd:YAG lasers (wavelength= 532 nm; power rating 350 mJ/pulse; LABest Optronics Co. Ltd., Beijing, China), each operating at 14 Hz (7 ns pulse duration) with a 0.5-2.0 ms separation between pulses. A V3V-8000 camera probe (TSI, Inc., Shoreview, MN, USA; three 12-bit, 2048x2048 pixel resolution cameras) was positioned orthogonally to the working section. Paired DDPTV images ($\Delta t \approx$ 0.5-2.0 ms) of the flow around the animal were captured at 7 Hz using a hyper-streaming image transfer and computer system.

Identification of 3D particle locations and calculation of particle displacements were performed using INSIGHT 4G V3V software (TSI, Inc., Shoreview, MN, USA) using approaches described in Pereira et al. (2000) and Troolin and Longmire (2009). On average, 100,000 particles were identified in each image with triplet yields of approximately 50,000-60,000 (50-60%). Using a relaxation method for particle tracking (Pereira et al., 2006) available within the INSIGHT 4G V3V software, approximately 18,000-25,000 particle vectors were obtained in the imaging volume. The vectors were interpolated onto a structured grid using a Gaussian weighting interpolation available in the software. A voxel size of 16 mm, percent overlap of 95% and a smoothing factor of 1.5 were used for the Gaussian weighting interpolation

in these experiments. Velocity vector fields were calculated using the INSIGHT 4G V3V

software.

During DDPTV experiments, high-speed video was collected using 3 high-speed DALSA

Falcon video cameras (Teledyne Dalsa, Inc., Waterloo, Ontario, Canada; 1400x1200 pixels, 100

fps). The cameras were positioned to view the squid from lateral and ventral perspectives in the

working section of the water tunnel. A series of 2-4 500 watt halogen lights, equipped with

optical filters having low transmission at 532 nm, provided illumination. To prevent

overexposure from the pulsed Nd:YAG laser (wavelength=532 nm), a notch filter to block 532

nm wavelengths was used with each Falcon camera. The V3V-8000 probe was also outfitted

with optical filters that transmitted wavelengths of 532 ± 5 nm so only laser light illuminated the

DDPTV CCD sensors. Two PCI NI-6602 timing boards, 2 BNC-2121 breakout boxes, and NI

timing software (National Instruments, Austin, TX, USA) were used to send timing signals to the

Falcon cameras, TSI synchronizer and BNC-565 pulse generator (Berkeley Nucleonics, San

Rafael, CA, USA). The synchronizer and pulse generator in turn sent triggering signals to the

V3V probe and Nd:YAG lasers, respectively.

Kinematic Analysis

Frame-by-frame position tracking of the squid body features was accomplished using

image tracking software (Hedrick, 2008). Five points were tracked on the paralarval squid: (1)

the squid eye, (2) the dorsal edge of the widest point of the mantle, (3) the ventral edge of the

widest point of the mantle, (4) the tip of the funnel and (5) the base of the funnel. The tracked

points were used to calculate several kinematic variables including: (1) mantle diameter changes,

(2) contraction and refill periods, (3) funnel angle, (4) mean velocity, (5) peak velocity, and (6)

peak acceleration. Swimming velocities of paralarvae were determined by dividing net displacement over the path of travel over complete jet cycles by the jet cycle period. Due to low resolution, fin motions and funnel diameter changes could not be determined.

For the juveniles and adults, six points were tracked: (1) the squid eye, (2) the most anterior point of the funnel opening, (3) the most posterior point of the funnel opening, (4) dorsal edge of the widest point of the mantle, (5) ventral edge of the widest point of the mantle, and (6) the tip of the fin at maximum chord length. The tracked points were used to determine the following kinematic variables: (1) mantle diameter changes, (2) contraction and refill periods, (3) funnel angle, (4) mean velocity, (5) peak velocity, (6) peak acceleration, (7) displacement of the fins and (7) diameter of the funnel. Swimming velocities of juveniles and adults were determined by measuring net displacement along the x-axis over complete jet cycles divided by the cycle period and adding this to the background water tunnel speed. Using a Matlab routine developed in house, acceleration, velocity and mantle diameter were calculated and smoothed with a fourth order Butterworth filter using a cutoff frequency between 3-5 Hz.

DPIV Analysis

Most of the approaches used for paralarval DPIV analysis are similar to those presented in Bartol et al. (2009a). For convenience, we report on the key features of the analysis below. Several Matlab (Mathworks, Inc., Natick, MA, USA) routines were developed in-house and used to calculate hydrodynamic impulse and kinetic energy. For the 2D DPIV data, axisymmetry about the axis of a shed vortex's jet centroid was assumed. The slope and y-intercept of the jet centerline were determined based on a best fit of the velocity and vorticity data. The length of the jet (L) was the extent of the velocity field above a set threshold of 0.2 along the jet centerline.

Using the angled centerline as the r = 0 axis, jet impulse (I) and kinetic energy (E) were

calculated using the following equations:

$$\frac{I}{\rho} = \pi \int \omega_\theta r^2 drdx \quad (1)$$

$$\frac{E}{\rho} = \pi \int \omega_\theta \psi drdx \quad (2)$$

where ω_θ is the azimuthal component of vorticity, r is the radial coordinate, I is the impulse

magnitude (directed along the jet axis) and ρ is the fluid density. The length of the jet was

computed based on the extent over which the jet vorticity field was above a specified magnitude

of 0.5 (L_ω) and the jet diameter was determined based on the distance between vorticity peaks

perpendicular to the jet centerline in the leading vortex ring at the beginning of the jet (D_ω).

Using the direction of squid motion during mantle contraction, which was measured using the

high-speed kinematic data, and the jet angle to the horizontal, the component of the impulse

aligned with the direction of displacement was computed. Thickness of the laser sheet varied

from 0.5-2.0 mm. Given that velocity field measurements are depth averaged over the laser sheet

thickness and laser thickness is similar in dimension to that of the funnel, a convolution

adjustment is needed for accurate velocity and vorticity measurements. Therefore, an interative

deconvolution algorithm described in Bartol et al. (2009) was applied to all velocity/vorticity

fields to estimate the non-averaged flow field on the jet midplane.

DDPTV Analysis

Most of the approaches used here for juvenile and adult DDPTV analysis are similar to

those presented in Bartol et al., (2016). For convenience, we report on the key features of the

analysis below. For the 3D DDPTV data, the jet impulse (I) was computed using the following equation:

$$\frac{I}{\rho} = \frac{1}{2}\int x \times \omega\, dV \quad (3)$$

where x is the position vector, ω is the vorticity vector ($\omega = \nabla \times u$ and u is the velocity vector), ρ is the fluid density, and the integral is computed over the volume of the vortex. The 3D volume surrounding the vortex of interest was selected using a graphical user interface (GUI) developed in-house in Matlab and the integral was computed over this volume to minimize the influence of measurement noise near the flow of interest. Since impulse is the time integral of the force vector that generated the flow, the average thrust vector (magnitude *and* 3D direction) was determined by dividing I by the period of the flow generation (T). Time-averaged jet thrust ($\bar{F}_{jt}$) was calculated using

$$\bar{F}_{jt} = -I \cdot \hat{x}/T \qquad (4)$$

where $\hat{x}$ is the unit vector opposite the direction of tunnel flow and T is the jet period of interest (see below). The negative sign is included because equation (3) computes the fluid impulse and the impulse applied to the squid is in the opposite direction by Newton's Third Law. For each escape jet, the length of jet vorticity field (L_ω) and distance between vorticity peaks perpendicular to the jet centerline (D_ω) were measured in the xy plane using ImageJ software (Rasband, W.S., ImageJ, U. S. National Institutes of Health, Bethesda, Maryland, USA, http://imagej.nih.gov/ij/, 1997-2015 (D_ω).

Several different approaches for calculating kinetic energy (E) of the jet wake are described by Bartol et al. (2016). Kinetic energy in the present study was computed using:

$$E/\rho = \frac{1}{2} \int |u|^2 \, dV \tag{5}$$

where $|u|$ is the velocity magnitude. The advantage of this approach is that it will always give a positive value for E. The disadvantage is that it does not necessarily isolate the E associated with only the vortex of interest because of the influence of the surface integral term. One consequence is that equation (5) provides a conservative measurement of the kinetic energy because the selected region can contain flow from neighboring vortices and any background noise in the selected region will increase the computed energy value. In application of equation (5), the background flow velocity was subtracted from the local velocity vector prior to computing the kinetic energy because only the excess kinetic energy is relevant for propulsive efficiency.

Propulsive Efficiency

Paralarvae tend to swim predominantly upward (vertical in the water column) during mantle contraction and sink during refilling (Fig. 17). Since we are interested in work done by the propulsive system, and not gravity, the effect of gravity on the net motion was factored out by considering only motion during jet ejection. To compare jet propulsive efficiency for paralarvae with that of juveniles and adults, which swim more horizontally, propulsive efficiency was computed for only the exhalant phase of the jet cycle using the equation:

$$\eta_{\rho(jet)} = \frac{\widetilde{F}_j x}{\widetilde{F}_j x + E} \tag{6}$$
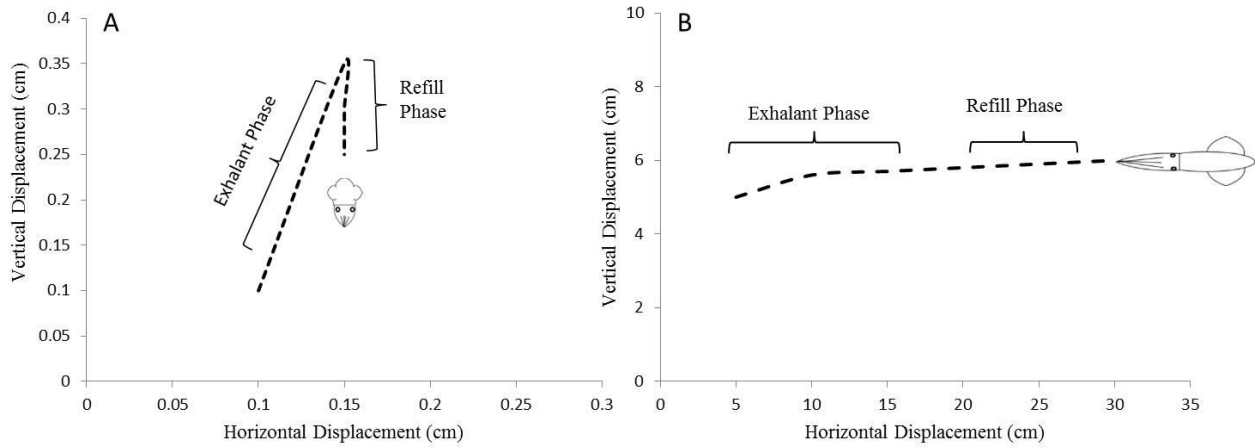
Figure 17. The exhalant and refill phase of A) the vertically oriented escape jet trajectory of a paralarvae and B) the exhalant and refill phase of the horizontally oriented trajectory of juveniles and adults. Only the exhalant phase was considered for propulsive efficiency comparisons across ontogeny.

where $\widetilde{F_j}$ = jet thrust time averaged over the mantle contraction (N), x = displacement during mantle contraction (m), and E = total excess kinetic energy of the jet (J). Time averaged jet thrust was determined by dividing the impulse ($N{\cdot}s$) component in the direction of displacement (variable for paralarvae; horizontal against free-stream for juveniles/adults) by the mantle contraction period (s), i.e., the mantle contraction period is T in equation 4.

RESULTS

Escape Jetting through Ontogeny

A total of 59 escape jets were considered for this study, including 29 paralarval jets, 12 juvenile jets, and 18 adult jet sequences. Only sequences in which the animal was away from the free-water surface or working section walls were analyzed. All of the data presented are for tail-first escape jets. In paralarvae, the mean mantle contraction period was 0.07 ± 0.02 s, which was only 21% of the mean total jet period of 0.32 ± 0.4 s; in juveniles, the mean mantle contraction period was 0.24 ± 0.28 s, which was 35% of the mean total jet period of 0.68 ± 0.21 s; and in adults, the mean mantle contraction period was 0.27 ± 0.02 s, which was 36% of the mean total jet period of 0.73 ± 0.14 s. Significant differences were found between kinematic variables throughout ontogeny (MANOVA: $F_{8,82} = 28.34$, p>0.001, Wilk's $_\Delta = 0.71$, $\eta^2=0.112$). The mean average squid swimming velocity was significantly different among the size classes ($F_{2,59}=46.27$, p<0.001), with the paralarvae having a higher relative average velocity (33.51 ± 13.79 DML s^{-1}; range=10.47-67.04 DML s^{-1}) than both the juveniles (7.82 ± 2.88 DML s^{-1}; range=2.48-10.88 DML s^{-1}; p<0.001) and adults (4.24 ± 1.84 DML s^{-1}; range= 1.80-8.39 DML s^{-1}; p<0.001). The mean peak swimming velocity was also significantly different across the size classes ($F_{2,59}=27.20$, p<0.001), where paralarvae showed higher relative peak swimming velocities

(52.80±28.25 DML s^{-1}; range= 12.11–120.28 DML s^{-1}) than juveniles (7.98±3.04 DML s^{-1}; range=4.81–12.00 DML s^{-1}; p<0.001) and adults 4.56±2.84 DML s^{-1}; range=1.70-11.18 DML s^{-1}; p<0.001). Additionally, significant differences were found in peak acceleration among the three size classes (F$_{2,59}$=15.36, p<0.001). Paralarvae had significantly higher peak acceleration (874.49±692.04 DML s^{-2}; range= 125.06-2936.28 DML s^{-2}), than juveniles (58.27±18.09 DML s^{-2}; range= 33.34-78.91 DML s^{-2}; p=0.002) and adults (35.26±26.77 DML s^{-2}; range= 13.36-98.96 DML s^{-2}; p<0.001). The funnel angle (relative to the horizon) at the beginning of the jet was significantly different between ontogenetic groups (F$_{2,59}$=146.79, p<0.001), with paralarvae having a higher funnel angle (76.34±13.64°) than juveniles (14.86±2.72°) and adults (20.84±8.09°).

Escape jets consisted of vortical regions of variable length. Two different hydrodynamic patterns were observed: (1) *escape jet I*, where the jet structures consisted of spherical vortex rings with an L$_\omega$/D$_\omega$<3, and (2) *escape jet II*, which consisted of elongated trails of concentrated vorticity and an L$_\omega$/D$_\omega$>3 (Table 2). An L$_\omega$/D$_\omega$ cutoff of three was used as jets with an L$_\omega$/D$_\omega$<3 formed a spherical vortex, while an L$_\omega$/D$_\omega$>3 typically had a trailing jet (Bartol et al., 2009b). These hydrodynamic patterns where observed in paralarvae (Fig. 18), juveniles and adults (Fig. 19). In juveniles and adults, some trailing jets (*escape jet II*) showed a long core of vorticity with no clearly discernible vortex ring structures, while others included several linked vortices, often with a leading edge ring structure. *Escape jet II* for paralarvae consisted primarily of long vorticity cores with no obvious leading edge vortex ring separation. No differences were found between the mean swimming velocity or acceleration between the two jet types throughout ontogeny (all p>0.05). For both types of jets, the peak in velocity was preceded by hyperinflation of the mantle and a forceful mantle contraction. Although not significant at p=0.05, *escape jet I*

exhibited a trend in shorter funnel aperture periods (0.06s) than *escape jet II* (0.13s)(t-test: t_5=2.60, p=0.08) in juveniles and adults (Fig. 20). Funnel aperture in paralarvae could not be measured due to low resolution, though the same pattern would likely be found. Throughout almost all of the juvenile and adult sequences, one fin flap occurred during the early stages of mantle contraction followed by a wrapping of the fins around the mantle for the remainder of the jet cycle. This pattern was repeated for each jet cycle. The thrust contribution from this fin flap was low compared to the more powerful jet. Although greater spatial resolution is necessary to fully resolve fin flows, the fin flow fields observed in this study for paralarvae were negligible relative to jet flows since they did not produce visible velocity fields.

Propulsive Efficiency through Ontogeny

The same three size classes (paralarvae, juvenile and adult) were considered for calculations of propulsive efficiency. Significant differences in propulsive efficiency were found among the three size classes (ANOVA: $F_{2,59}$=3.94, p=0.025). Tukey *post-hoc* tests revealed that paralarvae had higher propulsive efficiency (94.55±0.05%) than the adults (87.71±0.13%; p=0.03); however, neither paralarvae (p=0.98) nor adults (p=0.12) were found to have different propulsive efficiency than the juveniles (93.75±0.02%). In paralarvae, only 8 individuals produced *escape jet I* while 16 individuals produced *escape jet II*. No differences in propulsive efficiency were found between the two jet modes for paralarvae (t-test: t_{28}=0.89, p=0.40). Within the juveniles, equal numbers of individuals produced the two jet modes, with 6 juveniles producing *escape jet I* and 6 producing *escape jet II*. For the adults, however, only two individuals produced *escape jet I* while 17 produced *escape jet II*. Of the two hydrodynamic patterns in juveniles and adults, the short spherical vortex mode (*escape jet I*) had a higher

Table 2. Descriptive measurements of *escape jet I* and *escape jet II* in paralarvae, juveniles and adults

	Escape Jet I			Escape Jet II		
Size Group	L_{ω}/D_{ω} Mean	Swimming Velocity (DML s^{-1})	Propulsive Efficiency (%)	L_{ω}/D_{ω} Mean	Swimming Velocity (DML s^{-1})	Propulsive Efficiency (%)
Paralarvae	2.3±0.5	31.9±9.9	94.7±10.7	6.8±4.2	34.1±15.1	94.4±11.3
Juveniles	1.4±0.2	9.3±3.3	94.1±12.2	5.7±0.9	8.3±3.2	93.33±31.9
Adults	2.1±0.1	4.8±1.6	88.3±13.0	6.5±2.0	4.2±1.6	86.32±32.6
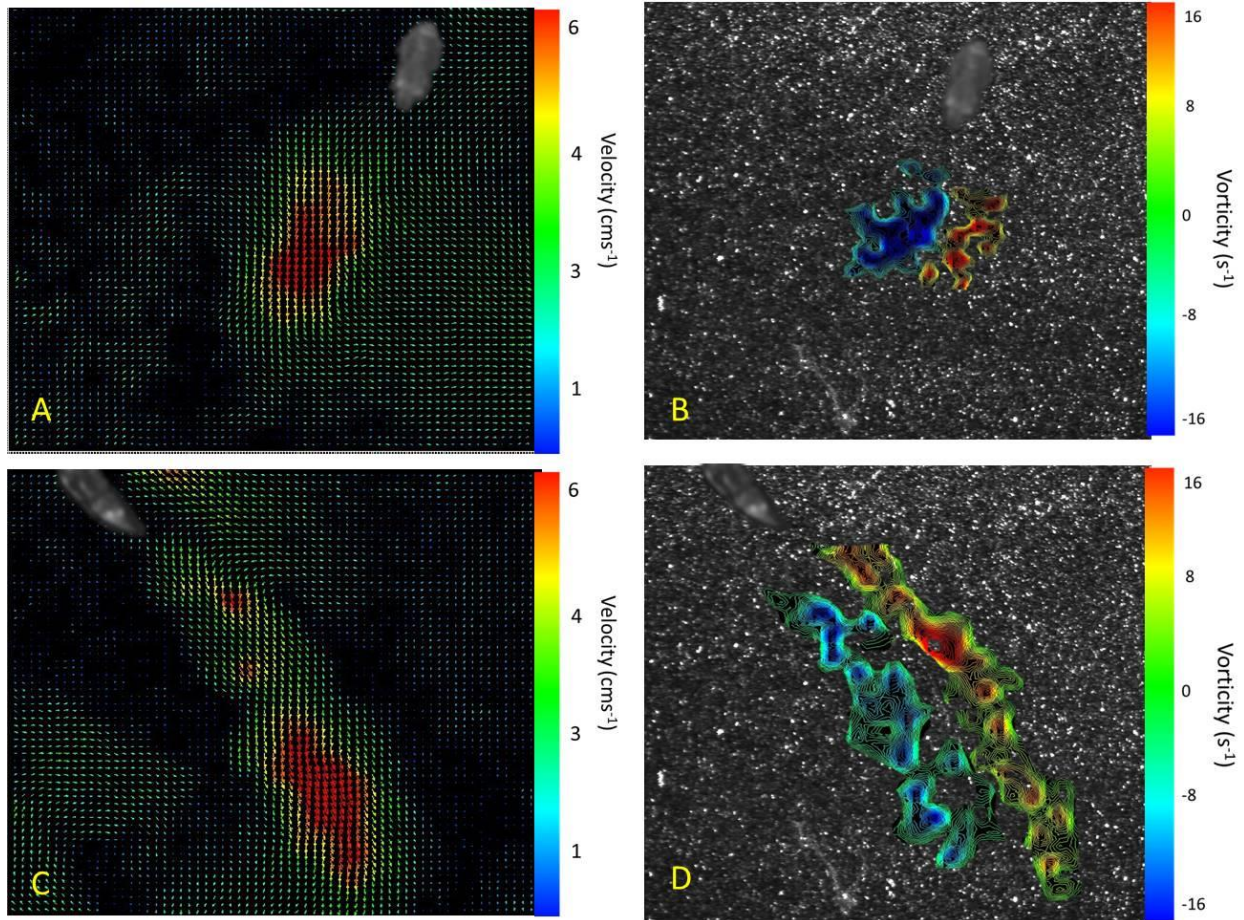
Figure 18. The two hydrodynamic jet modes observed in paralarvae *Doryteuthis pealeii*. A velocity vector field of *escape jet I* (A) (swimming velocity= 40.42 DML s^{-1}) with its corresponding vorticity contour field (B) (L_ω/D_ω= 2.77), and a velocity vector field of *escape jet II* (C) (swimming velocity= 30.11 DML s^{-1}) with its corresponding vorticity contour field (L_ω/D_ω= 16.91). The paralarvae in these images are 1.8 mm DML. Velocity and vorticity fields are based on the original data prior to deconvolution.
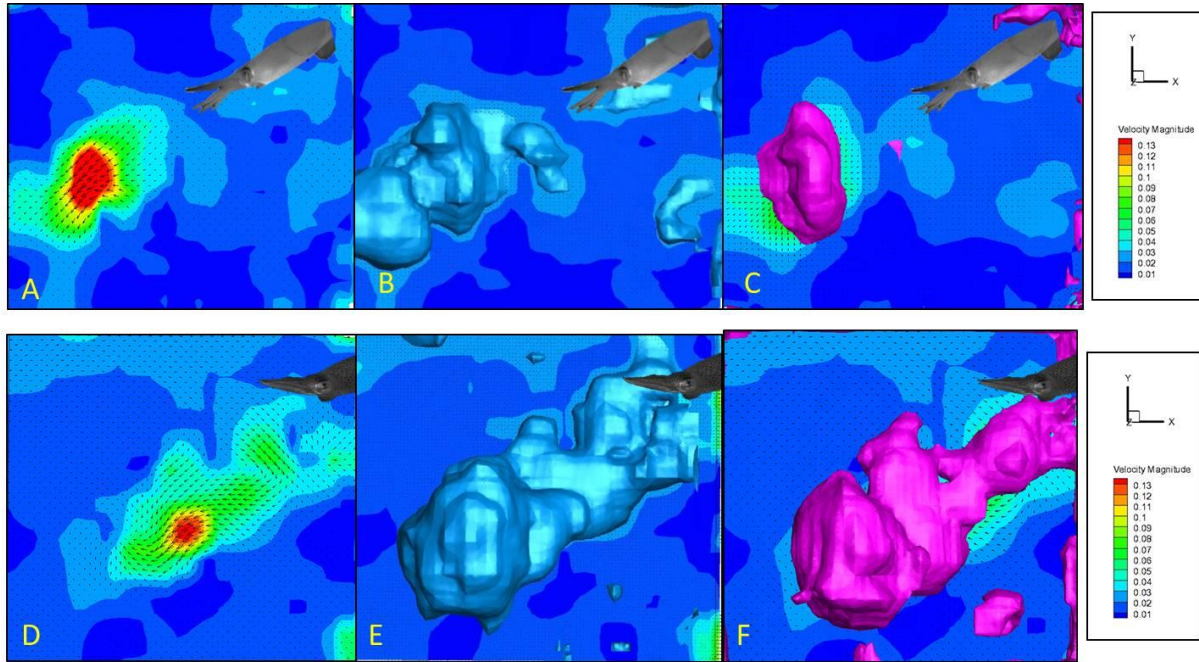
Figure 19. The two hydrodynamic jet modes observed in juvenile and adult *Lolliguncula brevis*. A 2D velocity vector field (A) (swimming velocity= 2.87 DML s^{-1}), velocity magnitude isosurface (B) and vorticity magnitude isosurface (C) of *escape jet I* (L_ω/D_ω=1.93)(DML =4.10 cm). A 2D velocity vector field (D) (swimming velocity= 7.95 DML s^{-1}), velocity magnitude isosurface (E), and vorticity magnitude isosurface (F) of *escape jet II* (L_ω/D_ω=5.97)(DML= 5.30 cm).
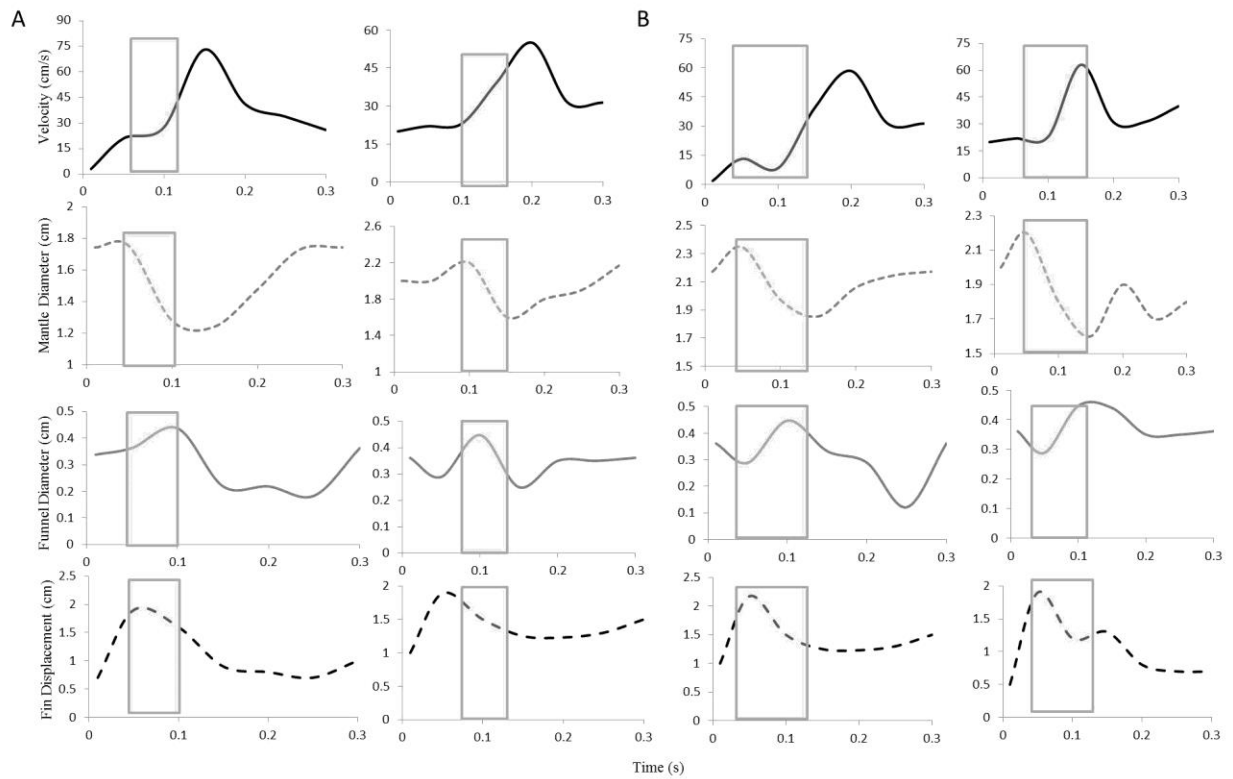
Figure 20. Swimming velocity, mantle diameter, funnel diameter, and fin displacement throughout the escape response for two examples of a pulsed vortex ring escape jet (*escape jet I*)(A) and a long escape jet (*escape jet II*)(B). Brief squid *L. brevis* ranging in size from 4.20 cm DML to 6.40 cm DML are depicted. Mantle contraction period is highlighted.
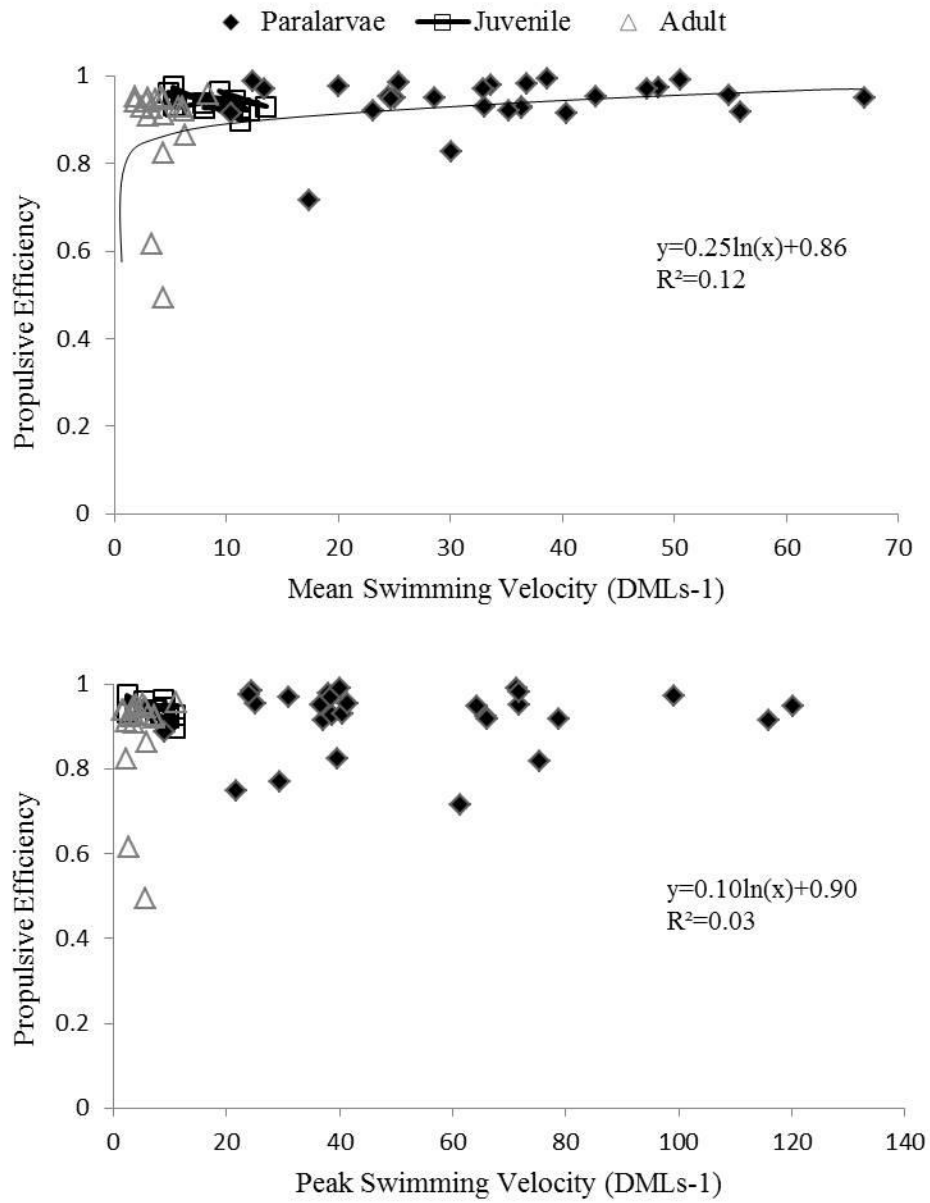
Figure 21. Propulsive efficiency plotted as function of mean velocity and peak velocity.

propulsive efficiency (94.84±8.05%) than jets with a large elongated vorticity core (*escape jet II*) (89.52±1.92%) (t-test: t_{29}=2.80, p=0.009). Propulsive efficiency increased as mean swimming speed increased (logarithmic regression: R^2= 0.12, p=0.01). However, propulsive efficiency did not necessarily increase as the peak velocity increased (R^2= 0.027, P=0.25; Fig. 21)**.**

DISCUSSION

The results of this study demonstrate that squid from all life history stages display locomotive flexibility when performing an escape jet. Throughout ontogeny, two distinct hydrodynamic patterns were produced (*escape jet I* and *escape jet II*). Although all life stages are capable of producing a similar range of flow patterns, there are important differences in propulsive efficiency and kinematics throughout ontogeny. The observed differences among paralarvae, juveniles and adults likely derive from morphological and ecological differences, as well as physical constraints associated with their Re environment. Paralarvae are largely planktonic, as opposed to juveniles and adults that are nektonic, and spend most of their time maintaining position in the water column or migrating vertically. Although paralarvae can reach impressive speeds, as documented in this study (peak velocity= 52.80±28.25 DML s^{-1}), they generally do not reach these speeds while swimming horizontally (Bartol et al., 2008). Instead, paralarvae are predominantly vertical swimmers, positively phototaxic and depend heavily on currents for horizontal displacement (Boletzky, 2003; Robin et al., 2014). This vertical swimming preference was reflected in the present study, whereby paralarvae used higher angle escape jets than juveniles and adults. Morphologically, the thick mantle muscle filaments that provide power for contractions are 1.5x shorter in paralarvae compared with juveniles and adults.

These shorter thick filaments allow paralarvae to contract their mantles at higher rates, including during escape jetting (Thompson and Kier, 2006). This is consistent with our finding that *D. pealeii* paralarvae have shorter contraction periods (0.07 ± 0.02 s) than juvenile and adult *L.brevis* (0.27 ± 0.02 s). Throughout ontogeny, the number and orientation of the mantle connective tissues fibers also change. These are important for limiting mantle deformation and storing elastic energy during jetting (Bone et al., 1981; Gosline et al., 1983; Macgillivray et al., 1999; Ward and Wainwright, 1972). Paralarvae swim in an intermediate Re fluid regime where both viscous and inertial forces are important (Bartol et al., 2009a). The mantle properties of paralarvae facilitate higher frequency mantle contraction, which is beneficial since coasting is inhibited in an intermediate Re regime, requiring constant jetting to translate. However, as juveniles and adults swim at higher Re, high rates of mantle contraction are less critical because gliding is more attainable as inertial forces increase.

Jet and fin kinematics

The paralarvae in this study showed significantly higher average escape jet velocities (33.51 ± 13.79 DML s^{-1}) than juveniles (7.82 ± 2.88 DML s^{-1}) and adults (4.24 ± 1.84 DML s^{-1}) when these jet velocities were normalized by dorsal mantle length. The same pattern was seen in peak velocity among the three size classes, where paralarvae reached 5x the peak velocity of juveniles and adults. Paralarvae also exhibited significantly greater peak acceleration than juveniles and adults. These results are consistent with the findings of Packard (1969), who found that *Loligo vulgaris* paralarvae exhibit maximum linear accelerations of 817 DML s^{-2} while juveniles reached accelerations of 316 DML s^{-2}, and adults only reached 162 DML s^{-2}. The ability of paralarvae to reach such high velocity and acceleration is a great advantage given the

high rate of predation at this early life history stage (Boyle and Rodhouse, 2008). The average

and peak velocities of the juveniles and adults reported here are lower than those reported in

other kinematic studies of *L. brevis*, where flow imaging was not involved (see Chapter 4).

These differences reflect some of the challenges of collecting DDPTV data, whereby the squid

are imaged in more confined experimental tanks.

Juveniles and adult *L. brevis* are capable of a wide diversity of fin motions ranging from

undulations to flapping (Bartol et al., 2001a; Hoar et al., 1994a; Anderson and Demont, 2010;

Bartol et al., 2008; Stewart et al., 2010; Bartol et al., in prep). Based on DPIV measurements of

the fin wake, Stewart et al. (2010) found that the fins of *L. brevis* function as stabilizers while

generating lift at low speeds and then shift to propulsors as speed increases during tail-first

swimming. During arms-first swimming, the fins primarily provide lift, playing a lesser role in

creating thrust (Stewart et al., 2010). Based on 3D velocimetry measurements, Bartol et al.

(2016) also found that the fins of *L. brevis* sometimes act as stabilizers, producing negative thrust

(drag), while consistently providing lift at low/intermediate speeds (<2.0 DML s^{-1}) to counteract

negative buoyancy. Both studies revealed that fin flows are complex during arms-first and tail-

first swimming, with Bartol et al (2016) providing 3D vorticity data of interconnected jet and fin

vortex flows. During escape jets, paralarvae, juveniles and adults typically only flapped their

fins once prior to mantle contraction in the present study, and subsequently wrapped them

around the mantle for the duration of the jet. Thrust production associated with these

synchronized flaps was low relative to the jet, particularly for paralarvae where the fin flows

were barely perceivable. This synchronized flapping pattern has been reported in other studies

(Bartol et al., 2001b; Hoar et al., 1994; O'Dor, 1988). The lack of complex fin activity and

appreciable thrust production during escape jets may be attributed to the constraints of the fin

musculature and its inability to produce high forces at the high shortening velocities required for

an escape jet (Kier, 1989; O'Dor and Webber, 1991). Nonetheless, when the goal is to escape a

predator for survival, every component of thrust, even limited thrust from the fins, adds to total

thrust and ultimately to escape. The consistent timing of the fin flap at the beginning of mantle

contraction is interesting as it suggests that the efficacy of the fin flap is maximized during this

narrow temporal window. It is also possible that, due to muscle constraints, the fins have limited

force they can apply and it is best to use this force at the beginning of the escape jet, when the

squid is moving slowly, to have the largest impact. This topic merits further exploration.

Propulsive efficiency

The measurements of propulsive efficiency derived from bulk properties of the jet wake

in this study indicate that paralarvae exhibit higher propulsive efficiency during jet ejection than

adult squid for escape jets. The efficiency advantage of paralarvae is a product of several factors.

In the present study, paralarvae produced a jet that is more aligned with the direction of motion

(mean paralarvae jet angle relative to direction of motion= 13.7°; mean juvenile/adult jet angle

relative to direction of motion= 18.7°). These results are consistent with Bartol et al. (2008,

2009a, 2009b), who considered propulsive efficiency throughout ontogeny for steady swimming

and found similar angle differences. As mentioned above, paralarvae also have larger funnel

apertures (Boletzky, 1974; Packard, 1969; Thompson and Kier, 2002), faster contraction

frequencies (8.6 mantle circumference lengths per second in paralarvae, versus 3.6 mantle

circumference lengths per second in adults)(Thompson and Kier, 2001) and hold proportionally

greater volumes of water in their mantle cavities (Gilly et al., 1991; Preuss et al., 1997b;

Thompson and Kier, 2001), which allow paralarvae to expel large volumes of water at relatively

low speeds but at high frequencies, all of which can improve propulsive efficiency (Bartol et al., 2009a).

The propulsive efficiencies reported in this study are in reasonable agreement to those reported in previous studies. Bartol et al. (2009a) found that paralarval *D. pealeii* have mean propulsive efficiencies of approximately 75% for speeds of 0.7–3.1 cm s^{-1} (Bartol et al., 2009a). The paralarval escape jets recorded here were higher (94.55%), but this is likely due to the consideration of higher swimming speeds (1.88-12.07 cm s^{-1}), as propulsive efficiency tends to increase with speed in squid (Bartol et al., 2009b, 2015). Indeed Bartol et al. (2009a) found that paralarvae have deconvolved propulsive efficiencies as high as 87.5% for speeds of ~2.5 cm s^{-1}. Using models and whole-cycle efficiency calculations, Staaf et al., (2014) reported efficiencies for ommastrephid paralarvae of ~20%. However, these results are difficult to compare directly to our results because they do not derive from direct bulk wake measurements of the wake and include a refill period penalty.

As was the case here for escape jetting, Bartol et al (2008) and Bartol et al. (2009a) found that paralarvae have higher propulsive efficiency than juveniles and adults during steady swimming. For steady swimming, mean propulsive jet efficiency of juveniles and adult *L. brevis* is ~64% based on DPIV measurements (Bartol et al., 2009b). In newer 3D analyses that incorporate both jet and fin contributions to steady swimming in *L. brevis,* overall propulsive efficiency was 65.5% (Bartol et al., 2016). In jellyfish (*Sarsia tubulosa*), swimming efficiency throughout ontogeny ranges from 56-75% (Katija et al., 2015). Our juvenile and adult escape jet mean propulsive efficiencies of 87.71% and 93.75%, respectively, are higher than the efficiencies above. However, when similar high-speed propulsive efficiencies are considered the values are in good agreement, with values as high as 91-96% being reported in Bartol et al.

(2009b, 2016). While not based on direct measures of the jet impulse and kinetic energy, propulsive efficiencies up to 93% were reported in adult *D. pealeii* when swimming at speeds >1.6 DML s^{-1} (Anderson and Grosenbaugh, 2005), which is similar to our highest recorded adult efficiency of 97%.

The use of different jet modes with dissimilar propulsive efficiencies in the present escape jet study is consistent with previous studies performed on steady swimming squid. In these prior studies, *Jet mode I*, where a well-defined spherical vortex is produced, has higher propulsive efficiency than *jet mode II*, where a leading edge ring component detaches from a long trailing jet (Bartol et al., 2008, 2009b). More recent 3D analysis considering both jet and fin contributions also revealed that jet wakes with clear isolated vortex rings have higher mean propulsive efficiencies (78.6%) than jet wakes with elongated regions of jet vorticity (67.9%) (Bartol et al., 2016). Our results show that longer jets (*escape jet II*) have lower efficiency than shorter pulses (*escape jet I*) during escape jet swimming as well. Overall, the observed high propulsive efficiencies of high velocity squid escape jets challenges previous studies that report that jets are inherently inefficient (Alexander, 1968; Lighthill, 1975; Vogel, 2003).

Estimating propulsive efficiency in squids throughout ontogeny is challenging given the different Re regimes and behaviors involved. As mentioned above, paralarvae swim predominantly along a vertical axis, and therefore paralarval displacement over a full jet cycle (mantle contraction and refill) is strongly dependent on the refill duration and sinking rate. To remove the impact of gravity on propulsive efficiency in paralarvae, we considered only the exhalant phase of the jet across our ontogenetic comparisons. Although juveniles and adults swim along a more horizontal axis where losing ground and gravity effects are not as significant, it was important to consider propulsive efficiencies for only the propulsive phase for these life

stages as well, so that fair comparisons could be made. Because the refill period involves no thrust component, it is feasible that our propulsive efficiencies are slightly overestimated. Even if this is true, however, the *relative* differences among the life stages are still accurate, as the same propulsive efficiency metric was used for all comparisons.

Ecological implications

Throughout all life history stages, squids are prey targets for many marine predators, including fish, marine mammals, sea birds, and even other cephalopods, making them an integral component of marine food webs (Clarke, 1996; Mather, 2010; Piatkowski et al., 2001; Wood et al., 2008). Therefore, it is vital that they have an effective response to predation. Our findings show that squids can select at least two escape responses, i.e., *escape jet I* or *escape jet II*, both of which have high propulsive efficiency. When faced with an oncoming predator, the escape response often consists of several sequential escape jets to move away from the predator. Thus, there is a benefit to having high efficiency for each escape jet within a long chain of responses, as it reduces overall energy expenditure. Considering that squid are prey targets for so many species, it is likely that they not only perform sequential escape jets for each interaction but also have lots of daily interactions, making a highly efficient response essential for survival. Although this study focused on individual escape jets, a next logical step would be to evaluate escape jets over multiple cycles to determine how many successive escape jets are routinely employed.

Paralarvae, juveniles and adult squid showed two distinctive types of escape jets: (1) a short spherical vortex pulse (*escape jet I*) and (2) a longer pulse with an extended region of concentrated vorticity (*escape jet II*). The fact that these two patterns were observed throughout

ontogeny indicates that squid have a two phase approach to the escape response, whereby they can use the highly efficient *escape jet I* when a predatory attack is not assured, and the less efficient but presumably more powerful *escape jet II* when an attack is more certain. If this were the case, one might expect swimming speeds and accelerations to be higher for *escape jet II* than *escape jet I*, as the goal of *escape jet II* is to flee quickly. Curiously, this was not observed, indicating that escape mode selection is complex with multiple factors in play. Indeed, the selected escape jet mode may be related, in part, to inking. Squid are capable of producing a variety of large and small ink shapes based on the mantle contraction and opening time of the funnel aperture (Bush and Robison, 2007; Hanlon and Messenger, 1996). When faced with an approaching predator, the most common ink shape utilized by *L. brevis* is a large pseudomorph (see Chapter 4). Since ink is produced in the mantle cavity and ejected out of the funnel when the mantle contracts, the cephalopod inking response is inextricably linked to their jet propulsion system (Hanlon and Messenger, 1996). While not significantly different, there was a clear trend in funnel aperture opening times between the two approaches; funnel aperture opening time was 0.13 s for *escape jet II*, and 0.6 s for *escape jet I*. These differences could potentially impact ink expulsion volume, with shorter and longer inking events being more associated with *escape jet I* and *escape jet II*, respectively. Inking behavior was employed during both *escape jet I* and *escape jet II* in this study; however the shape, volume, and overall mass of the ink was not readily quantifiable with our flow quantification set-up. Clearly, more research is needed to explore how various inking shapes are related to the escape jets observed in this study.

Concluding thoughts

In this study, we determined that squid have locomotive flexibility in escape responses, which was evident by the observation of *escape jet I* and *escape jet II* throughout ontogeny. *Escape jet I* is more efficient in juveniles and adults and may be the mode used when a threat is not eminent. *Escape jet II* is less efficient than *escape jet I* and may be used when a predatory attack is unavoidable (and perhaps even initiated), making a rapid escape integral for survival. Inking may be another important factor in escape jet selection. While all life history stages produced escape jets that are highly efficient, paralarvae were more efficient than adult squid, which likely derives from differences in morphology, ecology, and Re regime. Our observed high propulsive efficiencies for escape swimming, when the goal it to avoid capture at all costs and not necessarily maximize propulsive efficiency, was unexpected. However, when a squid is avoiding capture, the escape response usually consists of multiple sequential escape jets, and many daily interactions with predators are common for squid. Having high propulsive efficiency and the ability to swim quickly are key advantages for squid as they escape oncoming predators, which may have lower peak swimming speeds and propulsive efficiency during these predator/prey encounters. Throughout ontogeny, squid are prey targets for many marine predators, making predator avoidance an enormously important aspect of survival to reproductive age (Clarke, 1996; Piatkowski et al., 2001). Our results indicate that squid are extremely good at producing high velocity and highly efficient escape jets as soon as they hatch. Although squid undergo morphological, ecological and physiological transitions as they develop from planktonic paralarvae to larger nektonic adults, and while differences were found in kinematic patterns and propulsive efficiency through ontogeny, all life stages of squid are capable of a powerful and flexible escape jet response to maximize escape from predation.

CHAPTER 6

CONCLUSIONS

Cephalopods have a number of unique defenses against predators including multiple sensory modalities, an array of anti-predator behavior, and a powerful jet for quick escape (Budelmann, 1996; Hanlon and Messenger, 1996). Squid also undergo major morphological and ecological changes throughout their lives (Boletzky, 1974), which alter how they detect and respond to an oncoming predator. This dissertation provides new insights into the relative importance of the lateral line analogue and vision in predator detection for paralarval, juvenile, and adult squid (Chapters 2-3), the behavioral anti-predator strategies used by squid throughout ontogeny (Chapter 4), and the hydrodynamics of escape jetting employed by squid of different life stages (Chapter 5).

The findings of Chapter 2 and 3 demonstrate for the first time that both vision and the lateral line analogue provide sensory information for initiation of an escape response and successful predator evasion in squid throughout ontogeny. Cephalopod vision has been viewed as the dominant sensory modality used in predator detection due to the well-developed complex nature of cephalopod eyes (Budelmann, 1994; Budelmann, 1996). However, the sensitivity of the lateral line (0.06 µm), means that squid are capable of detecting a moving 1 meter fish from a distance of about 30 meters away, even when vision is disabled (Budelmann, 1994). The use of the lateral line analogue was evident in paralarval squid where in both light and dark conditions, the non-ablated groups showed a higher proportion of escape responses than the ablated groups. Interestingly, there was no difference in the initiation of an escape response of the paralarvae in the light non-ablated and dark non-ablated conditions, as would be expected if vision was used as

the dominant sense. Although differences were found in the initiation of an escape response, no differences were found in survival across treatment groups with the exception of the dark ablated condition, which was likely due to the higher mean velocity of the predator versus the paralarvae in the experimental trials. In juveniles/adults the light non-ablated group survived a higher number of interactions than the light ablated and dark treatment groups, highlighting the importance of both the lateral line analogue and vision. However, the observed higher proportion of interactions survived for the light non-ablated group relative to the dark ablated group, as well as the trend in higher proportion of interactions survived for the light non-ablated versus the dark non-ablated group demonstrate that vision is the more important modality for predator avoidance for life history stages older than paralarvae. Higher number of interactions survived in the light non-ablated than the light ablated group, however, suggests that the lateral line analogue also plays a key role in predator evasion even when vision can be utilized.

Overall, juveniles/adults performed more escape responses than paralarvae, which led to a significantly higher rate of survival. This result may be due to the different anti-predator strategies of squid throughout ontogeny to compensate for an underdeveloped nervous system and planktonic nature (Chen et al., 1996). In juveniles/adults the mean velocity of the escape response was significantly higher in non-ablated versus ablated conditions. Additionally, the time for the squid to reach maximum velocity was almost half a second longer in the ablated versus non-ablated group. It is likely that, similar to the zebrafish, squid respond to the bow wave generated by an approaching predator which stimulates the lateral line analogue. Throughout all of the predator-prey interactions, the squid oriented themselves so the predator approached them anteriorly at angles between 0° and 90°, which is advantageous for both tail-first escape jetting (preferred mode) and sensory perception, as the epidermal hairs are located at

the head and arms. Our findings indicate that the lateral line analogue plays a role in predator detection and initiation of an escape response at the earliest life stages, and continues to contribute to successful evasion by aiding visual cues in juvenile/adult squid. These results provide novel insight into the sensory modalities used by squid to evade predators from the earliest life stages and to maturity.

The results of Chapter 4 reveal the unique differences in anti-predator behavioral strategies of squid as they undergo morphological and ecological transformations throughout ontogeny. Paralarval squid did not react to an oncoming predator with posturing or consistent inking responses. Instead, they produced an escape jet in only 35% of encounters while demonstrating routine stereotypical behaviors in 65% of encounters in the presence of a predator. One of the most striking ontogenetic differences was the presence of these unique stereotyped behaviors by paralarvae, but not other life history stages. Since the paralarvae often did not change their behavior as a predator was approaching, it is possible that they rely heavily on their repertoire of stereotyped behaviors and clear body patterning to elude potential predators in the water column until they develop better neural and motor control. In contrast, juvenile and adult squid exhibited frequent inking/escape jetting and postural responses to an oncoming predator, with the selection of anti-predator behavior being impacted by characteristics of the predator's approach. During the slower predator approaches, the juvenile/adult squid were more likely to posture, while faster approaches triggered inking and escape jet responses. In juveniles/adults, postural responses were favored when the predator was positioned at large distances from the squid while inking responses were selected when the predator was close to the squid. Additionally, postural displays were selected when the predator travelled only a short distance toward the squid, while ink responses were used when the predator travelled a significantly

greater distance toward the squid. In adults and juveniles, the banded body pattern was demonstrated far more than a dark body, clear body or dark arms with a clear body pattern. Furthermore, the proportion of total inking events varied with angular direction of the squid relative to the predator, with anterior and lateral approaches (46-90º) triggering more inking and escape events than approaches from other angles. These findings indicate that hydrodynamic cues received by the lateral line analogue (as discussed in Chapter 3) play a role in inking behavior. The variability in anti-predator behaviors in paralarvae through adults indicates that squid utilize suitable adaptations for their changing morphology and ecological niches to maximize survival throughout ontogeny.

In Chapter 5, the hydrodynamic properties of escape jets produced by paralarvae, juveniles and adult squid are examined. Throughout ontogeny, squid generated two escape jet patterns: (1) *escape jet I* characterized by short rapid pulses resulting in vortex ring formation and (2) *escape jet II* characterized by long high volume jets, often with a leading edge vortex ring. The presence of two escape jet modes indicates that squid have greater complexity in their escape jet behavior than previously thought, i.e., escape jets are not simply produced in an all-or-none fashion. *Escape jet I* is more efficient in juveniles and adults and may be the mode used when the threat is unclear. *Escape jet II* is less efficient than *escape jet I* and may be used when an attack is imminent and escape is of utmost importance. No differences were found in the propulsive efficiency of *escape jet I* and *II* at the paralarval stage, which may be a product of Re and morphology. In addition to efficiency differences, jet mode selection may be a function of ink patterns, as *escape jet II* involves a longer duration of funnel aperture opening than *escape jet I*, allowing the squid to produce larger volume ink signatures. Given that few inking responses were observed in the paralarval predator-prey trials in Chapter 4, it is possible that these modes

become increasingly important for ink pattern diversity as the squid becomes more neurologically advanced and less resources are being allocated towards growth (Russo et al., 2003). While all life history stages produced escape jets that are highly efficient, paralarvae were more efficient than adult squid. This result is likely due to morphological differences in the life stages, where paralarvae have larger funnel apertures (Boletzky, 1974; Packard, 1969; Thompson and Kier, 2002), faster contraction frequencies (Thompson and Kier, 2001) and hold proportionally greater volumes of water in their mantle cavities (Gilly et al., 1991; Preuss et al., 1997a; Thompson and Kier, 2001), which allow paralarvae to expel large volumes of water at relatively low speeds but at high frequencies, all of which can improve efficiency (Bartol et al., 2009a). The overall high efficiencies of the escape jets are surprising, given that energy conservation is not the goal of an escape response. However, when a squid is avoiding capture, the escape response usually consists of multiple sequential escape jets to reach a safe distance from the predator. Moreover, squid have many daily encounters with predators given they are a highly sought after protein-rich food source. Thus, having high efficiencies and high escape velocities is essential for their survival during encounters with seemingly relentless predators. The results of this chapter confirm that as squid develop from planktonic paralarvae to larger nektonic adults, they are capable of a powerful and flexible escape jet response to maximize escape from predation throughout ontogeny.

Overall, the findings of these studies indicate that squid are extremely well adapted for predator avoidance. With multiple sensory modalities to detect an approaching predator, a variety of anti-predator behavioral responses, and a highly efficient and flexible escape jet, all life stages of squid have anti-predator strategies specific to their ecological, physiological and morphological stage to maximize survival.

REFERENCES

Alcock, J. (1993). *Animal Behavior: An Evolutionary Approach*.

Alexander, R. (1968). *Animal Mechanics*. Seattle, WA: University of Washington Press.

Anderson, E. J. and Grosenbaugh, M. a (2005). Jet flow in steadily swimming adult squid. *J. Exp. Biol.* **208**, 1125–46.

Barbato, M., Bernard, M., Borrelli, L. and Fiorito, G. (2007). Body patterns in cephalopods. *Pattern Recognit. Lett.* **28**, 1854–1864.

Barbosa, A., Litman, L., Litman, L. and Hanlon, R. T. (2008). Changeable cuttlefish camouflage is influenced by horizontal and vertical aspects of the visual background. *J. Comp. Physiol. A. Neuroethol. Sens. Neural. Behav. Physiol.* **194**, 405–13.

Bartol, I. K., Patterson, M. R. R. and Mann, R. (2001a). Swimming mechanics and behavior of the shallow-water brief squid Lolliguncula brevis. *J. Exp. Biol.* **204**, 59–66.

Bartol, I. K., Mann, R. and Patterson, M. R. (2001b). Aerobic respiratory costs of swimming in the negatively buoyant brief squid Lolliguncula brevis. *J. Exp. Biol.* **204**, 3639–3653.

Bartol, I. K., Patterson, M. R. and Mann, R. (2001c). Swimming mechanics and behavior of the shallow-water brief squid Lolliguncula brevis. *J. Exp. Biol.* **204**, 3655–3682.

Bartol, I., Mann, R. and Vecchione, M. (2002). Distribution of the euryhaline squid Lolliguncula brevis in Chesapeake Bay: effects of selected abiotic factors. *Mar. Ecol. Prog. Ser.* **226**, 235–247.

Bartol, I. K., Krueger, P. S., Thompson, J. T. and Stewart, W. J. (2008). Swimming dynamics and propulsive efficiency of squids throughout ontogeny. *Integr. Comp. Biol.* **48**, 720–33.

Bartol, I. K., Krueger, P. S., Stewart, W. J. and Thompson, J. T. (2009a). Pulsed jet dynamics of squid hatchlings at intermediate Reynolds numbers. *J. Exp. Biol.* **212**, 1506–18.

Bartol, I. K., Krueger, P. S., Stewart, W. J. and Thompson, J. T. (2009b). Hydrodynamics of pulsed jetting in juvenile and adult brief squid Lolliguncula brevis: evidence of multiple jet "modes" and their implications for propulsive efficiency. *J. Exp. Biol.* **212**, 1889–903.

Bartol, I. K., Krueger, P. S., Jastrebsky, R. A., Williams, S. and Thomspon, J. T. (2016). Volumetric flow imaging reveals the importance of vortex ring formation in squid swimming at different orientations. *J. Exp. Biol.* **in press**,.

Blaxter, J. H. S. and Fuiman, L. a (1990). The role of the sensory systems of herring larvae in evading predatory fishes. *J Mar Biol Ass U K* **70**, 413–427.

Bleckmann, H. (1994). Reception of Hydrodynamic Stimuli in Aquatic and Semiaquatic Animals (Progress in Zoology). In *Progress in Zoology*, p. 115.

Bleckmann, H. and Zelick, R. (2009). Lateral line system of fish. *Integr. Zool.* **4**, 13–25.

Bleckmann, H., Budelmann, B. U. and Bullock, T. H. (1991). Peripheral and central nervous responses evoked by small water movements in a cephalopod. *J. Comp. Physiol. A* **168**, 247–257.

Boletzky, S. . (1974). The "larvae" of Cephalopod: A review. *Thalass. Jugoslavica*.

Boletzky, S. . (2003). Biology of early life stages in cephalopod molluscs. *Adv. Mar. Biol.* **44**, 143–203.

Bone, Q. and Trueman, E. R. (2009). Jet propulsion in salps (Tunicata: Thaliacea). *J. Zool.* **201**, 481–506.

Bone, Q., Pulsford, A. and Chubb, A. D. (1981). Squid mantle muscle. *J. Mar. Biol. Assoc. United Kingdom* **61**, 327.

Boyle, P. R. and Boletzky, S. v. (1996). Cephalopod Populations: Definition and Dynamics. *Philos. Trans. R. Soc. B Biol. Sci.* **351**, 985–1002.

Boyle, P. and Rodhouse, P. (2008). *Cephalopods: Ecology and Fisheries*. John Wiley & Sons.

Browman, H. I., Yen, J., Fields, D. M., St-Pierre, J.-F. and Skiftesvik, A. B. (2011). Fine-scale observations of the predatory behaviour of the carnivorous copepod Paraeuchaeta norvegica and the escape responses of their ichthyoplankton prey, Atlantic cod (Gadus morhua). *Mar. Biol.* **158**, 2653–2660.

Budelmann, B. U. (1994). Cephalopod sense organs, nerves and the brain: adaptations for high performance and life style. *Mar. Freshw. Behav. Physiol.* **25**, 13–33.

Budelmann, B. U. (1996). Active Marine Predators: The Sensory World of Cephalopods. *Mar. Freshw. Behav. Physiol.* **27**, 59–75.

Budelmann, B. U. and Bleckmann, H. (1988). A lateral line analogue in cephalopods: water waves generate microphonic potentials in the epidermal head lines of Sepia and Lolliguncula. *J. Comp. Physiol. A. Neuroethol. Sens. Neural. Behav. Physiol.* **164**, 1–5.

Bullock, T. H. (1984). *Neural Mechanisms of Startle Behavior*. (ed. Eaton, R. C.) Boston, MA: Springer US.

Bullock, T. H. and Budelmann, B. U. (1991). Sensory evoked potentials in unanesthetized unrestrained cuttlefish: a new preparation for brain physiology in cephalopods. *J. Comp. Physiol. A.* **168**, 141–50.

Burighel, P., Lane, N. J., Fabio, G., Stefano, T., Zaniolo, G., Candia Carnevali, M. D. and Manni, L. (2003). Novel, secondary sensory cell organ in ascidians: In search of the ancestor of the vertebrate lateral line. *J. Comp. Neurol.* **461**, 236–249.

Bush, S. L. and Robison, B. H. (2007). Ink utilization by mesopelagic squid. *Mar. Biol.* **152**, 485–494.

Bush, S. L., Robison, B. H. and Caldwell, R. L. (2009). Behaving in the dark: locomotor, chromatic, postural, and bioluminescent behaviors of the deep-sea squid Octopoteuthis deletron young 1972. *Biol. Bull.* **216**, 7–22.

Caldwell, R. L. (2005). An Observation of Inking Behavior Protecting Adult Octopus bocki from Predation by Green Turtle (Chelonia mydas) Hatchlings. *Pacific Sci.* **59**, 69–72.

Chen, D. S., Dykhuizen, G. V., Hodge, J. and Gilly, W. F. (1996). Ontogeny of Copepod Predation in Juvenile Squid (Loligo opalescens). *Biol. Bull.* **190**, 69–81.

Cheng, J. Y. and DeMont, M. E. (1996). Jet-propelled swimming in scallops: swimming mechanics and ontogenic scaling. *Can. J. Zool.* **74**, 1734–1748.

Cheng, J.-Y., Davison, I. G. and Demont, M. E. (1996). Dynamics and energetics of scallop locomotion. *J. Exp. Biol.* **199**, 1931–1946.

Clarke, M. R. (1996). The role of cephalopods in the world's oceans: general conclusions and the future. *Philos. Trans. Biol. Sci.* **351**, 1105–1112.

Coombs, S., Görner, P. and Münz, H. eds. (1989a). *The Mechanosensory Lateral Line*. New York, NY: Springer New York.

Coombs, S., Goerner, P. and Muenz, H. (1989b). *The mechanosensory lateral line : neurobiology and evolution*. New York: Springer.

Coombs, S., Braun, C. B. and Donovan, B. (2001). The orienting response of lake michigan mottled sculpin is mediated by canal neuromasts. **348**, 337–348.

Cornwell, C. J., Messenger, J. B. and Hanlon, R. T. (2009). Chromatophores and Body Patterning in the Squid Alloteuthis Subulata. *J. Mar. Biol. Assoc. United Kingdom* **77**, 1243.

Cronin, T. W. (2005). A visual ecology of predator-prey interactions. In *Ecology of Predator-Prey Interactions* (ed. Barbosa, P.) and Castelllanos, I.), pp. 105–138. Oxford: Oxford University Press.

Cronin, T. W. and Jinks, R. N. (2001). Ontogeny of Vision in Marine Crustaceans1. *Am. Zool.* **41**, 1098–1107.

Dadswell, M. J. and Weihs, D. (1990). Size-related hydrodynamic characteristics of the giant scallop, Placopecten magellanicus (Bivalvia: Pectinidae). *Can. J. Zool.* **68**, 778–785.

Daniel, T. L. (1983). Mechanics and energetics of medusan jet propulsion. *Can. J. Zool.* **61**, 1406–1420.

Daniel, T. L. (1985). Cost of Locomotion: Unsteady Medusan Swimming. *J. Exp. Biol.* **119**, 149–164.

Demont, M. E. and Gosline, M. (1988). Mechanics of Jet Propulsion in the Hydromedusan Jellyfish, Polyorchis Pexicillatus: I. Mechanical Properties of the Locomotor Structure. *J. Exp. Biol.* **134**, 313–332.

Derby, C. D. (2007). Escape by Inking and Secreting : Marine Molluscs Avoid Predators Through a Rich Array of Chemicals and Mechanisms. **213**, 274–289.

Doall, M., Strickler, J., Fields, D. and Yen, J. (2002). Mapping the free-swimming attack volume of a planktonic copepod, Euchaeta rimana. *Mar. Biol.* **140**, 871–879.

Domenici, P. (2002). The Visually Mediated Escape Response in Fish: Predicting Prey Responsiveness and the Locomotor Behaviour of Predators and Prey. *Mar. Freshw. Behav. Physiol.* **35**, 87–110.

Domenici, P., Blagburn, J. M. and Bacon, J. P. (2011). Animal escapology I: theoretical issues and emerging trends in escape trajectories. *J. Exp. Biol.* **214**, 2463–2473.

Douglas, R. H., Williamson, R. and Wagner, H.-J. (2005). The pupillary response of cephalopods. *J. Exp. Biol.* **208**, 261–5.

Dubas, F., Leonard, R. B. and Hanlon, R. T. (1986). Chromatophore motoneurons in the brain of the squid, Lolliguncula brevis: an HRP study. *Brain Res.* **374**, 21–29.

Engelmann, J., Hanke, W., Mogdans, J. and Bleckmann, H. (2000). Hydrodynamic stimuli

and the fish lateral line. *Nature* **408**, 51–2.

Feitl, K. E., Ngo, V. and McHenry, M. J. (2010). Are fish less responsive to a flow stimulus when swimming? *J. Exp. Biol.* **213**, 3131–7.

Fields, D. M. and Yen, J. (2002). Fluid mechanosensory stimulation of behaviour from a planktonic marine copepod, Euchaeta rimana Bradford. *J. Plankton Res.* **24**, 747–755.

Fingerman, M. (1970). Comparative physiology: chromatophores1 1048.

Finke, E., Portner, H. O., Lee, P. G. and Webber, D. M. (1996). Squid (Lolliguncula brevis) life in shallow waters: oxygen limitation of metabolism and swimming performance. *J. Exp. Biol.* **199**, 911–921.

Fish, F. E. (1987). Kinematics and Power Output of Jet Propulsion by the Frogfish Genus Antennarius (Lophiiformes: Antennariidae). *Copeia* 1046–1048.

Florey, E. (1966). Nervous control and spontaneous activity of the chromatophores of a cephalopod, Loligo opalescens. *Comp. Biochem. Physiol.* **18**, 305–324.

Gibb, A. C., Swanson, B. O., Wesp, H., Landels, C. and Liu, C. (2006). Development of the escape response in teleost fishes: do ontogenetic changes enable improved performance? *Physiol. Biochem. Zool.* **79**, 7–19.

Gilly, W. F. and Lucero, M. T. (1992). Behavioral responses to chemical stimulation of the olfactory organ in the squid Loligo opalescens. *J. Exp. Biol.* **162**, 209–229.

Gilly, W. F., Hopkins, B. and Mackie, G. O. (1991). Development of giant motor axons and neural control of escape responses in squid embryos and hatchlings. *Biol. Bull.* **180**, 209–220.

Gilly, W. F., Preuss, T. and Mcfarlane, M. B. (1996). All-or-none contraction and sodium channels in a subset of circular muscle fibers of squid mantle. *Biol. Bull.* **191**, 337–340.

Gosline, B. Y. J. M., Steeves, J. D., Anthony, D. and Demont, M. E. (1983). Patterns of circular and radial mantle muscle activity in respriation and jetting of the squid Loligo opalescens. *J. Comp. Physiol. A. Neuroethol. Sens. Neural. Behav. Physiol.* **104**, 97–109.

Hale, M. (1999). Locomotor mechanics during early life history: effects of size and ontogeny on fast-start performance of salmonid fishes. *J. Exp. Biol.* **202**, 1465–1479.

Hanlon, R. T. (1990). Maintenance, rearing and culture of teuthoid and sepioid squids. In *Squid as Experimental Animals* (ed. Gilbert, D. L.), Adelman, W. J.), and Arnold, J. M.), pp. 35–62. New York: Plenum Press.

Hanlon, R. T. and Messenger, J. B. (1996). *Cephalopod Behaviour*. New York: Cambridge University Press.

Hanlon, R. T., Hixon, R. F. and Hulet, W. H. (1983). Survival, growth and behavior of the loliginid squids Loligo plei, Loligo pealei, and Lolliguncula brevis (Mollusca: cephalopoda) in closed sea water systems. *Biol. Bull.* **165**, 637–685.

Hanlon, R. T., Smale, M. J. and Sauer, W. H. H. W. (1994). An Ethogram of Body Patterning Behavior in the Squid Loligo vulgaris reynaudii on Spawning Grounds in South Africa. *Biol. Bull.* **187**, 363–372.

Hanlon, R. T., Maxwell, M. R., Shashar, N., Loew, E. R. and Boyle, K. L. (1999). An

ethogram of body patterning behavior in the biomedically and commercially valuable squid Loligo pealei off Cape Cod, Massachusetts. *Biol. Bull.* **197**, 49–62.

Harris, J. a, Cheng, A. G., Cunningham, L. L., MacDonald, G., Raible, D. W. and Rubel, E. W. (2003). Neomycin-induced hair cell death and rapid regeneration in the lateral line of zebrafish (Danio rerio). *J. Assoc. Res. Otolaryngol.* **4**, 219–34.

Hedrick, T. L. (2008). Software techniques for two- and three-dimensional kinematic measurements of biological and biomimetic systems. *Bioinspir. Biomim.* **3**, 034001.

Heuch, P. A., Doall, M. H. and Yen, J. (2007). Water flow around a fish mimic attracts a parasitic and deters a planktonic copepod. In *Journal of Plankton Research*, .

Hoar, J. A., E, S., M, W. D. and K, O´d. R. (1994a). The role of fins in the competition between squid and fish. In *Mechanics and Physiology of Animal Swimming*, pp. 27–43.

Hoar, J., Sim, E., Webber, D. and O´Dor, R. (1994b). The role of fins in the competition between squid and fish. In *Mechanics and Physiology of Animal Swimming*, pp. 27–43.

Horodysky, A. Z., Brill, R. W., Warrant, E. J., Musick, J. a and Latour, R. J. (2010). Comparative visual function in four piscivorous fishes inhabiting Chesapeake Bay. *J. Exp. Biol.* **213**, 1751–61.

Huffard, C. L. (2006). Locomotion by Abdopus aculeatus (Cephalopoda: Octopodidae): walking the line between primary and secondary defenses. *J. Exp. Biol.* **209**, 3697–707.

Jantzen, T. M. and Havenhand, J. N. (2003). Reproductive Behavior in the Squid Sepioteuthis australis From South Australia: Ethogram of Reproductive Body Patterns. *Biol. Bull.* **204**, 290–304.

Katija, K., Colin, S. P., Costello, J. H. and Jiang, H. (2015). Ontogenetic propulsive transitions by Sarsia tubulosa medusae. *J. Exp. Biol.* **218**, 2333–43.

Kier, W. M. (1988). The arrangement and function of molluscan muscle. *The Mollusca* **11**, 211–252.

Kier, W. M. (1989). The fin musculature of cuttlefish and squid (Moolusca, Cephalopoda): morphology and mechanics. *J. Zool.* **217**, 23–38.

Kobayashi, S., Takayama, C. and Ikeda, Y. (2013). Ontogeny of the brain in oval squid Sepioteuthis lessoniana (Cephalopoda : Loliginidae) during the post-hatching phase. **93**, 1663–1671.

Komak, S., Boal, J. G., Dickel, L. and Budelmann, B. U. (2005). Behavioural responses of juvenile cuttlefish (Sepia officinalis) to local water movements. *Mar. Freshw. Behav. Physiol.* **38**, 117–125.

Kröger, B., Vinther, J. and Fuchs, D. (2011). Cephalopod origin and evolution: A congruent picture emerging from fossils, development and molecules: Extant cephalopods are younger than previously realised and were under major selection to become agile, shell-less predators. *Bioessays* **33**, 602–13.

Krueger, P. S. and Gharib, M. (2003). The significance of vortex ring formation to the impulse and thrust of a starting jet. *Phys. Fluids* **15**, 1271.

Lighthill, M. (1975). *Mathematical Biofluidynamics*. Philadelphia, PA: Society for Industrial and Applied Mathematics.

Lucero, M. T., Farrington, H. and Gilly, W. F. (1994). Quantification of L-Dopa and Dopamine in Squid Ink: Implications for Chemoreception. *Biol. Bull.* **187**, 55–63.

Macgillivray, P., Anderson, E., Wright, G. and Demont, M. (1999). Structure and mechanics of the squid mantle. *J. Exp. Biol.* **202**, 683–695.

Madin, L. P. (1990). Aspects of jet propulsion in salps. *Can. J. Zool.* **68**, 765–777.

Marthy, H. J. (1987). Ontogenesis of the nervous system in cephalopods. In *Nervous Systems in Invertebrates* (ed. Ali, M. A.), pp. 443–459. New York: Plenum.

Martin, R. (1965). On the structure and embryonic development of the giant fibre system of the squid Loligo vulgaris. *Zeitschrift Zellforsch. und Mikroskopische Anat.* **67**, 77–85.

Mather, J. a. (2010). Vigilance and antipredator responses of Caribbean reef squid. *Mar. Freshw. Behav. Physiol.* **43**, 357–370.

Mäthger, L. M. and Hanlon, R. T. (2006). Anatomical basis for camouflaged polarized light communication in squid. *Biol. Lett.* **2**, 494–6.

Mäthger, L. M. and Hanlon, R. T. (2007). Malleable skin coloration in cephalopods: selective reflectance, transmission and absorbance of light by chromatophores and iridophores. *Cell Tissue Res.* **329**, 179–86.

Mäthger, L. M., Shashar, N. and Hanlon, R. T. (2009). Do cephalopods communicate using polarized light reflections from their skin? *J. Exp. Biol.* **212**, 2133–40.

McCormick, L. R. and Cohen, J. H. (2012). Pupil light reflex in the Atlantic brief squid, Lolliguncula brevis. *J. Exp. Biol.* **215**, 2677–83.

McHenry, M. J., Feitl, K. E., Strother, J. A. and Van Trump, W. J. (2009). Larval zebrafish rapidly sense the water flow of a predator's strike. *Biol. Lett.* **5**, 477–479.

Messenger, J. B. (1968). The visual attack of the cuttlefish, Sepia officinalis. *Anim. Behav.* **16**, 342–357.

Messenger, J. B. (2001). Cephalopod chromatophores : neurobiology and natural history. 473–528.

Miller, T. J., Crowder, L. B. and Rice, J. A. (1993). Ontogenetic changes in behavioural and histological measures of visual acuity in three species of fish. *Environ. Biol. Fishes* **37**, 1–8.

Mommsen, T. P., Ballantyne, J., Macdonald, D., Gosline, J. and Hochachka, P. W. (1981). Analogues of red and white muscle in squid mantle. *Proc. Natl. Acad. Sci.* **78**, 3274–3278.

Montgomery, J., Coombs, S. and Halstead, M. (1995). Biology of the mechanosensory lateral line in fishes. *Rev. Fish Biol. Fish.* **5**, 399–416.

Montgomery, J. C., Coombs, S. and Baker, C. F. (2001). The mechanosensory lateral line system of the hypogean form of Astyanax fasciatus. *Environ. Biol. Fishes* **62**, 87–96.

Muntz, W. R. A. and Johnson, M. S. (1978). Rhodopsins of oceanic decapods. *Vision Res.* **18**, 601–602.

O'Dor, R. K. (1982). Respiratory Metabolism and Swimming Performance of the Squid, Loligo opalescens. *Can. J. Fish. Aquat. Sci.* **39**, 580–587.

O'Dor, R. K. (1988). The forces acting on swimming squid. *J. Exp. Biol.* **442**, 421–442.

O'Dor, R. (2002). Telemetered cephalopod energetics: swimming, soaring, and climping. *Integr Comp Biol* **42**, 1065–1070.

O'Dor, R. K. and Webber, D. M. (1986). The constraints on cephalopods: why squid aren't fish. *Can. J. Zool.* **64**, 1591–1605.

O'Dor, R. K. and Webber, D. M. (1991). Invertebrate Athletes: Trade-Offs between Transport Efficiency and Power Density in Cephalopod Evolution. *J. Exp. Biol.* **160**, 93–112.

O'dor, R. K., Webber, D. M. and Scotia, N. (1991). Invertebrate athletes: trade-offs between transport efficiency and power density in cephalopod evolution. *J Exp Biol* **160**, 93–112.

O'Dor, R. K., Hoar, J. A., Webber, D. M., Carey, F. G., Tanaka, S., Martins, H. R. and Porteiro, F. M. (1995). Squid (Loligo forbesi) performance and metabolic rates in nature. *Mar. Freshw. Behav. Physiol.* **25**, 163–177.

Okutani, T. (1987). Juvenile Morphology. In *Cephalopod Life Cycles* (ed. Boyle, P. R.), Miami FL: Associated Press.

Otis, T. S. and Gilly, W. F. (1990). Jet-propelled escape in the squid Loligo opalescens: concerted control by giant and non-giant motor axon pathways. *Proc Natl Acad Sci U S A* **87**, 2911–5.

Packard, A. (1969). Jet Propulsion and the Giant Fibre Response of Loligoa. *Nature* **221**, 875–877.

Pereira, F., Stüer, H., Graff, E. C. and Gharib, M. (2006). Two-frame 3D particle tracking. *Meas. Sci. Technol.* **17**, 1680–1692.

Piatkowski, U., Pierce, G. J. and Morais, M. (2001). Impact of cephalopods in the food chain and their interaction with the environment and fisheries : an overview. **52**, 3–8.

Polis, G. A. (1981). The evolution and dynamics of intraspecific predation. *Annu. Rev. Ecol. S* **12**, 225–251.

Preuss, T. and Gilly, W. (2000). Role of prey-capture experience in the development of the escape response in the squid Loligo opalescens: a physiological correlate in an identified neuron. *J. Exp. Biol.* **203**, 559–565.

Preuss, T., Lebaric, Z. N. and Gilly, W. F. (1997a). Post-Hatching Development of Circular Mantle Muscles in the Squid Loligo opalescens. *Biol. Bull.* **192**, 375–387.

Preuss, T., Lebaric, Z. N. and Gilly, W. F. (1997b). Post-Hatching Development of Circular Mantle Muscles in the Squid Loligo opalescens. *Biol. Bull.* **192**, 375–387.

Prosser, C. L. and Young, J. Z. (1937). Responses of muscles of the squid to repetitive stimulation of the giant nerve fibers. *Biol. Bull.* **73**, 237–241.

Robin, J.-P., Roberts, M., Zeidberg, L., Bloor, I., Rodriguez, A., Briceño, F., Downey, N., Mascaró, M., Navarro, M., Guerra, A., et al. (2014). Transitions during cephalopod life history: the role of habitat, environment, functional morphology and behaviour. *Adv. Mar. Biol.* **67**, 361–437.

Russo, G. L., De Nisco, E., Fiore, G., Di Donato, P., D'Ischia, M. and Palumbo, A. (2003). Toxicity of melanin-free ink of Sepia officinalis to transformed cell lines: Identification of the active factor as tyrosinase. *Biochem. Biophys. Res. Commun.* **308**, 293–299.

Shadwick, R. E. (1995). Mechanical organization of the mantle and circulatory system of cephalopods. *Mar. Freshw. Behav. Physiol.* **25**, 69–85.

Shadwick, R. E. and Lauder (2006). *Fish Physiology: Fish Biomechanics: Fish Biomechanics*. Academic Press.

Shea, E. K. and Vecchione, M. (2010). Ontogenic changes in diel vertical migration patterns compared with known allometric changes in three mesopelagic squid species suggest an expanded definition of a paralarva. *ICES J. Mar. Sci.* **67**, 1436–1443.

Staaf, D. J., Gilly, W. F. and Denny, M. W. (2014). Aperture effects in squid jet propulsion. *J. Exp. Biol.* **217**, 1588–600.

Staudinger, M. D. and Juanes, F. (2010). Size-dependent susceptibility of longfin inshore squid (Loligo pealeii) to attack and capture by two predators. *J. Exp. Mar. Bio. Ecol.* **393**, 106–113.

Staudinger, M. D., Hanlon, R. T. and Juanes, F. (2011). Primary and secondary defences of squid to cruising and ambush fish predators: variable tactics and their survival value. *Anim. Behav.* **81**, 585–594.

Stewart, W. J., Bartol, I. K. and Krueger, P. S. (2010). Hydrodynamic fin function of brief squid, Lolliguncula brevis. *J. Exp. Biol.* **213**, 2009–2024.

Stewart, W. J., Cardenas, G. S. and McHenry, M. J. (2013). Zebrafish larvae evade predators by sensing water flow. *J. Exp. Biol.* **216**, 388–98.

Stewart, W. J., Nair, A., Jiang, H. and McHenry, M. J. (2014). Prey fish escape by sensing the bow wave of a predator. *J. Exp. Biol.* **217**, 4328–36.

Sundermann, G. (1983). The fine structure of epidermal lines on arms and head of postembryonic Sepia officinalis and Loligo vulgaris (Mollusca, Cephalopoda). *Cell Tissue Res.* **232**, 669–677.

Sutherland, R. L., Mäthger, L. M., Hanlon, R. T., Urbas, A. M. and Stone, M. O. (2008). Cephalopod coloration model . I . Squid chromatophores and iridophores. **25**, 588–599.

Thompson, J. T. and Kier, W. M. (2001). Ontogenetic changes in mantle kinematics during escape-jet locomotion in the oval squid, Sepioteuthis lessoniana Lesson, 1830. *Biol. Bull.* **201**, 154–166.

Thompson, J. T. and Kier, W. M. (2002). Ontogeny of Squid Mantle Function : Changes in the Mechanics of Escape-Jet Locomotion in the Oval Squid , Sepioteuthis lessoniana Lesson , 1830. 14–26.

Thompson, J. T. and Kier, W. M. (2006). Ontogeny of mantle musculature and implications for jet locomotion in oval squid Sepioteuthis lessoniana. *J. Exp. Biol.* **209**, 433–43.

Thompson, J. T., Szczepanski, J. A. and Brody, J. (2008). Mechanical specialization of the obliquely striated circular mantle muscle fibres of the long-finned squid Doryteuthis pealeii. *J. Exp. Biol.* **211**, 1463–74.

Troolin, D. R. and Longmire, E. K. (2009). Volumetric velocity measurements of vortex rings from inclined exits. *Exp. Fluids* **48**, 409–420.

Viitasalo, M., Kiørboe, T., Flinkman, J., Pedersen, L. and Visser, A. (1998). Predation vulnerability of planktonic copepods:consequences of predator foraging strategies and prey

sensory abilities. *Mar. Ecol. Prog. Ser.* **175**, 129–142.

Visser, A. (2001). Hydromechanical signals in the plankton. *Mar. Ecol. Prog. Ser.* **222**, 1–24.

Vogel, S. (2003). *Comparative Biomechanics: Life's Physical World*. Princeton, NJ: Princeton University Press.

Vogel, S. (2013). *Comparative Biomechanics: Life's Physical World (Second Edition)*. Princeton University Press.

Wainwright, P., Carroll, A. M., Collar, D. C., Day, S. W., Higham, T. E. and Holzman, R. a (2007). Suction feeding mechanics, performance, and diversity in fishes. *Integr. Comp. Biol.* **47**, 96–106.

Ward, D. V. and Wainwright, S. (1972). Locomotory function of the squid mantle. *J. Zool.* **167**, 487–499.

Webber, D. M. and O'Dor, R. K. (1986). Monitoring the Metabolic Rate and Activity of Free-Swimming squid With Telemetered Jet Pressure. *J. Exp. Biol.* **126**, 205–224.

Weihs, D. and Webb, P. W. (1984). Optimal avoidance and evasion tactics in predator-prey interactions. *J. Theor. Biol.* **106**, 189–206.

Wells, M. J. and O'Dor, R. K. (1991). Jet propulsion and the evolution of the cephalopods. *Bull. Mar. Sci.* **49**, 419–432.

Westerweel, J., Dabiri, D. and Gharib, M. (1997). The effect of a discrete window offset on the accuracy of cross-correlation analysis of digital PIV recordings. *Exp. Fluids* **23**, 20–28.

Williams, P. J., Brown, J. a, Gotceitas, V. and Pepin, P. (1996). Developmental changes in escape response performance of five species of marine larval fish. *Can. J. Fish. Aquat. Sci.* **53**, 1246–1253.

Wood, J. B., Pennoyer, K. E. and Derby, C. D. (2008). Ink is a conspecific alarm cue in the Caribbean reef squid, Sepioteuthis sepioidea. *J. Exp. Mar. Bio. Ecol.* **367**, 11–16.

Wood, J. B., Maynard, A. E., Lawlor, A. G., Sawyer, E. K., Simmons, D. M., Pennoyer, K. E. and Derby, C. D. (2010). Caribbean reef squid, Sepioteuthis sepioidea, use ink as a defense against predatory French grunts, Haemulon flavolineatum. *J. Exp. Mar. Bio. Ecol.* **388**, 20–27.

Yen, J., Lenz, P. H., Gassie, D. V. and Hartline, D. K. (1992). Mechanoreception in marine copepods: Electrophysiological studies on the first antennae. *J. Plankton Res.* **14**, 495–512.

York, C. A. and Bartol, I. K. (2014). Lateral line analogue aids vision in successful predator evasion for brief squid Lolliguncula brevis. *J. Exp. Biol.* 2437–2439.

Young, J. Z. (1938). The functioning of the giant nerve fibres of the squid. *J. Exp. Biol.* **15**, 170–185.

Young, J. Z. (1962). The optic lobes of octopus vulgaris. *Philos. Trans. R. Soc. London Ser. B Biol. Sci.* **245**, 19–58.

Young, R. E. and Harman, R. F. (1988). "Larva,""paralarva" and "subadult" in cephalopod terminology. *Malacologia* **29**, 201–207.

Zylinski, S. and Johnsen, S. (2011). Mesopelagic cephalopods switch between transparency and pigmentation to optimize camouflage in the deep. *Curr. Biol.* **21**, 1937–41.

VITA

Carly Anne York

Department of Biology, Old Dominion University, Norfolk, VA 23529 USA

Education

2011-2016   Ph.D Candidate, Old Dominion University, Norfolk VA
Ecological Sciences. Advisor: Dr. Ian Bartol
Dissertation: The anti-predator responses of squids throughout ontogeny

2009-2011   M.S.,Western Kentucky University, Bowling Green KY
Biological Sciences. Advisor: Dr. Bruce Schulte
Thesis: The relationship of dominance, reproductive state and stress in a non-cooperative breeder, the domestic horse (Equus caballus)

2004-2007   B.S., Elon University, Burlington NC
Exercise Science. Advisor: Dr. Paul Miller

Peer Reviewed Publications

York, C.A**.,** Bartol, I.K. (2016) Anti-predator behavior of squid throughout ontogeny. *In press* at *Journal of Experimental Marine Biology and Ecology.*

York, C.A., Bartol, I.K. (2014). Lateral line analogue aids vision in successful predator evasion for brief squid *Lolliguncula brevis. Journal of Experimental Biology*, 217, 2437-2439.

York, C.A., Schulte, B.A. (2014) The relationship of dominance, reproductive state and stress in female horses (*Equus caballus*). *Behavioural Processes*, 107, 15-21.

Miller, P.C., Hall, E.E., Mulcahy, T.K., Bulow, K., Scoggin, M., Sinderbrand, C., Bixby, W.R.,Bailey, S.P. (2008) Recovery of contractile function following eccentric exercise with protease supplementation. *Medicine and Science in Sports and Exercise*, 40, 195.